University of Tennessee, Knoxville

TRACE: Tennessee Research and Creative Exchange

Doctoral Dissertations

Graduate School

12-2010

Multivariate Optimization of Neutron Detectors Through Modeling

Martin Rodney Williamson
University of Tennessee - Knoxville, mwillia3@utk.edu

Follow this and additional works at: https://trace.tennessee.edu/utk_graddiss

 Part of the Nuclear Engineering Commons

Recommended Citation

Williamson, Martin Rodney, "Multivariate Optimization of Neutron Detectors Through Modeling. " PhD diss., University of Tennessee, 2010.
https://trace.tennessee.edu/utk_graddiss/924

This Dissertation is brought to you for free and open access by the Graduate School at TRACE: Tennessee Research and Creative Exchange. It has been accepted for inclusion in Doctoral Dissertations by an authorized administrator of TRACE: Tennessee Research and Creative Exchange. For more information, please contact trace@utk.edu.

To the Graduate Council:

I am submitting herewith a dissertation written by Martin Rodney Williamson entitled "Multivariate Optimization of Neutron Detectors Through Modeling." I have examined the final electronic copy of this dissertation for form and content and recommend that it be accepted in partial fulfillment of the requirements for the degree of Doctor of Philosophy, with a major in Nuclear Engineering.

Laurence F. Miller, Major Professor

We have read this dissertation and recommend its acceptance:

Dayakar Penumadu, Lawrence W. Townsend, Ronald E. Pevey

Accepted for the Council:

Carolyn R. Hodges

Vice Provost and Dean of the Graduate School

(Original signatures are on file with official student records.)

To the Graduate Council:

I am submitting herewith a dissertation written by Martin Rodney Williamson entitled "Multivariate Optimization of Neutron Detectors Through Modeling." I have examined the final electronic copy of this dissertation for form and content and recommend that it be accepted in partial fulfillment of the requirements for the degree of Doctor of Philosophy, with a major in Nuclear Engineering.

Laurence F. Miller, Major Professor

We have read this dissertation
and recommend its acceptance:

Dayakar Penumadu

Lawrence W. Townsend

Ronald E. Pevey

Accepted for the Council:

Carolyn R. Hodges
Vice Provost and Dean of the Graduate School

(Original signatures are on file with official student records.)

MULTIVARIATE OPTIMIZATION OF NEUTRON DETECTORS THROUGH MODELING

A Dissertation Presented for the
Doctor of Philosophy Degree
The University of Tennessee, Knoxville

Martin Rodney Williamson
December 2010

Copyright ©, Martin Rodney Williamson

All rights reserved.

DEDICATION

This dissertation is dedicated to my family, who truly are a gift from God. My loving wife and best friend Jenny has generously given her love, support, and encouragement throughout this long process. My children, Tom and Nate, have given me a love and purpose which I never could have fathomed without them. I love you all!

ACKNOWLEDGMENTS

I am enormously grateful to everyone who helped me during the creation of this dissertation. Special thanks are extended to Drs. Lawrence Townsend, Dayakar Penumadu, and Ronald Pevey for agreeing to spend their time and effort to be on my committee and for providing insight and recommendations which have enriched the depth of this dissertation. I would like to thank the other researchers working on this grant, specifically Alex Green, Stephen Young, Merry Koschan, and Drs. Neel Sen, George Schweitzer, and Chuck Melcher for sharing their expertise regarding detectors and the physics associated with them through our weekly discussions. My participation in this research was made possible by my employer, the Y-12 National Security Complex, by providing me with a sabbatical to complete this work. Specifically, I would like to thank John Sherwood, Chris Robinson, and John Gertsen of Y-12 who lobbied for my being granted the sabbatical. I would also like to thank David Davis, now a fellow employee at Y-12, for his programming expertise which was required during the development of the Matlab® PTRAC post-processing code. I am grateful to Dr. Michael James of LANL and Dr. Edward Siciliano of PNNL for their discussions and guidance related to modeling radiation detectors with MCNPX for DNDO applications. Finally, I would like to thank Dr. Laurence F. Miller, my committee chair and faculty advisor, for giving me the opportunity to be a part of this research. Dr. Miller has been an exceptional mentor by sharing his knowledge and experience in neutron detection which was instrumental in shaping the direction of this project. My sincerest thanks to you all.

ABSTRACT

Due to the eminent shortage of ^{3}He, there exists a significant need to develop a new (or optimize an existing) neutron detection system which would reduce the dependency on the current ^{3}He-based detectors for Domestic Nuclear Detection Office (DNDO) applications. The purpose of this research is to develop a novel methodology for optimizing candidate neutron detector designs using multivariate statistical analysis of Monte Carlo radiation transport code (MCNPX) models. The developed methodology allows the simultaneous optimization of multiple detector parameters with respect to multiple response parameters which measure the overall performance of a candidate neutron detector. This is achieved by applying three statistical strategies in a sequential manner (namely factorial design experiments, response surface methodology, and constrained multivariate optimization) to results generated from MCNPX calculations. Additionally, for organic scintillators, a methodology incorporating the light yield non-proportionality is developed for inclusion into the simulated pulse height spectra (PHS). A Matlab® program was developed to post-process the MCNPX standard and PTRAC output files to automate the process of generating the PHS thus allowing the inclusion of nonlinear light yield equations (Birks equations) into the simulation of the PHS for organic scintillators.

The functionality of the developed methodology is demonstrated on the successful multivariate optimization of three neutron detection systems which utilize varied approaches to satisfying the DNDO criteria for an acceptable alternative neutron detector. The first neutron detection system optimized is a ^{3}He-based radiation portal monitor (RPM) based on a generalized version of a currently deployed system. The second system optimized is a ^{6}Li-loaded polymer composite scintillator in the form of a thin film. The final system optimized is a ^{10}B-based plastic scintillator sandwiched between two standard plastic scintillators. Results from the multivariate optimization analysis include not only the identification of which factors significantly affect detector performance, but also the determination of optimum levels for those factors with simultaneous consideration of multiple detector performance responses. Based on the demonstrated functionality of the developed multivariate optimization methodology,

application of the methodology in the development process of new candidate neutron detector designs is warranted.

TABLE OF CONTENTS

LIST OF TABLES

LIST OF FIGURES

ACRONYMS

ANOVA	Analysis of Variance
CCD	Central Composite Design
DF	Degrees of Freedom
DHS	Department of Homeland Security
DNDO	Domestic Nuclear Detection Office
FWHM	Full-Width Half Maximum
GARRn	Gamma Absolute Rejection Ration for Neutrons
GUI	Graphical User Interface
GRG	Generalized Reduced Gradient
HDPE	High Density Polyethylene
HVPS	High Voltage Power Supply
IAT	Innovative American Technologies
LANL	Los Alamos National Laboratory
LiF	Lithium Fluoride
Li-Sal	Lithium Salicylate
LLD	Lower Level Discriminator
LSM	Least Squares Means
MCNP	Monte Carlo N-Particle
MCNPX	Monte Carlo N-Particle eXtended
MeVee	Mega-Electron Volt (Electron Equivalent)
NSF	National Science Foundation
P2VN	Poly(2-Vinylnaphthalene)
PHD	Pulse Height Discrimination
PHL	Pulse Height Light
PHS	Pulse Height Spectra
PMT	Photomultiplier Tube
PNNL	Pacific Northwestern National Laboratory
PSD	Pulse Shape Discrimination
RPM	Radiation Portal Monitor
RSM	Response Surface Methodology
PTRAC	Particle Track
SAIC	Science Applications International Corporation
SAS	Statistical Analysis Software
SNM	Special Nuclear Material
UT	The University of Tennessee

1 INTRODUCTION

1.1 PROBLEM STATEMENT AND MOTIVATION

The Domestic Nuclear Detection Office (DNDO) is a national office within the Department of Homeland Security (DHS) which provides a single accountable organization with dedicated responsibilities to protect against nuclear terrorism. The ability to accurately detect and identify neutron signatures from Special Nuclear Material (SNM) is paramount to the success of the DNDO mission. The current standard for neutron detection is the ^{3}He gas proportional counter due to the stability, sensitivity, and gamma/neutron discrimination these detectors offer. Currently, no other commercially available neutron detector is comparable to the ^{3}He neutron tubes in these respects. The lack of an equivalent neutron detection system has resulted in neutron detection for DNDO applications being performed almost exclusively using ^{3}He gas proportional counters [1,2]. However, recent studies show that the production rates and current stockpile of ^{3}He are not sufficient to keep pace with increasing demand [3]. Therefore, there exists a significant need to develop a new (or optimize an existing) neutron detection system which would reduce the dependency on the current ^{3}He-based detectors. This research was initiated under a grant awarded to a multidisciplinary team from the University of Tennessee (UT) to develop a viable alternative to current ^{3}He-based detectors for DNDO applications [4]. Due to the volume of ^{3}He required for Radiation Portal Monitors (RPMs), this research focuses only on finding a replacement technology for ^{3}He in RPM applications.

Many diverse methods of neutron detection exist, and fabrication and testing of new detector designs can be costly and time-consuming. The purpose of this research is to develop a novel methodology for optimizing candidate neutron detector designs using multivariate statistical analysis of Monte Carlo radiation transport code (MCNPX) models. This methodology is applicable to any neutron detection design and its functionality is demonstrated on the successful multivariate optimization of three neutron detection systems which utilize varied approaches to satisfying the DNDO criteria for an acceptable alternative neutron detector.

1.2 ORGANIZATION OF DISSERTATION

This work is described in the next four chapters. Chapter two provides a literature survey which includes background information related to the field of neutron detection with a focus on discussion of the detection of SNM, potential alternative DHS detector designs, and the criteria which must be satisfied for an acceptable ^{3}He replacement detector. Chapter two also presents an introduction to the statistical methods utilized for this research as well as an overview of previous research related to these fields. Chapter three presents a description of the experimental system used to generate the measured results as well as the Monte Carlo radiation transport code used to generate the simulated detector results presented within this report. Chapter three also provides a description of the detector response parameters of interest (and how to calculate them), an overview of the Matlab® code used to post-process the MCNPX results, and the methodology used for multivariate optimization. Chapter four presents the detailed results of the optimization methodology applied to three neutron detection systems which use varied approaches to satisfy the DNDO criteria. Chapter five presents the conclusions reached during this research and recommendations for future work.

1.3 ORIGINALITY AND RELEVANCY

While the use of Monte Carlo radiation transport codes to simulate the performance of neutron detectors is commonplace, this research is novel in the fact that it utilizes the multivariate statistical analysis of the Monte Carlo simulations for simultaneously optimizing multiple detector parameters with respect to multiple response parameters which measure the overall performance of a candidate neutron detector. These response parameters are taken directly from DNDO criteria and include measures of the detection system's neutron sensitivity, neutron-gamma discrimination ability, and cost. Additionally, for organic scintillation neutron detectors, original work includes the use of semi-empirical models to calculate the light yield generated from the energy deposition in a scintillator for a given charged particle. These models are used to convert the typical pulse height spectra (PHS) generated by MCNPX from energy deposited by the charged particles into light output from the scintillator. This conversion required the development

of a custom Matlab® code capable of analyzing and post-processing the MCNPX particle track (PTRAC) output. This detector optimization methodology is original in that the simulated detector responses are analyzed using statistical software to determine which detector parameters (and interrelationships among those parameters) impact each of the detector response parameters. These parameters (or factors) are then used to build quadratic models of each response parameter. Finally, the quadratic models are used to determine optimum values for each of the factors with DNDO-defined minimum constraints placed on each of the detector's response functions. Lastly, this work is novel in that these optimization techniques are performed on new neutron detection systems which have been developed at the University of Tennessee and have not previously been studied.

2 LITERATURE SURVEY

2.1 RADIATION AND RADIATION MEASUREMENT OF SPECIAL NUCLEAR MATERIAL

Special Nuclear Material is defined by the Atomic Energy Act of 1954 as plutonium or uranium enriched in isotopes uranium-233 or uranium-235 [5]. While these materials are only mildly radioactive, in sufficient quantities they can be used as nuclear explosives. Each of these materials emits a gamma radiation signature (or unique energy spectrum), while plutonium also emits a detectable neutron radiation signature. Detection of concealed SNM through a gamma radiation signature is complicated by the inherent presence of other background gamma radiation such as natural background radiation, naturally occurring radioactive material in commerce, the possibility of individuals who have undergone radioisotope therapy, etc. Detection of concealed SNM through neutrons has the advantages of lower natural background and fewer sources being carried in the normal flow of commerce. However, due to uranium emitting a very low rate of spontaneous fission neutrons, active interrogation with neutron or gamma ray sources is required. Both detection methods are further complicated by the potential presence of radiation shielding which can impact the energy spectra and flux intensity observed by the detection system. Due to the large scope associated with the detection of illicit SNM trafficking, the focus of this research is limited to the optimization of systems used to detect neutrons generated from SNM (from either induced or spontaneous fission) to complement gamma-ray detectors.

2.2 NEUTRON DETECTION BACKGROUND

Since neutrons do not directly ionize atoms, they can only be detected indirectly through nuclear reactions induced by neutrons which subsequently produce energetic charged particle(s) or photon(s). These secondary particles are then recorded with a conventional radiation detector, such as a scintillation detector (which is the detection method of choice for this developmental research). The following sub-sections provide background information related to the physics for each of the particles involved in neutron detection.

2.2.1 NEUTRON INTERACTIONS AND TRANSPORT

Neutrons do not experience the electrostatic repulsion force (i.e., Coulomb force) from a nucleus since they have no net electric charge. Subsequently, neutrons have a higher probability (or cross section) for a nuclear absorption by a nucleus and generally travel further than charged particles. Neutron interactions are limited to two broad categories: scattering (either elastic or inelastic) and absorption (which includes many types of reactions such as (n, p), (n,α), (n,γ), and (n, fission)). In a scattering reaction, the neutron interacts with a nucleus and both particles reappear after the collision. The total kinetic energy is conserved for elastic scattering with the energy being redistributed between the two particles. For inelastic scattering part of the kinetic energy is given to the nucleus leaving it in an excited state and one or more γ-rays are emitted to bring the nucleus back to the ground state. In neutron absorption reactions, the neutron is captured by the nucleus forming a heavier nucleus which, if unstable, decays into other particles.

The probability of a given neutron interaction (also known as the cross section) varies drastically with respect to the incident neutron energy. For example, neutron absorption cross sections for nuclides commonly used for neutron detectors are presented in Figure 1.

As shown in Figure 1, the neutron absorption cross section decreases rapidly with increasing incident neutron energy. Therefore, detectors utilizing neutron absorption as the detection mechanism are better suited for the detection of lower energy (or "slow") neutrons. Neutron detection systems utilizing these absorption reactions are normally encased in a moderator (usually polyethylene) in order to slow-down (thermalize) the neutrons and maximize the absorption probability. As incident neutron energy increases, neutrons may also be detected from their elastic scattering with light nuclei. This is accomplished by detection of the charged recoil nucleus generated from this collision. Further discussion of these detection mechanisms and their use for DNDO applications is presented in the following sub-sections. Detection systems are organized by the type of nuclear reaction employed for detection.

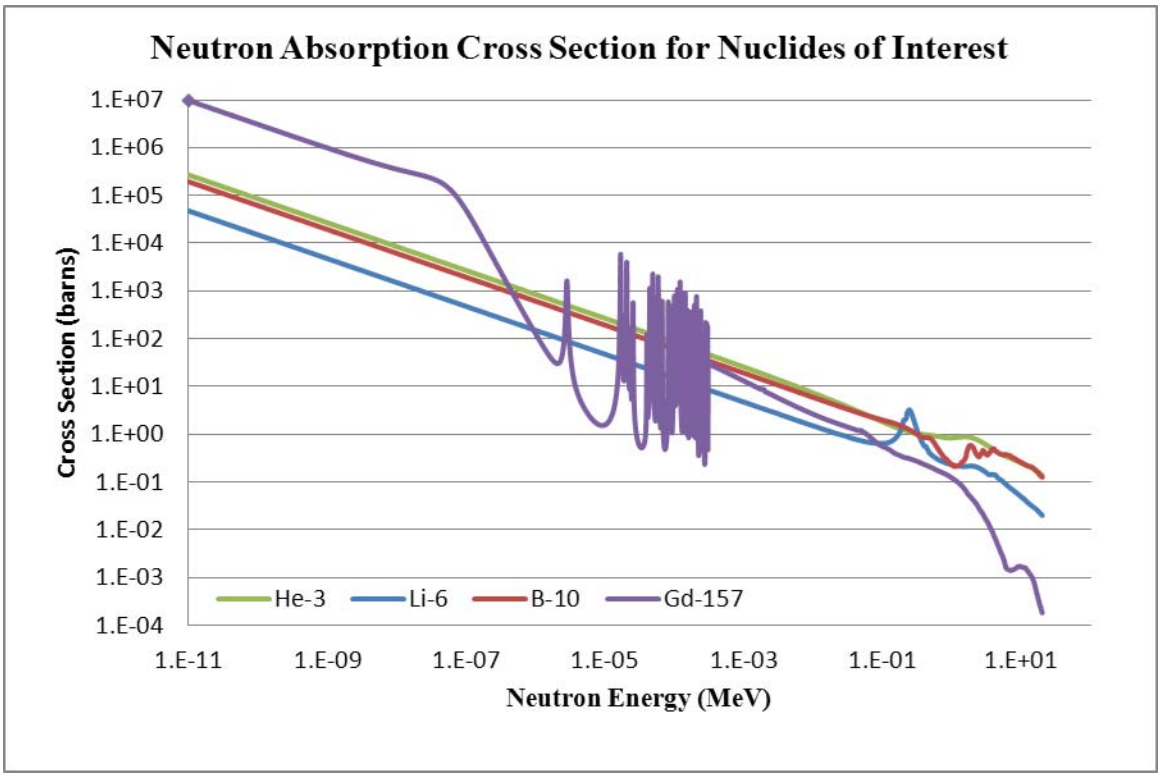

Figure 1. ENDFB/6.1 Absorption Cross Section vs. Energy for Reactions of Interest (Source: Korea Atomic Energy Research Institute, 2000 [6])

2.2.1.1 Neutron Detection by the ^{3}He(n,p) Reaction

Neutron detection by ^{3}He is based on the following exothermic reaction:

$$^{3}_{2}\mathrm{He}+^{1}_{0}n \rightarrow ^{1}_{1}\mathrm{p}+^{3}_{1}\mathrm{H}+765\mathrm{keV}$$

For reactions induced by thermal neutrons, the oppositely directed reaction product energies are 573 keV for the proton and 191 keV for the triton. As shown in Figure 1, ^{3}He has a very large thermal neutron (0.025 eV) capture cross section of ~5400 barns [7]. As shown in Figure 2, the potential exists for large neutron detection efficiencies, especially given the fact that this efficiency can be significantly increased with the ability to increase the ^{3}He gas pressure [8]. However, as the pressure of ^{3}He within the detector increases, so does the system's cost. Another significant advantage of ^{3}He counters is their negligible response to gamma rays in relatively low gamma radiation fields (pile-up effects only become an issue in fields which exceed ~ 1 R/hr) which results in excellent neutron/gamma discrimination [9]. Currently deployed ^{3}He-

based neutron detectors have achieved neutron to photon discrimination abilities of ~$1x10^{-7}$ at an exposure rate of 10 mR/hr [2].

Due to the potential for highly efficient neutron detection, durability, discrimination capabilities, as well as the limited degradation over time, ^{3}He counters are widely used for DNDO applications in personal radiation detectors, man-portable detectors, and radiation portal monitors [3].

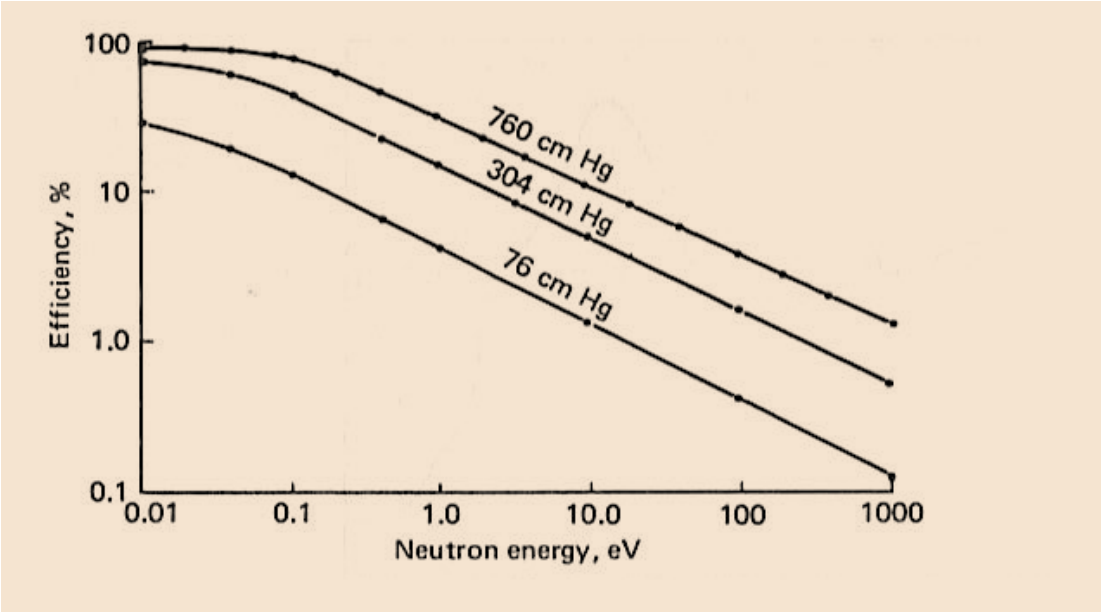

Figure 2. Efficiency of ^{3}He Proportional Counter (Source: Tsoulfanidis, 1995 [8])

2.2.1.2 Neutron Detection by the ^{6}Li(n,α) Reaction

Neutron detection by ^{6}Li is based on the following exothermic reaction:

$$^{6}\mathrm{Li}+{}^{1}_{0}n \rightarrow {}^{4}_{2}\mathrm{He}+{}^{3}_{1}\mathrm{H}+4.78\ \mathrm{MeV}$$

As seen in Figure 1, the ^{6}Li neutron capture cross section is significantly lower than that of ^{157}Gd, ^{3}He, or ^{10}B for most neutron energies. However, this weakness is somewhat offset by the relatively large Q-value of 4.78 MeV which aids in neutron discrimination utilizing pulse height discrimination (PHD). For reactions induced by thermal neutrons, the oppositely directed reaction product energies are 2.73 MeV for the triton and 2.05 MeV for the alpha. Detectors based on the ^{6}Li neutron absorption currently being used in DHS applications include LiI glass detectors in personal radiation detectors and Li loaded glass fibers in man-portable detectors [1]. Additionally, as presented in Section 2.3.2, several of the proposed alternative ^{3}He detector designs also utilize the ^{6}Li isotope.

2.2.1.3 Neutron Detection by the ^{10}B(n,α) Reaction

Neutron detection by ^{10}B is based on the following exothermic reaction:

$$^{10}B + {}^{1}_{0}n \rightarrow \begin{cases} {}^{7}_{3}Li + {}^{4}_{2}He + 2.792\ MeV\ \ (6\%) \\ {}^{7}_{3}Li^{*} + {}^{4}_{2}He + 2.310\ MeV\ (94\%) \end{cases}$$

With thermal neutrons, about 94% of the ^{10}B absorptions lead to an excited state (^{7}Li*), while the other 6% lead directly to the ground state (^{7}Li). In the case of the excited nucleus (^{7}Li*), a photon is promptly emitted with an energy of 0.478 MeV which results in a stable ^{7}Li nucleus. Coincidence counting of this gamma could be used as a discrimination technique to identify the neutrons. For reactions induced by thermal neutrons, the oppositely directed reaction product energies are:

$$E_{Li}=1.01\ \mathrm{MeV}\ \mathrm{and}\ E_{\alpha}=1.78\ \mathrm{MeV}\ \ (\mathrm{Ground\ State\ -\ 6\%})$$

$$E_{Li}=0.84\ \mathrm{MeV}\ \mathrm{and}\ E_{\alpha}=1.47\ \mathrm{MeV}\ \ (\mathrm{Excited\ State\ -\ 94\%})$$

While ^{10}B-based neutron detectors are not currently utilized for widespread DNDO applications, several of the proposed alternative neutron detector designs discussed in Section 2.3 are based on this reaction.

2.2.1.4 Neutron Detection by the ^{157}Gd(n,α) Reaction

Neutron detection by ^{157}Gd is based on the following exothermic reaction:

$$^{157}\mathrm{Gd} + {}^{1}_{0}n \rightarrow {}^{158}Gd^{*} + 7.94\ MeV$$

Gadolinium neutron capture reactions release an assortment of prompt reaction products including gamma rays, internal conversion electrons, X-rays and Auger electrons. While ^{157}Gd has the largest thermal neutron cross section of all the stable isotopes at ~255,000 barns, detectors based upon this reaction have limited value in DNDO applications due to the low energy of the reaction products (which subsequently makes neutron/photon discrimination difficult). Subsequently, no detectors based on the ^{157}Gd reaction are currently used or identified as proposed alternative candidate detectors for DNDO applications.

2.2.1.5 Neutron Detection by Proton Recoil

In this interaction, the incident neutron transfers a portion of its kinetic energy to the scattering nucleus, resulting in a charged recoil nucleus which can then be detected. Since neutrons and protons have approximately the same mass, it is possible that the neutron may transfer all of its kinetic energy to the proton in one collision; therefore, hydrogen is almost exclusively used as the scattering nucleus. Additionally, since this reaction has a Q-value of zero, incoming neutron energies may be determined. Due to the presence of gamma rays or other low energy background, detection (and subsequent discrimination) of neutrons by proton recoil is only feasible for neutrons with energies above ~ 1 keV. Therefore, this type of detector is not well suited (and not currently utilized) for DNDO applications.

2.2.2 PHOTON INTERACTIONS AND TRANSPORT

While the detectors discussed here are intended for neutron detection, most neutron detectors are also gamma ray detectors. Like neutrons, photons have no charge and do not ionize directly. However, photons can transfer their energy to charged electrons. In scintillation detectors, these electrons can then cause scintillations which

are used to detect neutrons. These effects can lead to neutron/photon discrimination difficulties. There are three main processes in which photons can transfer energy to electrons: the photoelectric effect; Compton scattering; and pair production. Determining which of these processes occurs depends both on the energy of the incident radiation as well as the composition of the absorbing medium. The relative importance of these three processes is presented in Figure 3.

In the photoelectric process, a photon interacts with a whole atom, is completely absorbed, and the atom then ejects an electron (called a photoelectron). Compton scattering occurs when a photon has an inelastic collision with a free or loosely bound electron which is at rest. As a result of this collision, the incident photon has a reduced energy and the electron recoils from the atom with a transferred energy ranging from zero to a large fraction of the incident gamma rays initial energy. Pair production refers to the creation of an electron-positron pair from a photon. This conversion is only possible if the photon energy exceeds the rest masses of two electrons (1.02 MeV). Due to the energy required for this process, pair production is not of major importance in neutron detection.

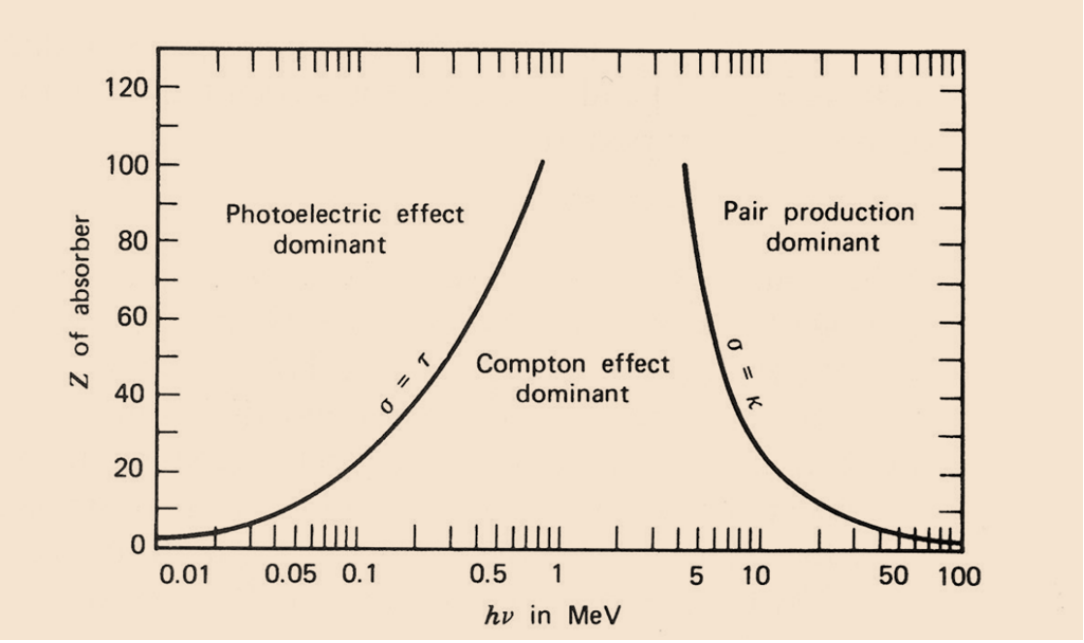

Figure 3. Relative Importance of Photon Interactions (Source: Knoll, 2000 [7])

2.2.3 CHARGED PARTICLE INTERACTIONS AND TRANSPORT

The charged particles discussed in this section are intended to include the light ions (electrons, protons, tritons, and alphas) generated from the neutron capture or proton recoil reactions discussed in Section 2.2.1. Coulomb interactions (electrostatic repulsion between charges) account for the vast majority of the energy loss experienced by charged particles. However, they may also lose energy by emission of electromagnetic radiation (Bremsstrahlung or Cerenkov) or by nuclear reactions [8]. The following two sub-sections provide an overview of the energy loss mechanisms for heavy charged particles and electrons, respectively.

2.2.3.1 Heavy Charged Particle Interactions and Transport

Due to the electric charge carried by heavy charged particles (such as protons, tritons, and alphas), they continuously interact through the electrostatic repulsion force (i.e., Coulomb force) with multiple orbital electrons present in the medium in which they travel. The result of these interactions is the transfer of a small portion of the charged particle's energy to each of the electrons, with the amount of energy transferred being dependent on the distance between the particles. Depending on the amount of energy transferred, an electron may either be excited or ionized. Excitation occurs when the electron gains enough energy to move to a higher energy orbital shell within the absorber atom. Ionization occurs when the electron gains enough energy (known as the ionization energy) to be removed from the absorber atom and become a free particle, leaving the residual atom (which was formerly neutral) with a net positive charge.

The average energy loss per unit path length (–dE/dx) experienced by a charged particle within a medium is referred to as the stopping power of that medium. The classical expression for the stopping power of heavy charged particles derived by Bethe is:

$$S\left(\frac{MeV}{m}\right) = -\frac{dE}{dx} = \frac{4\pi e^4 z^2}{m_o v^2} NZ \left[ln\frac{2m_o v^2}{I} - ln\left(1 - \frac{v^2}{c^2}\right) - \frac{v^2}{c^2} \right] \qquad 2.2\text{-}1$$

Where: ze and v are the electric charge and velocity of the particle, respectively; N and Z are the number density and atomic number of the absorbing medium, respectively; c is

the speed at which light travels in a vacuum; m_o is the electron mass; and I represents the average excitation and ionization potential (or ionization energy) [7]. The stopping power for different mediums depends primarily on NZ, which represents the medium's electron density. The stopping power of a material for different charged particles with the same velocity varies as the square of the charge, so that the stopping power for an alpha particle is four times as great as that for a proton moving with the same velocity. Stopping powers in air for several particles is presented graphically in Figure 4 over a range of particle energies.

The range of a charged particle is defined as the average distance traversed by a particle (without relation to direction) in a medium [10]. Due to the difference in charge (and subsequently in stopping power), the range of an alpha particle is much less than the range of a proton of the same initial energy in the same medium. This effect is shown in Figure 5, which presents the range (in cm) of electrons, protons, and alpha particles in air at standard temperature and pressure (STP).

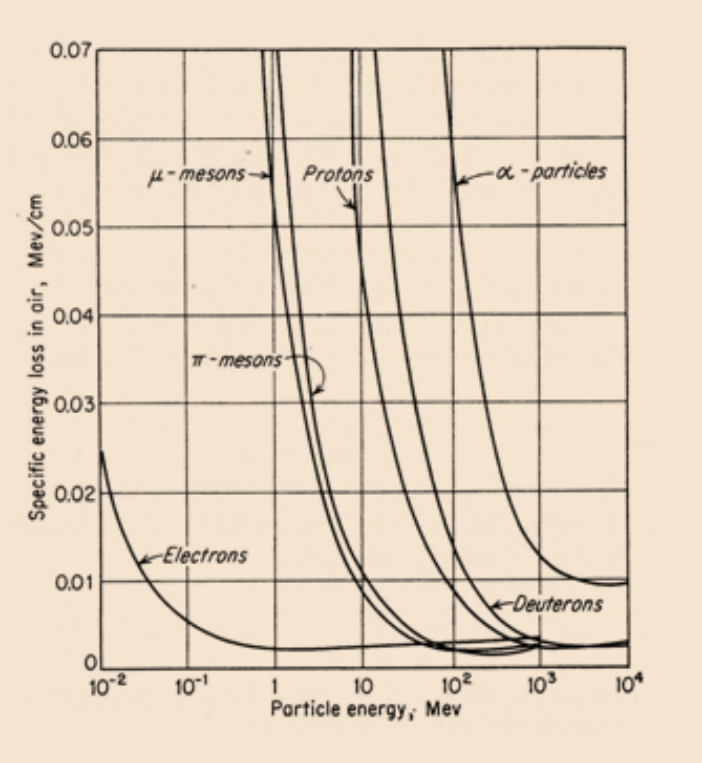

Figure 4. Stopping Power in Air for Charged Particles (Source: Knoll, 2000 [7])

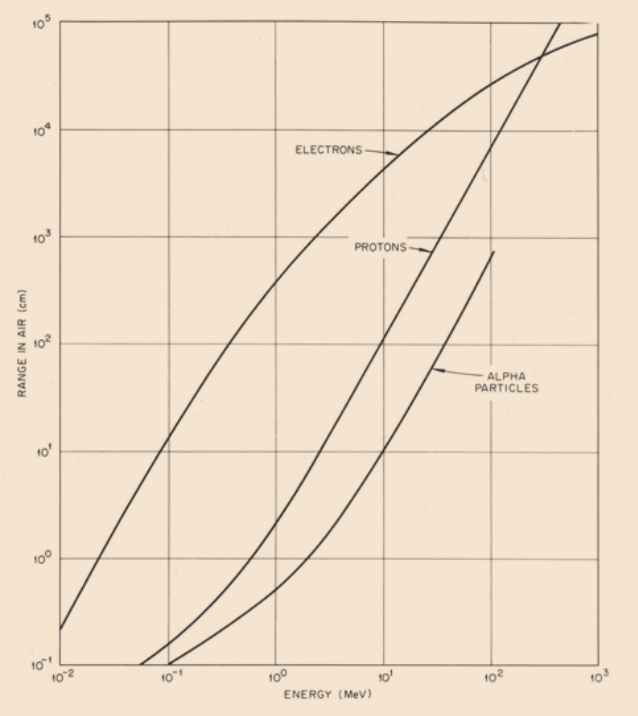

Figure 5. Range of Electrons, Protons, and Alpha Particles in Air at STP (in cm) (Source: Turner, 1995 [11])

2.2.3.2 Electron Interactions and Transport

The passage of electrons through matter is similar to heavy charged particles in that electrons can excite and ionize atoms. However, due to the mass of the travelling electron being equal to the atomic electrons, the effects of elastic scattering are considerable. Electron-nuclei interactions may also occur. These elastic interactions may result in large deflection angles as well as large energy losses in a single collision. Therefore, whereas a heavy charged particle may move through the electron cloud in a practically straight line, the electron pursues a random torturous path. Electrons may also lose energy by emission of electromagnetic radiation (Bremsstrahlung or Cerenkov), but these effects only becomes important at the higher energies (>10 MeV) [12]. The classical expression for the stopping power for electrons due to ionization and excitation (neglecting radiative processes) derived by Bethe is:

$$-\frac{dE}{dx}=\frac{2\pi e^4 NZ}{m_o v^2}\left[ln\frac{m_o v^2 E}{2I^2(1-(v/c)^2)}-(ln(2))\left(2\sqrt{1-(v/c)^2}-1+(v/c)^2\right)+(1-(v/c)^2)+\frac{1}{8}\left(1-\sqrt{1-(v/c)^2}\right)^2\right] \quad 2.2\text{-}2$$

The symbols for Equation 2.2-2 are the same as those utilized in Equation 2.2-1 [7]. As shown in Figure 5, the range of electrons is much greater than those of heavy charged particles for a given energy due to the electrons losing their energy at a lower rate (see relative stopping powers in Figure 4).

2.2.4 SCINTILLATION DETECTORS

Scintillators are materials (known as phosphors) which possess the property of luminescence. Ionizing radiation causes electronic transitions to short-lived excited states in luminescent materials. These excited states decay back to the ground state by emitting scintillation light in the visible part of the electromagnetic spectrum. A scintillation detector can be obtained by coupling either a photomultiplier tube (PMT) or a photodiode to a scintillator, thus allowing the scintillation light to be collected and counted.

Two main categories (each containing a wide range of materials) of scintillators exist: organic and inorganic, with the luminescence mechanism differing between the two. Selecting the appropriate scintillator depends upon the intended application. For detection of thermal neutrons, the scintillator must be doped with elements with high neutron absorption cross sections such as ^{6}Li or ^{10}B (which were discussed in detail in Section 2.2.1). Neutron detection relies upon the detection of the ionizing radiation produced by these neutron absorptions. Fast neutron detection in scintillators is achieved through the detection of recoil protons, so the scintillator should be rich in hydrogen content. For this reason, organics are generally preferred for neutron scintillation detectors due to having a lower Z number and density.

2.2.4.1 Light Yield Response of Scintillators

A relatively small fraction of the ionization energy lost by a charged particle goes into exciting molecules, while the remainder of the kinetic energy is dissipated non-radiatively by either heat or increasing lattice vibrations [7]. The fraction of ionization energy converted to fluorescent light energy, the scintillation efficiency, is of great significance as the degree of the n/γ discrimination from PHD improves with increasing light output. The scintillation efficiency differs for each type of scintillator and also

depends on the type of charged particle producing the ionization. For inorganic scintillators, the amount of light output is nearly proportional to the amount of energy deposited by the charged particle. However, for organic scintillators, while the response to electrons is linear for particle energies above ~ 125 keV, the response to heavier particles is nonlinear up to much higher energies [7]. This non-linearity effect is often referred to as the scintillator's light yield non-proportionality. Figure 6 shows the relative light yield with respect to the energy deposited for several charged particles in anthracene (a common organic scintillator).

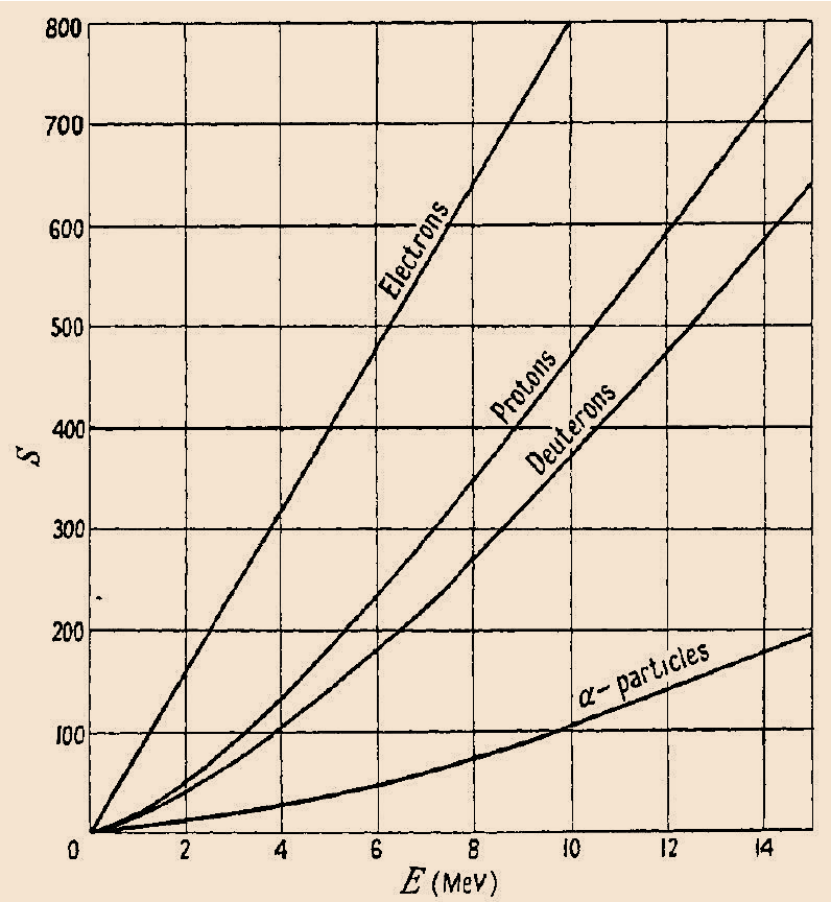

Figure 6. Relative Light Yield vs. Energy Deposited (Source: Birks, 1951 [13])

The light yield non-proportionality may be explained by noting that as the stopping power increases, more molecules get excited per unit path length of the charged particle, thus more light is output. However, eventually this response becomes asymptotic since the scintillator has a finite number of molecules that can be excited. This indicates that there is a value of stopping power at which all available molecules will have been excited. A scintillator in this state is said to have reached a point of saturation. At this point, delivering more energy will not yield more scintillation light. Therefore, due to the stopping power of an electron being less than an alpha particle of equal energy, the electron will generate significantly more light output than the alpha when traversing through a scintillator. This relationship between light yield for a scintillator and the energy deposited by ionizing particles is expressed as Birks Saturation Law, and is mathematically represented by Birks formula as shown in Equation 2.2-3 [13].

$$\frac{dL}{dx} = \frac{S\left(\frac{dE}{dx}\right)}{1 + kB\left(\frac{dE}{dx}\right)} \qquad 2.2\text{-}3$$

The left hand side of the Birks formula represents the fluorescent light energy (L) emitted per unit path length of the charged particle track. The S is the scintillation efficiency as defined earlier in this section, and dE/dx is the stopping power ($MeV\ cm^2\ g^{-1}$) of the ionizing particle. The term k is a quenching or saturation parameter, while B is the Birks constant. In practice, the term kB is taken as a single adjustable parameter with units of $g\ cm^{-2}\ MeV^{-1}$, and is determined empirically for a specific scintillator and charged particle with S giving the absolute normalization to fit measured data. The saturation effect expressed as Birks Law is presented graphically in Figure 7. Based on extensive analysis on a number of organic scintillators, Craun and Smith recommended the use of an extended version of the Birks equation developed by Chou which contained an additional adjustable parameter C with units of $g^2\ cm^{-4}\ MeV^{-2}$, which provided a better fit to experimental measurements [14]. The two-parameter Birks/Chou formula is given below:

$$\frac{dL}{dx} = S\left(\frac{dE}{dx}\right)\left[1 + kB\left(\frac{dE}{dx}\right) + C\left(\frac{dE}{dx}\right)^2\right]^{-1} \qquad 2.2\text{-}4$$

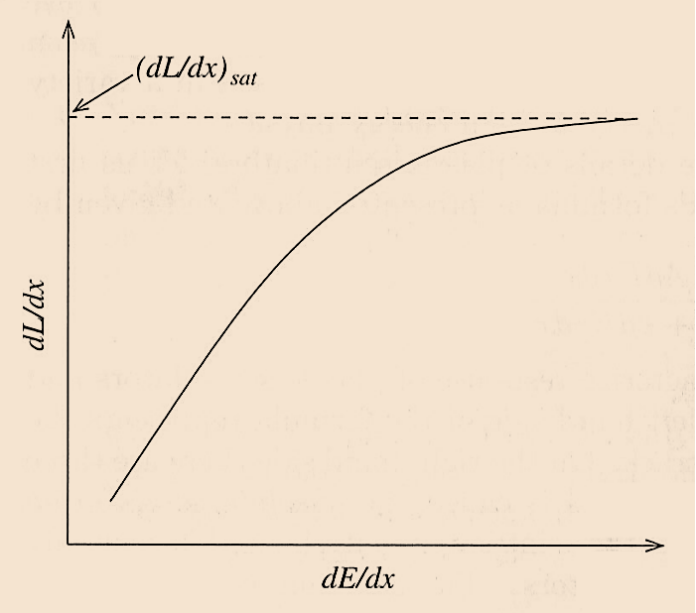

Figure 7. Birks Saturation Law
(Source: Ahmed, 2007 [12])

By assuming that the scintillation efficiency, *S*, is independent of the stopping power, Equation 2.2-4 can be written as [15]:

$$\frac{dL}{dE} = S\left[1 + kB\left(\frac{dE}{dx}\right) + C\left(\frac{dE}{dx}\right)^2\right]^{-1} \qquad 2.2\text{-}5$$

Rewriting Equation 2.2-5 in terms of the light output, *dL*, results in:

$$dL = dE * S\left[1 + kB\left(\frac{dE}{dx}\right) + C\left(\frac{dE}{dx}\right)^2\right]^{-1} \qquad 2.2\text{-}6$$

The amount of light output, *dL*, is commonly presented in terms of electron equivalent energy or (MeVee). This is necessary due to the dependence of light yield in organics on the type of particle depositing energy in the scintillating medium. Expressing the light output in terms of MeVee allows representation of the light yield on an absolute basis for easier interpretation of results.

2.3 DNDO ALTERNATIVE NEUTRON DETECTOR CRITERIA AND TECHNOLOGIES

As mentioned previously, the dominant type of neutron detector for DHS applications is the ^{3}He gas proportional counter. However, due to the imminent ^{3}He shortage, a replacement type of detector with similar capabilities is required. DNDO has been aware of this upcoming shortage for some time, and in 2009 a comprehensive review of possible alternatives was completed [2]. Due to the volume of ^{3}He required for Radiation Portal Monitors (RPMs), this review focused on alternative neutron detectors to ^{3}He for RPM applications. While several potential alternative neutron detection technologies were identified, none of the systems have thus far proven to have the appropriate capabilities to match the current ^{3}He-based systems. Summaries of the requirements that a replacement detector must satisfy and the existing alternative designs identified from the comprehensive review are provided in Sections 2.3.1 and 2.3.2, respectively.

2.3.1 REPLACMENT DETECTOR REQUIREMENTS

In order to preserve the same detection and operational capabilities of the ^{3}He-based RPM systems, an acceptable alternative neutron detector's capabilities must meet or exceed those of the currently deployed systems. Table 1 presents the functional specifications outlined by DNDO for current RPMs.

Table 1. Functional Specifications for Current RPM Neutron Detection Capability

Parameter	Specification
Absolute neutron detection efficiency	$\epsilon_{abs\ n} \geq 1.2 \times 10^{-3}$ (or 2.5 cps/ng of ^{252}Cf in the DNDO specified test configuration) [2]
Intrinsic gamma-neutron detection efficiency	$\epsilon_{int\ \gamma n} \leq 10^{-6}$ [16]
Gamma absolute rejection ratio for neutrons (GARRn)	$0.9 \leq$ GARRn ≤ 1.1 at 10 mR/h exposure [16]
Cost	~$30,000 per system [2]

The absolute neutron detection efficiency ($\varepsilon_{abs,n}$) is defined as the number of neutron pulses recorded divided by the number of neutrons emitted by the source (with only a neutron source present) as shown in Equation 2.3-1 [2].

$$\varepsilon_{abs,n} = \frac{Number\ of neutron\ pulses\ recorded}{Number\ of\ neutrons\ emitted\ from\ source} \quad 2.3\text{-}1$$

DNDO guidelines state that a ^{252}Cf source is to be used for the determination of the absolute neutron detection efficiency [2]. While ^{252}Cf also emits photons, the photon flux incident upon a candidate detector from the DNDO specified ^{252}Cf source configuration is negligible due to the requirement for 0.5 cm of lead shielding surrounding the source [17]. The intrinsic gamma-neutron detection efficiency ($\varepsilon_{int,\gamma n}$) is defined as the number of neutron pulses detected divided by the number of photons striking the detector, thus measuring the response of a neutron detector to the presence of a gamma ray field when no neutron source is present as shown in Equation 2.3-2 [16].

$$\varepsilon_{int,\gamma n} = \frac{Number\ of\ photons\ that\ produce\ neutron\ counts}{Number\ of\ photons\ incident\ upon\ the\ detector} \quad 2.3\text{-}2$$

Per PNNL-14716, the intrinsic gamma-neutron detection efficiency is to be measured using either a ^{192}Ir or ^{60}Co source placed at an appropriate distance so as to produce an exposure rate of 10 mR/hour at the detector [31]. The gamma absolute rejection ratio for neutrons (GARRn) is a parameter defined by Pacific Northwestern National Laboratory (PNNL) which measures the detector response in the presence of both a large gamma ray source and a ^{252}Cf neutron source (configured as it would be for an absolute efficiency measurement). The GARRn is defined as the absolute neutron detection efficiency in the presence of both sources ($\varepsilon_{abs,\gamma,n}$), divided by the absolute neutron detection efficiency of the neutron detector in the presence of only the neutron source as shown in Equation 2.3-3.

$$GARRn = \frac{\varepsilon_{abs,\gamma,n}}{\varepsilon_{abs,n}} \quad 2.3\text{-}3$$

The GARRn would be equal to 1 if the gamma ray source had no impact. As an example of the calculation of the performance criteria here, consider the following measured results and calculated performance parameters for a hypothetical ^{3}He-based RPM system. The detector registered 2.82 counts per second from a 1 nano-gram ^{252}Cf source in the DNDO specified configuration (no photon source present). From Martin

and Kos, a pure ^{252}Cf source emits ~2,314 neutrons per second [29]. Therefore, using Equation 2.3-1, the absolute neutron detection efficiency is:

$$\varepsilon_{abs,n} = \frac{2.82\ neutron\ pulses\ per\ second}{2{,}314\ neutrons\ from\ source\ per\ second} = 1.22E-3$$

Using a ^{60}Co source at an exposure rate of 10 mR/hr (and no neutron source), the detector registered 1.95 counts per second. At this exposure rate and distance from the detector, say that the ^{60}Co source emits 1.12E9 photons per second isotropically, and that due to the solid angle subtended by the detector to the source only 1.7% of the source photons are incident upon the detector. The intrinsic gamma-neutron detection efficiency is then calculated using Equation 2.3-2 as:

$$\varepsilon_{int,\gamma n} = \frac{1.95\ \ photons\ producing\ neutron\ counts\ per\ second}{(0.017)(1.12E9)\ photons\ incident\ upon\ the\ detector\ per\ sec} = 1.02E-7$$

Finally, the absolute gamma-neutron detection efficiency is calculated to be 1.19E-3 using Equation 2.3-1 with both the ^{252}Cf and ^{60}Co sources present in the same configuration as the previous measurements. The gamma absolute rejection ratio for neutrons is then calculated using Equation 2.3-3 as:

$$GARRn = \frac{\varepsilon_{abs,\gamma,n}}{\varepsilon_{abs,n}} = \frac{1.19E-3}{1.22E-3} = 0.98$$

These results show that the hypothetical ^{3}He-based RPM system tube meets all three criteria for an acceptable neutron detector as defined in this document. Additional details regarding these parameters and the methodology used to calculate them are presented in Sections 3.3 and 3.5.

2.3.2 EXISTING ALTERNATIVE NEUTRON DETECTOR DESIGNS

PNNL analysts performed a comprehensive review of existing detectors which could be potential replacement candidates for ^{3}He-based neutron detectors for DHS applications in June of 2009 [2]. Promising candidate designs include BF_3 gas-filled tubes, boron-lined proportional counters, glass and plastic neutron-sensitive scintillating fiber detectors, and detectors composed of non-scintillating fibers coated with scintillating and neutron-absorbing materials. Table 2 provides a summary and comparison of the performance of the candidate designs relative to that of the currently deployed ^{3}He-based RPM systems.

While the non-scintillating plastic fiber detectors from IAT provide neutron sensitivity and discrimination ability comparable to ^{3}He tubes, these detectors have not yet been produced in large sizes such as are needed in an RPM and their current cost is very high [2]. Subsequently, as shown in Table 2, the PNNL report concluded that none of the identified candidate designs can currently demonstrate capabilities equal to those of ^{3}He counters. Therefore, either these designs must be further tested and optimized, or new detection systems must be developed.

2.4 MULTIVARIATE STATISTICAL ANALYSIS

Due to the many parameters which affect detector performance, an elegant optimization methodology is required. The optimization methodology utilized in this research applies three statistical strategies to the results generated from MCNPX calculations, in a sequential manner (namely factorial design analysis, response surface methodology, and constrained multivariate optimization). These statistical strategies are described in the following subsections. The statistical analysis of MCNPX results discussed in this section is performed using the Statistical Analysis Software (SAS), Version 9.2, code. The SAS software package includes features such as statistical analysis of variance, regression, multivariate analysis, and visualization techniques which were utilized in this research [18]. Examples of SAS input files generated as a part of this research are included in Appendix C.

Table 2. ^{3}He Replacement Design Candidate Summary (Source: Van Ginhoven et al, 2009 [2])

Detector	Relative absolute neutron detection efficiency	Relative intrinsic gamma-neutron detection efficiency	Vendor	Cost
^{3}He tubes	1	1	LND Inc., Reuter Stokes	Increasing
BF_3 tubes	~0.2-0.5	>1	LND Inc.	Low
B lined tubes	~0.14	1	LND Inc., Reuter Stokes	Low
Li Glass Fiber	1	~0.1	NucSafe, Inc.	Medium
Non-Scintillating Plastic Fiber	~1	1	Innovative American Technologies (IAT)	High

2.4.1 FACTORIAL DESIGN ANALYSIS

Factorial design of experiments (DOE) with two-level factors (independent variables) are widely used because they are easy to design, efficient to run, straightforward to analyze, and full of information. Therefore, two-level factorial DOE are very useful as screening tools to determine the few vital features (usually main effects and two factor interactions) that significantly affect each of the detector response parameters. A main effect is an outcome that can show consistent difference between the levels of a factor. Interaction effects exist when some independent variable has different effects on some dependent variable as a function of some other independent variable (i.e., when differences on one factor depend on the level of other factor). The two levels of the factor are usually taken to be high and low values for the independent parameter and are normally coded as +1 and -1, respectively.

A full factorial design involves all possible combinations of factors and levels (known as treatment combinations), with the number of combinations growing rapidly as the number of factors increases. Thus, if there are k factors, with two levels for each factor, the full factorial design consists of: $2 \times 2 \times \ldots \times 2 = 2^k$ treatment combinations. It follows that full factorial experiments can be unwieldy if the system contains many factors. Fractional factorial designs are better suited for a system containing five or more factors. A fractional factorial design uses only a portion (fraction) of the experimental runs required for a full factorial design. The fraction of experimental runs are chosen to expose information about the most important features (usually main effects and two-factor interactions) of the problem while assuming that higher order interactions have no distinguishable effects on the response. Multiple linear regression is performed on the results of the factorial analysis to construct two-factor interaction models for the 2^k factorial. The two-factor interaction model may be written as:

$$y = \beta_0 + \sum_{j=1}^{k} \beta_j x_j + \sum_{i=1}^{k-1} \sum_{j=i+1}^{k} \beta_{i*j} x_i x_j + \epsilon \qquad 2.4\text{-}1$$

Where y is an observation value of a response variable at the treatment combination, β values are regression coefficients which are calculated using least squares regression such that the sum of the squared residuals is minimized, x values are treatment combinations ($x_i x_j$ is the product of levels for factors x_i and x_j) , and ϵ is a error term [19].

To test whether or not an effect or interaction is significant, analysis of variance (ANOVA) is performed. The first step in ANOVA is the calculation of the sum of squares (SS) and the degrees of freedom (DF). For example, suppose one fits a least squares regression model to the results of a 2^2 factorial analysis of effects A and B. The total sum of squares (SS_T) is a measure of the total variation in the whole data set and is a combination of the sum of squares associated with the main effect of A (SS_A), the main effect of B (SS_B), the interaction between the two effects A and B (SS_{AB}), and the variability due to error ($SS\epsilon$) as shown below:

$$SS_T = SS_A + SS_B + SS_{AB} + SS_\epsilon \qquad 2.4\text{-}2$$

Which can be written in statistical notation as:

$$SS_T = \sum_{i=1}^{a}\sum_{j=1}^{b}\sum_{k=1}^{n}\left(y_{ijk} - \bar{y}\right)^2$$

$$= bn\sum_{i=1}^{a}(\bar{y}_i - \bar{y})^2 + an\sum_{j=1}^{b}\left(\bar{y}_j - \bar{y}\right)^2 \qquad 2.4\text{-}3$$

$$+ n\sum_{i=1}^{a}\sum_{j=1}^{b}\left(\bar{y}_{ij} - \bar{y}_i - \bar{y}_j + \bar{y}\right)^2 + \sum_{i=1}^{a}\sum_{j=1}^{b}\sum_{k=1}^{n}\left(y_{ijk} - \bar{y}_{ij}\right)^2$$

Where a is the number of levels of factor A, b is the number of levels of factor B, n is the number of replicate experimental observations, $\bar{y}_i$ is the sample mean of the i^{th} group, and $\bar{y}$ is the overall mean of the data [19]. The number of degrees of freedom associated with each sum of squares is presented in Table 3.

Table 3. Degrees of Freedom for Two-Factor Factorial Design

Effect	Degrees of Freedom
A	a-1
B	b-1
AB interaction	(a-1)(b-1)
Error	ab(n-1)
Total	abn-1

The sum of squares and the degrees of freedom are used to calculate the means squares by dividing sums of squares by their degrees of freedom. In ANOVA, mean squares are used in the F-test to see if the corresponding effect is statistically significant. The F-test tests the hypothesis that the means of several normally distributed populations, all having the same standard deviation, are equal. This is accomplished by comparing the calculated F_0 value to F-critical values from a table with the appropriate degrees of freedom. The F_0 value is calculated by dividing the mean square of the factor of interest by the mean square of the error. If the calculated F_0 is larger than the F-critical value, then the null hypothesis that the means are equal would be rejected with the conclusion that the corresponding effect is statistically significant [20].

The results of the factorial design are sufficient to determine which explanatory variables have an impact on the response variable(s) of interest. The explanatory variables which are identified as non-significant can then be screened out and omitted from the more robust analysis discussed in the following section.

2.4.2 RESPONSE SURFACE METHODOLOGY

Once it is suspected that only statistically significant explanatory variables are left, a more robust design can be implemented to estimate a second-degree polynomial model of each response. The quadratic models of the responses can then be used to achieve a quantitative understanding of the detector's behavior over the range of factors analyzed. This method of developing second-order models to explore the relationships between the explanatory and response variables and their subsequent use to optimize the system is referred to response surface methodology (RSM). The quadratic models are generated by performing multiple least squares regression on the response data to fit an equation which minimizes the sum of the squares of the residuals made in solving every equation (where a residual is the difference between an observed value and the value predicted by the model).

The most popular second order design is the central composite design (CCD). The CCD matrix contains the embedded factorial design matrix (with two levels coded as +1 and -1) and is augmented with center points (coded as 0) and a group of axial points

known as star points at coded levels of +α and -α. Figure 8 shows a schematic of how a central composite design for two factors is constructed.

The value of α depends on certain properties desired for the design and the number of factors involved. A central composite design is said to be rotatable if the variance of any predicted value of the response depends only on the distance of the point from the center of the design, and is not a function of the axis or direction from the point to the center. In other words, all points at the same radial distance from the center point have the same magnitude of prediction error. To maintain rotatability, the value of α depends on the number of experimental runs in the factorial portion of the central composite design, and can be calculated using Equation 2.4-4 [21]:

$$\alpha = (number\ of\ design\ cases)^{1/4} \qquad 2.4\text{-}4$$

If the design is a full design (not a fractional design), then α can be calculated using Equation 2.4-5 [21].

$$\alpha = (2^k)^{1/4} \qquad 2.4\text{-}5$$

Where k is the number of factors being studied. Multiple linear regression is performed on the results of the CCD analysis to construct the second-order model. The second-order model has the following form:

$$y = \beta_0 + \sum_{i=1}^{k} \beta_i x_i + \sum_{i=1}^{k-1} \sum_{j=i+1}^{k} \beta_{i*j} x_i x_j + \sum_{i=1}^{k} \beta_{ii} x_{i\ i}^2 + \epsilon \qquad 2.4\text{-}6$$

The symbols for Equation 12 are the same as those in Equation 2.4-1, and least squares regression is again used to calculate the regression coefficients such that the sum of the squared residuals is minimized.

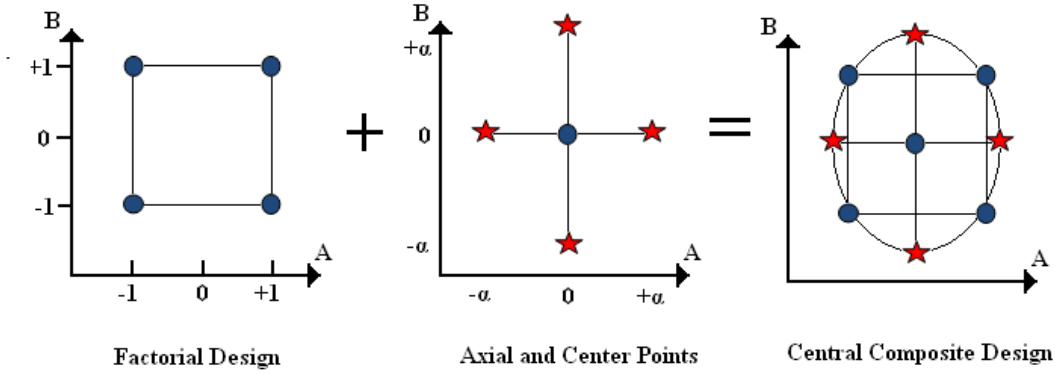

Figure 8. Central Composite Design for Two Factors

2.4.3 CONSTRAINED MULTIVARIATE OPTIMIZATION

As outlined in Table 1, multiple response parameters measure the overall performance of the neutron detection system. Simultaneous consideration of multiple responses involves first building an appropriate response surface model for each response (which was accomplished by the CCD analysis described in Section 2.4.2) and then determining a set of operating conditions that in some sense optimizes all responses (or at least keeps them in desired ranges). The approach used for this research is known as constrained optimization where the response parameters from Table 1 are held to the constraints outlined by DNDO. This analysis is performed by SAS after generating the response surface models from the CCD analysis, using the limits from Table 1 as the optimization constraints.

2.5 RESEARCH BY OTHERS

The use of Monte Carlo radiation transport codes to simulate neutron detector performance is common, with publications existing for both MCNPX and Geant4 [22,23]. Factorial design experiments are widely used to identify statistically significant factors on a response due to the ease of design and the amount of information which they produce. Response surface methodology is often used to optimize the response variables using the quadric model for the response variables from the CCD. The investigation of the use of factorial designs paired with RSM and a constrained multivariate optimization as a toolkit for optimizing neutron detector's parameters with respect to multiple performance measures is significantly novel; that is, no equivalent work has been published. Examples of research performed by others for both single detector parameter optimization using Monte Carlo codes and response optimization by factorial designs and response surface methodology on non-nuclear systems are further discussed in the following paragraphs.

Monte Carlo radiation transport code simulations have been successfully utilized to optimize a single parameter with respect to detector efficiency. Dingley et al [24] used the Geant4 toolkit to optimize the dimensions of sub-micron structures within a ^{10}B based neutron detector to maximize detector efficiency. In this analysis, four different detector configurations were analyzed (a parallel-trench design, a pillar-type design, and two

etched hole-type designs) with one detector parameter studied for each configuration. Childress and Miller [25] used MCNP to optimize the thickness of a triple crystal phoswich detector (which was used to simultaneously detect alpha, beta, and gamma radiation). In this analysis, the effects of varying the detector thickness was studied for trade-offs between charged particle energy deposition and detector efficiency individually. While trade-offs (or correlations) were considered, no statistical analysis was performed and the cases were evaluated on a "one factor at a time" basis. Subsequently, a true multivariate optimization of the detector's parameters was not performed.

Several authors have optimized response variables using factorial design experiments and response surface methodology. Gomis et al [26] performed multivariate optimization of a capillary electrophoresis method for medical applications using factorial designs. This research studied four independent (predictor) variables at two levels each (high and low values), and two response variables in a full factorial design. Optimum values for the predictor variables were obtained using central composite design and response surface methodology. Ng et al [27] presented a sequential approach to optimizing multiple response variables when interdependencies exist among the factors. Ng et al studied improving a radiography inspection process with two conflicting response variables which were measures of radiograph quality (contrast sensitivity and spatial resolution) and a secondary response variable (image density). The secondary response variable (image density) had to be within a certain range to make the image readable and enable further processing to obtain good radiograph quality response variables (contrast sensitivity and spatial resolution). Therefore, a constraint (or limit) was placed the secondary response variable (image density) in order to optimize the other response variables (measures of radiograph quality). Using this approach, optimal settings for the four independent factors were determined which satisfied not only the image density constraint, but also both the maximization of resolution and minimization of contrast responses simultaneously. The authors note however that in other scenarios there may be competing response characteristics, in which case tradeoff studies would have to be done.

3 METHODOLOGY

The proposed work is to develop a novel methodology for optimizing candidate neutron detector designs using multivariate statistical analysis of Monte Carlo radiation transport code (MCNPX) models. This section presents the methodology used to complete this objective, including: (1) a description of the neutron source systems used to irradiate the neutron detectors and collect experimental results; (2) a description of the Monte Carlo radiation transport code used to simulate detector responses; (3) a description of the response parameters chosen to measure the performance of the neutron detector, and a discussion of how to calculate them; (4) a description of the suite of Matlab® program files used to post-process the MCNPX generic and PTRAC output files; and (5) the step-by-step methodology for the multivariate optimization of any given neutron detection system.

3.1 NEUTRON IRRADIATIOR

The neutron source system is a custom-built high density polyethylene (HDPE) box containing a 0.59 μg ^{252}Cf source. The neutron irradiator is constructed of 2-inch thick blocks of HDPE, and has outside dimensions of ~20-inches long, ~12-inches wide, and ~14 inches tall. The HDPE box includes two 1/16-inch thick acrylic tubes (or wells) to contain the detector and associated PMT. The first acrylic tube is considered to be a bare detector well, while the other acrylic tube is shielded with a 1/16-inch thick cadmium cover to shield out low energy neutrons. The ^{252}Cf source is encased in a ~¼-inch diameter and ~1 ½-inch tall stainless steel cylinder. In order to reduce the gamma ray flux, the stainless steel-encased ^{252}Cf source is contained within a ~2-inch diameter and ~5 ¼-inch tall lead vessel which is ~½-inch thick radially. Two inches of HDPE separate the source and the detector measurement wells. The MCNPX model of neutron irradiator is presented in Figure 9.

The ^{252}Cf isotope is included in the MCNPX nuclear data library as a spontaneous fission neutron source. The spontaneous fission neutron energy spectra obtained from MCNPX for the ^{252}Cf source is shown in Figure 10.

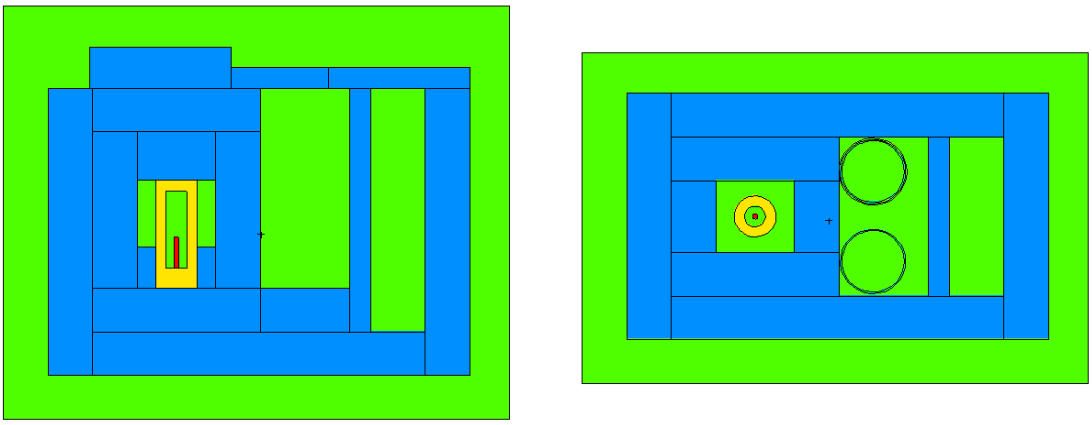

Figure 9. MCNPX Model of the Neutron Irradiator

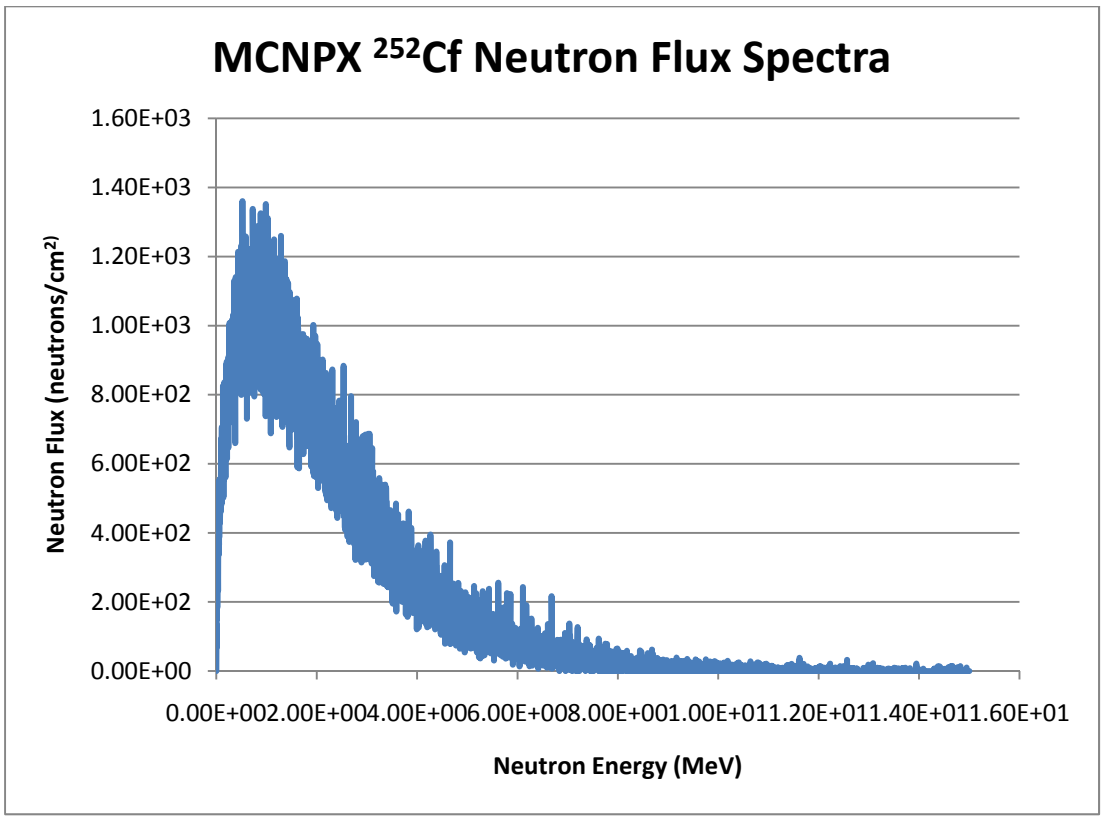

Figure 10. Spontaneous Fission Neutron Energy Spectra for ^{252}Cf

The source strength can be calculated based upon the ^{252}Cf source mass of 0.59 µg using the following methodology. The spontaneous fission activity, A_{sf}, is calculated using Equation 3.1-1 [8]:

$$A_{sf} = \lambda_{sf} N = \frac{ln2}{T_{sf}} m \frac{N_A}{A} \qquad 3.1\text{-}1$$

Where λ_{sf} is the radioisotope decay constant, N is the number of radioactive nuclei, m is the source mass, N_A is Avogadro's number, A is the atomic mass, and T_{sf} is the spontaneous fission half-life which is equal to [8]:

$$T_{sf} = \frac{T_t T_\alpha}{T_\alpha - T_t} = \frac{(2.646\ years * 2.731\ years)}{(2.731\ years - 2.646\ years)} = 85.01\ years = 2.68E9\ seconds$$

Where T_t is the total half-life and T_α is the half-life for alpha decay. After substitution, the spontaneous fission activity is calculated as:

$$A_{sf} = \frac{ln2}{2.68E9\ seconds}(0.59E-7\ grams)\frac{6.022E22\frac{atoms}{mol}}{252\frac{grams}{mol}}$$

$$= 3.644E5\ spontaneous\ fissions/second$$

The neutron yield ($\bar{\nu}$), or average number of neutrons emitted per fission event, of ^{252}Cf has been measured by Axton and Bardell to be 3.7509+/-0.0107 neutrons/fission [28]. The neutron source strength is determined by multiplying the spontaneous fission activity by the neutron yield. The resulting neutron source strength is 1.367 x 10^6 neutrons/second. An equation proposed by Martin and Kos can be used to verify the calculated source strength where the neutron emission rate from spontaneous fission of 1.0 micrograms of ^{252}Cf is equated to 2.314 x 10^6 neutrons/second [29]. Using this relationship and our ^{252}Cf source mass of 0.59 µg, the resulting neutron source strength is 1.365 x 10^6 neutrons/second, which is only slightly less than the calculated source strength of 1.367 x 10^6 neutrons/second.

3.2 MONTE CARLO SIMULATION

Monte Carlo radiation transport simulations were performed using the MCNPX Version 2.7c code. MCNPX, which stands for Monte Carlo N-Particle eXtended, was developed at the Los Alamos National Laboratory (LANL). MCNPX is based on MCNP4C3 and is capable of simulating the interaction of radiation (nearly all particles

and energies) with any environment. MCNPX is fully three-dimensional and time dependent. It utilizes the latest nuclear cross section libraries and uses physics models for particle types and energies where tabular data are not available. MCNPX is used for a broad range of applications including nuclear medicine, nuclear safeguards, accelerator applications, homeland security, and nuclear criticality safety [30]. Examples of MCNPX inputs generated as a part of this research are included in Appendix B.

3.3 DETECTOR RESPONSE PARAMETERS FOR STATISTICAL ANALYSIS

Based upon the DHS criteria shown in Table 1, a candidate replacement detector's performance is measured by its ability to be sensitive to neutrons, provide excellent γ-n discrimination, to limit false alarms, and to be reasonably priced. The four response variables used to measure these performance critera are taken directly from the functional specifications outlined in Table 1 from DNDO. An overview of each response variable as well as the methodology for its calculation is provided in the following sub-sections.

3.3.1 ABSOLUTE NEUTRON DETECTION EFFICIENCY

The absolute neutron detection efficiency ($\varepsilon_{abs,n}$) is defined as the number of neutron pulses recorded divided by the number of neutrons emitted by the source (with only a neutron source present) as shown in Equation 3.3-1.

$$\varepsilon_{abs,n} = \frac{Number\ of neutron\ pulses\ recorded}{Number\ of\ neutrons\ emitted\ from\ source} \qquad 3.3\text{-}1$$

Per PNNL-14716, the absolute neutron detection efficiency is to be measured using a ^{252}Cf source which is to be shielded by 0.5 cm of lead to reduce the gamma-ray flux and 2.5 cm of polyethylene to moderate the neutron spectra. No photon source is to be present. The source is to be placed 2 meters perpendicular to the geometric midpoint of the neutron detector's face, and the detector center shall be 1.5 m above grade for this test [31].

The absolute neutron detection efficiency can be measured for a candidate detector by placing the neutron sensor in the neutron irradiator described in Section 3.1, and calculating the ratio of the number of measured pulses by the calculated neutron source

strength of 1.367 x 10^6 neutrons/second. Depending on the type of neutron sensor, the absolute neutron detection efficiency may be relatively straight-forward to calculate in MCNPX requiring no post-processing outside of MCNPX. For example, for ^{3}He-based neutron detector, this is accomplished using the following procedure:

1. Set up F6 tallies for each of the charged particle reaction products. The F6 tally calculates the energy deposited by a charged particle in a given cell. For ^{3}He-based system, the neutron absorber is ^{3}He with proton and triton reaction products. Therefore, one F6 tally is generated for each particle and the cell(s) of concern is defined as the ^{3}He tube(s).
2. Set up an F8 tally (which has units of pulses/source particle) which provides the energy distribution of pulses created in the detector by radiation.
3. Energy bins are set up on the F8 tally to simulate a lower level discriminator (LLD) energy cutoff. Three energy bins are normally defined with the energy identifying the energy of the histogram bin upper boundary. A zero energy bin is recommended by the MCNPX manual to "catch non-analog knock-on electron negative scores" [30]. The next energy bin is set at the LLD energy cutoff, and the charged particle pairs depositing energy greater than the LLD cutoff are collected in the last energy bin.
4. A special treatment for tallies card (FT) must then be used with the pulse height light (PHL) option. This allows the energy from each of the charged particles defined in the F6 tallies to be combined and tallied together in the simulated pulse.

The third energy bin of the resulting F8 tally output is now the fraction of source neutrons which result in a pulse with an energy greater than the defined LLD level, which is effectively the absolute neutron detection efficiency. An example of the MCNPX input for calculating the absolute neutron detection efficiency in cell 60, with a LLD energy cutoff of 100 keV is shown below.

```
FC6  F6 tallies to set up the pulse height tallies
F6:H  60         $ F6 tally for the proton in cell #60
F16:T 60         $ F6 tally for the triton in cell #60
FC8  F8 Pulse height tally for cell 60 - 3He tube (H+T)-Q-val=0.764 MeV
F8:H  60         $ F8 tally for cell #60 (the 3He tube volume)
E8   0 0.1 1     $ Three energy bins to simulate LLD cutoff
FT8  PHL 2 6 1 16 1 0   $ Combines the F6 and F16 tallies in F8 tally
```

For organic scintillators, the process of calculating the absolute neutron detection efficiency is a much more cumbersome process accomplished using the process flow outlined in Section 3.5 by fitting the Birks/Chou equation to measured data and incorporating these equations into the custom Matlab® code written to post-process MCNPX PTRAC output as described in Sections 3.4 and 3.5.

3.3.2 INTRINSIC GAMMA-NEUTRON DETECTION EFFICIENCY

The intrinsic gamma-neutron detection efficiency ($\varepsilon_{int,\gamma n}$) is defined as the number of neutron pulses detected divided by the number of photons striking the detector, thus measuring the response of a neutron detector to the presence of a gamma ray field when no neutron source is present as shown in Equation 3.3-2 [16].

$$\varepsilon_{int,\gamma n} = \frac{Number\ of\ photons\ that\ produce\ neutron\ counts}{Number\ of\ photons\ incident\ upon\ the\ detector} \qquad 3.3\text{-}2$$

Per PNNL-14716, the intrinsic gamma-neutron detection efficiency is to be measured using either a ^{192}Ir or ^{60}Co source placed at an appropriate distance so as to produce an exposure rate of 10 mR/hour at the detector [31]. The distance required to produce this exposure rate can be calculated using the following relation for the exposure rate from a radiation source [12].

$$X = \Gamma \frac{\lambda_d N t}{r^2} \qquad 3.3\text{-}3$$

Where: X is the exposure; $\lambda_d N$ is the activity of the radioactive sample; t is the exposure time, r is the distance from the source, and Γ is generally known as the gamma constant. The distance required to produce an exposure rate of 10 mR/hour from a 1 mCi ^{60}Co source can be calculated by rearranging the terms from Equation 3.3-3 as follows:

$$r = \sqrt{\left(\frac{\lambda_d N t \Gamma}{X}\right)} = \sqrt{\left(\frac{(1\ mCi)\left(\frac{13.2\ R - cm^2}{mCi - hr}\right)}{\left(\frac{10\ mR}{hr}\right)\left(\frac{1\ R}{1000\ mR}\right)}\right)} = 36.33\ cm$$

The intrinsic gamma-neutron detection efficiency is relatively straight-forward to calculate in MCNPX requiring only minimal post-processing outside of MCNPX. This post-processing is usually performed with Microsoft Excel. This is accomplished using a similar procedure used to calculate the absolute neutron detection efficiency described in Section 3.3.1, with the exception that a ^{60}Co source is placed at an appropriate distance so as to produce an exposure rate of 10 mR/h at the detector, and the F6 tally is modified to only include pulses caused by secondary electrons generated from photon interactions. The third energy bin of the resulting F8 tally output is now the fraction of source photons which result in a pulse with an energy greater than the defined LLD level, which is effectively the absolute photon detection efficiency. The intrinsic gamma-neutron detection efficiency is thus calculated by multiplying the result of the F8 tally by the number of source photons (to get the count rate), and dividing the result by the number of photons incident on the detector. The number of photons incident upon the detector is determined by review of Table 130 of the standard MCNPX output which provides the fraction of source particles which enter each cell of the model. An example of the MCNPX input for calculating the intrinsic gamma-neutron detection efficiency in cell 60, with a LLD energy cutoff of 100 keV is shown below.

```
FC6  F6 tallies to set up the pulse height tallies
F6:E 60             $ F6 tally for the electron in cell #60
FC8 - F8 Fraction of source g/n pulses in cell 60 - 3He Tube (Electron)
F8:E  60            $ F8 tally for cell #60 (the 3He tube volume)
E8   0 0.1 1        $ Three energy bins to simulate LLD cutoff
FT8  PHL 1 6 1 0    $ PHL option to include the F6 tally in F8 tally
```

3.3.3 GAMMA ABSOLUTE REJECTION RATIO FOR NEUTRONS

The gamma absolute rejection ratio for neutrons (GARRn) measures the detector response in the presence of both a large gamma ray source and a ^{252}Cf neutron source (configured as it would be for an absolute efficiency measurement). The GARRn is defined as the absolute neutron detection efficiency in the presence of both sources

($\varepsilon_{abs,\gamma,n}$), divided by the absolute neutron detection efficiency of the neutron detector in the presence of only the neutron source as shown in Equation 3.3-4.

$$GARRn = \frac{\varepsilon_{abs,\gamma,n}}{\varepsilon_{abs,n}} \quad \text{3.3-4}$$

The GARRn would be equal to 1 if the gamma ray source had no impact. Per PNNL-14716, the GARRn is to be measured using either a ^{192}Ir or ^{60}Co source placed at an appropriate distance so as to produce an exposure rate of 10 mR/hour at the detector, and the same neutron source shall be placed at 2 meters in the same configuration as for the measurement for the absolute neutron detection efficiency [31]. The distance required to produce this exposure rate can be calculated using the following relation for the exposure rate from a radiation source [12]. It is preferred that ^{60}Co be used for the gamma source due to be consistent with the ANSI N42.38 standard [16].

Regardless of the type of neutron sensor, the GARRn is straight-forward to calculate, requiring minimal post-processing outside of MCNPX. Again, this post-processing is usually accomplished using Microsoft Excel. The GARRn is calculated by simply adding the absolute neutron detection efficiency calculated as described in Section 3.3.1 to the absolute photon detection efficiency which was calculated as part of the procedure to calculate the intrinsic photon detection efficiency as described in Section 3.3.2, and then dividing by the absolute neutron detection efficiency calculated as described in Section 3.3.1.

3.3.4 COST

The cost response function is dependent on the type of detection system, and is approximated by a generic equation for the neutron sensors analyzed for this research. As shown in Equation 3.3-5, the generic equation used to estimate the cost of a given neutron detection system is based on the parameters which are assumed to most significantly contribute to the overall cost, and are multiplied by a generic factor to account for manufacturing costs.

$$Cost = \left(\frac{manufacturing\ cost}{materials\ cost}\right) * \left(\sum_{i=1}^{n} V_i C_i\right) \quad \text{3.3-5}$$

Where the ratio of manufacturing cost to materials cost was taken to be equal to 2, V_i is the volume of the material, and C_i is the cost per unit volume of the material.

3.4 MATLAB® PTRAC POST-PROCESSING PROGRAM SUITE

A suite of Matlab® program files were developed to post-process the MCNPX generic and PTRAC output files. The Matlab® program suite automates the process of generating the PHS and allows the inclusion of nonlinear light yield equations into the simulation of the PHS for organic scintillators. Matlab® is a high-performance language for technical computing which integrates computation, visualization, and programming in an easy-to-use environment where problems and solutions are expressed in familiar mathematical notation [32]. The main script file, named MCNPX_GRABBER, calls a total of 16 Matlab® function m-files to perform various operatiosn such as sorting, tracking, and tallying charged particles (and the energy that they deposit) as they traverse through the detector's geometry. A brief overview of each Matlab® function m-file is provided in the following sub-sections. Matlab® version 7.9.0.529 (Release 2009b) was used during the code's development. Figure 11 shows the process flow of MCNPX_GRABBER.

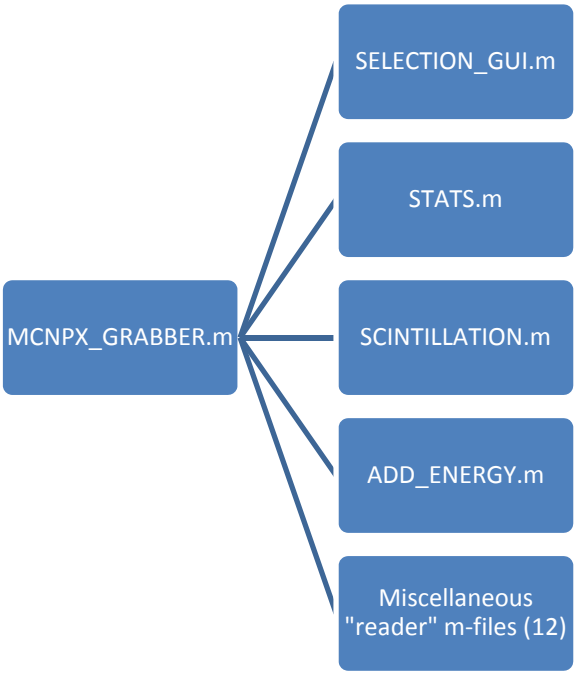

Figure 11. MCNPX_GRABBER.m Code Flow Chart

3.4.1 MCNPX_GRABBER.M

This Matlab® m-file is the main script file which performs functions including opening, importing, and organizing the MCNPX generic and MCNPX PTRAC-output file as well as plotting histograms showing energy the losses of each type of charged particle and simulated pulse height spectra (PHS) for each cell. Finally, MCNPX_GRABBER.m is responsible for passing information between the various other Matlab® function m-files as shown in Figure 11 in order to generate the energy deposition histograms and to calculate the various detector response data. For each type of charged particle, the stopping power tables generated from MCNXP for the scintillating material as well as the parameters for the Birks/Chou equations are also included in the MCNPX_GRABBER.m file. The MCNPX_GRABBER.m script is presented in Appendix D.

3.4.2 SELECTION_GUI.M

This Matlab® function m-file generates the graphical user interface (GUI) which prompts the user to define the MCNPX generic and PTRAC output files and to select the formatting of the PTRAC output by way of selecting check boxes if the PTRAC output is filtered by either the cell number or particle type. This information is eventually passed back to MCNPX_GRABBER.m for use in interpreting the MCNPX output files. Figure 12 shows the GUI presented to the user of the Matlab® PTRAC post-processing suite called by MCNPX_GRABBER.m. The SELECTION_GUI.m script is presented in Appendix D.

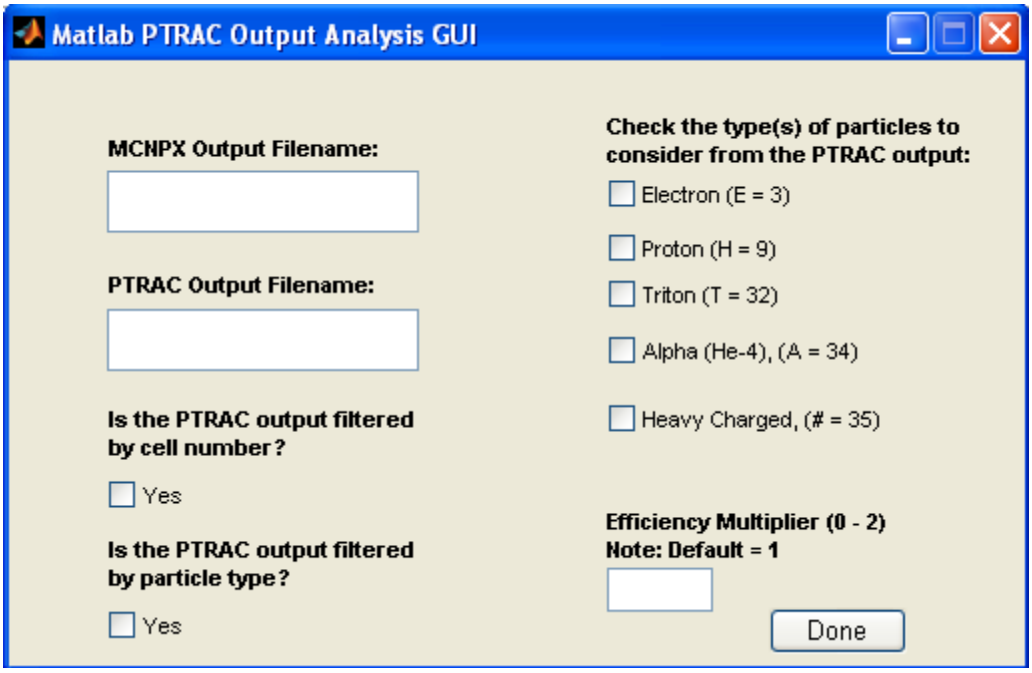

Figure 12. GUI Interface for Matlab® PTRAC Post-Processing Suite

3.4.3 STATS.M

This Matlab® function m-file follows each charged particle from "birth" to "death", calculating the distance travelled as well as the energy deposited within each cell. This includes the possibility that the particle may traverse through multiple cells along its track. If the detector which is being analyzed is an organic scintillator and the parameters from the Birks/Chou equations (Equation 2.2-6) are input, this m-file converts the energy deposited into the light yield for each event. The STATS.m script is presented in Appendix D.

3.4.4 SCINTILLATION.M

This Matlab® function m-file utilizes the particle information calculated from STATS.m to track the total number of charged particles entering and the number of tracks passing through each cell. This information is used to calculate the probability of scintillation given a minimum energy deposition as well as the average, total, and standard deviation of the energy deposited within each cell. The SCINTILLATION.m script is presented in Appendix D.

3.4.5 ADD_ENERGY.M

This Matlab® function m-file utilizes the particle information calculated from STATS.m to track the total energy lost by the charged particle for each neutron absorption event for each cell number. This information is passed back to MCNPX_GRABBER.m for use in generating histograms for the simulation of PHS. The ADD_ENERGY.m script is presented in Appendix D.

3.4.6 MISCELLANEOUS "READER" M-FILES

These Matlab® function m-files read the user defined MCNPX generic output file and search for various types of information. This information is mostly related to photon events as photons are not normally included in the MCNPX PTRAC output file in order to keep the PTRAC output file size (and subsequently Matlab® processing time) to a minimum. Some information related to neutrons is also collected in order to perform cross-checks with data calculated from MCNPX PTRAC output. This provides some assurance that the code is functioning as intended. Table 4 provides the names and a brief description of the purpose of each of the twelve reader m-files. The twelve "reader" m-file scripts are presented in Appendix D.

Table 4. Matlab® "Reader" M-File Summary

M-File Name	Purpose
NUM_SOURCE_READER.m	Tallies the number of source particles from the MCNPX output file
G_FROM_BREM_READER.m	Tallies the number of photons generated from Bremsstrahlung
G_FROM_N_READER.m	Tallies the number of photons generated from neutrons
N_ABS_READER.m	Tallies the number of neutron absorption events
N_ESCAPE_READER.m	Tallies the number of neutron escapes
P_CAPTURE_READER.m	Tallies the number of photon captures
P_COMPT_SCATT_READER.m	Tallies the number of photon Compton scattering events
P_ENERGY_CUT_READER.m	Tallies the number of photons whose history ended due to the low energy cutoff
P_ESCAPE_READER.m	Tallies the number of photon escapes
P_FLUORESCENCE_READER.m	Tallies the number of photons generated from fluorescence
P_PAIR_PROD_READER.m	Tallies the number of photons lost from Pair Production events
P_PHOTONUCLEAR_ABS_READER.m	Tallies the number of photons lost from photonuclear absorption events

3.5 METHODOLOGY FOR MULTIVARIATE OPTIMIZATION

The methodology used to optimize a given neutron detection system depends on whether or not the detector being optimized is a scintillator. Figure 13 shows a flowchart outlining the entire process for the optimization of a candidate neutron sensor. If N*n*, where *n* is an integer, appears next to an outlined step in the flow chart, then that step is explained or discussed in more detail in Note N*n* in the text following the figure.

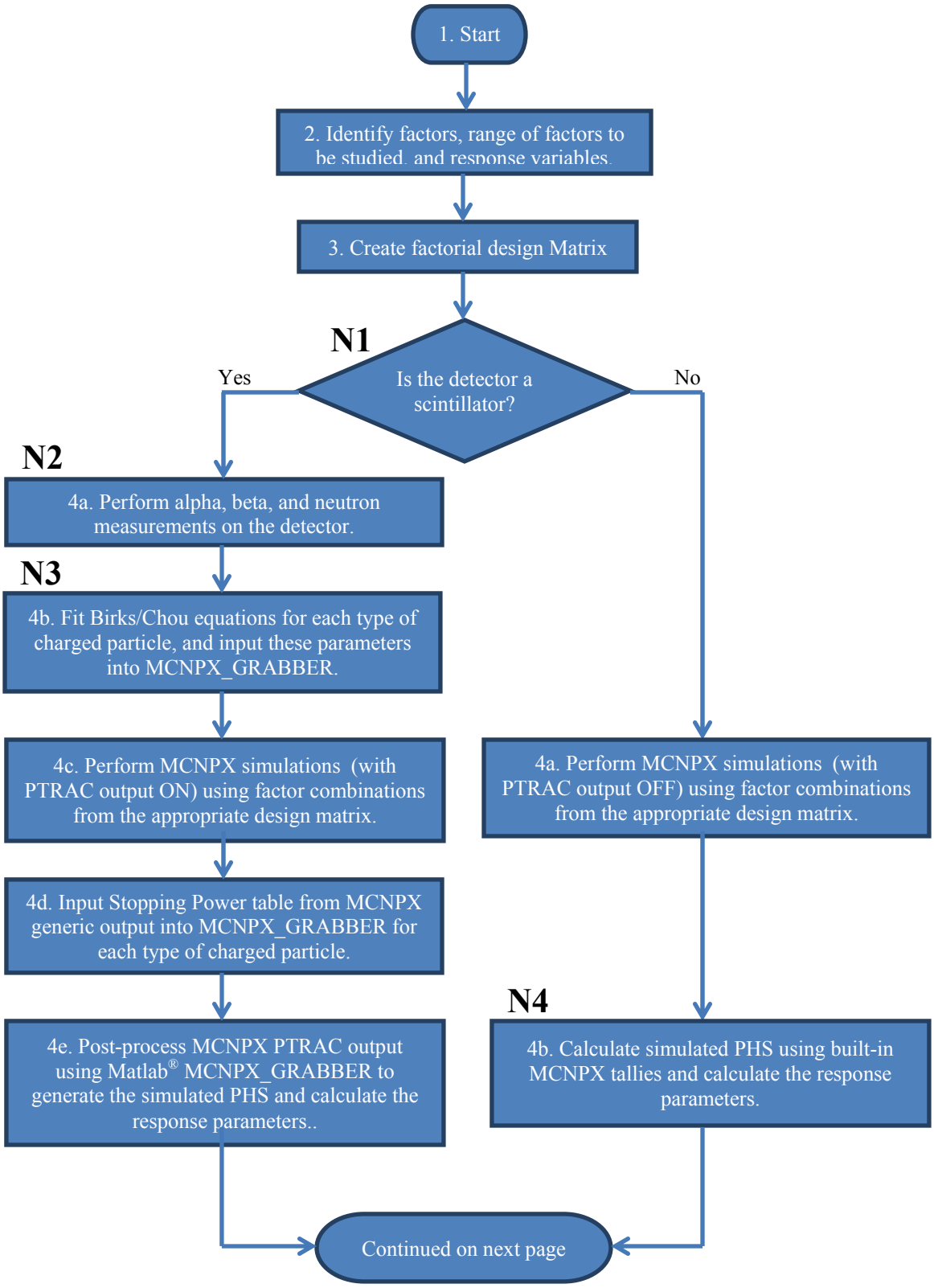

Figure 13. Optimization Process Flowchart

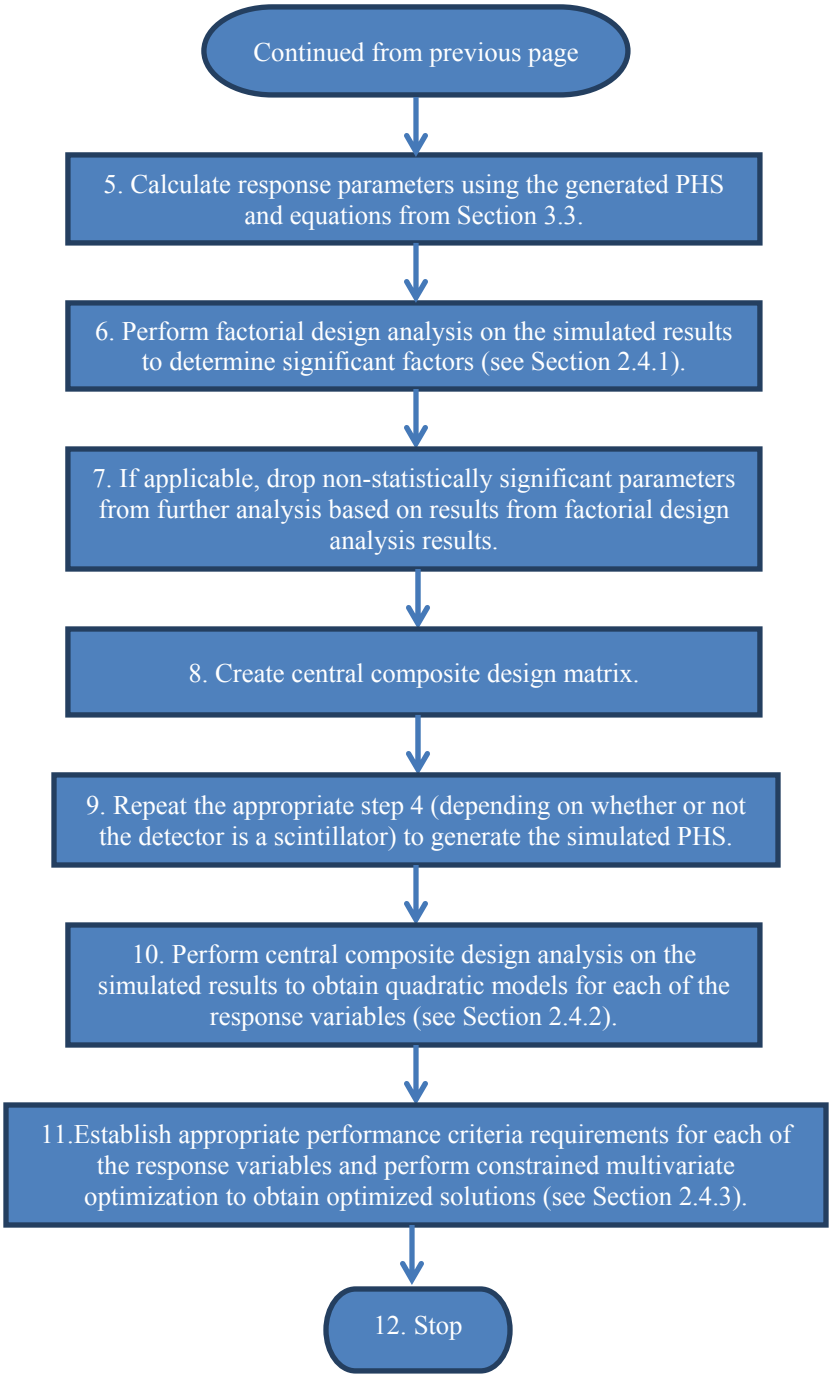

Figure 13. Continued.

N1: For some neutron detection systems, response parameters can be calculated using built-in MCNPX tallies with minimal post-processing. However, for organic scintillators (which have been the focus of research for this DNDO grant), it is not possible to accurately simulate the PHS due to the inability of any currently available software to predict the light output as a function of the energy deposited for a scintillating material. This response must be experimentally measured and incorporated into the Birks/Chou equations (Equation 2.2-6) described in Section 2.2.4.1. However, once measured for each type of charged particle for a given scintillating medium, these equations can be paired with the simulated results of the amount of energy deposited by each charged particle in a scintillator to obtain an accurate representation of the PHS.

N2: In order to solve for the fitting parameters, *kB* and *C*, required for the Birks/Chou equations, the amount of light output *L(E)* must be measured using alpha and beta sources at multiple energy levels as well as a neutron source. Stopping power tables are generated using MCNPX for each scintillating material (print table 85 from the standard MCNPX output) and the Matlab computer program (MCNPX_GRABBER) interpolates the appropriate *dE/dx* value at each of the measured charged particle energies.

N3: For each type of charged particle, the two fitting parameters are solved for by fitting the measured results with the Birks/Chou formula (Equation 2.2-6) and minimizing the sum square of errors (SSE) between experimental and predicted data. Fitted light yield equations for each charged particle type are then incorporated into the Matlab® code to generate a simulated pulse height spectra based on the energy deposited by the neutron absorption reaction products in the scintillating medium.

N4: For non-scintillating detectors, the response variables can be calculated using the built-in MCNPX tallies and minimal post-processing as presented in Section 3.3.

4 RESULTS AND DISCUSSION

Multivariate optimization has been successfully performed on three different neutron detection systems using the methodology outlined in this dissertation. The first neutron detection system presented is a based on a generic radiation portal monitor from PNNL which is similar to the currently deployed ^{3}He-based systems and utilizes PHD for n/γ discrimination. The second system optimized is a ^{6}Li-loaded polymer composite scintillator developed at UT which relies upon PHD for discrimination between neutrons and photons. The final system optimized is a ^{10}B-based plastic scintillator based on commercial detectors procured from Eljen Technologies. Both PHD and coincidence counting are considered for n/γ discrimination ability in the ^{10}B-based detectors.

Multiple parameters (factors) for each of these systems are optimized with the goal of satisfying the minimum DNDO requirements for a candidate replacement detector from Table 1. The generic ^{3}He model from PNNL is included to show that this technology can satisfy the DNDO requirements and to validate the results of the multivariate optimization methodology by comparison to measured data. Results from each multivariate optimization analysis will include which combinations of factors result in the best detector performance, with simultaneous consideration of each of the response functions. Results of the analysis will also provide insight into how each of the factors (and interrelationships between factors) analyzed impacts the detector performance.

4.1 ^{3}HE RADIATION PORTAL MONITOR DETECTOR OPTIMIZATION ANALYSIS

The ^{3}He Radiation Portal Monitor model is a generalized version of the Science Applications International Corporation (SAIC) RPM8 system described in PNNL-18471 [2]. The system modeled for this analysis consisted of two ^{3}He tubes inside a polyethylene box with a height of 87 inches, a width of 12 inches, and a variable thickness. The polyethylene box was surrounded by a ¼-inch thick steel shield around the back and sides. A ^{252}Cf source surrounded by 0.5 cm of lead and 2.5 cm of polyethylene was modeled at 2 meters perpendicular to the geometric midpoint of the

RPM in accordance with the DNDO test configuration specifications. Figure 14 shows a typical RPM with a pair of ^{3}He tubes inside of a moderating polyethylene box.

4.1.1 EXPLANATORY VARIABLE OVERVIEW

From the optimization methodology outlined in Section 3.5, the first step is to identify the explanatory detector variables (factors) which will be varied to measure the impact on the detector performance. Next, ranges over which to vary the explanatory parameters are chosen (usually high and low levels). For this detector system, the following five detector parameters and levels were chosen based of a review of PNNL reports on the generic RPM8 system:

1. The ^{3}He tube height
    a. 3 feet
    b. 5 feet

2. The thickness of polyethylene in the front of the detector (T_{front})
    a. 5 cm
    b. 8 cm

3. The thickness of polyethylene in the back of the detector (T_{rear})
    a. 7.2 cm
    b. 10.4 cm

4. The ^{3}He tube pressure
    a. 1 atmosphere
    b. 3 atmospheres

5. The separation distance between the two ^{3}He tubes from the center of the RPM (D_{CL})
    a. 3 cm
    b. 5.25 cm

Figure 15 shows X-Z and X-Y views of the MCNPX ^{3}He RPM model with the explanatory variables outlined, respectively.

Figure 14. Typical Radiation Portal Monitor (Source: Van Ginhoven, et al, 2009 [2])

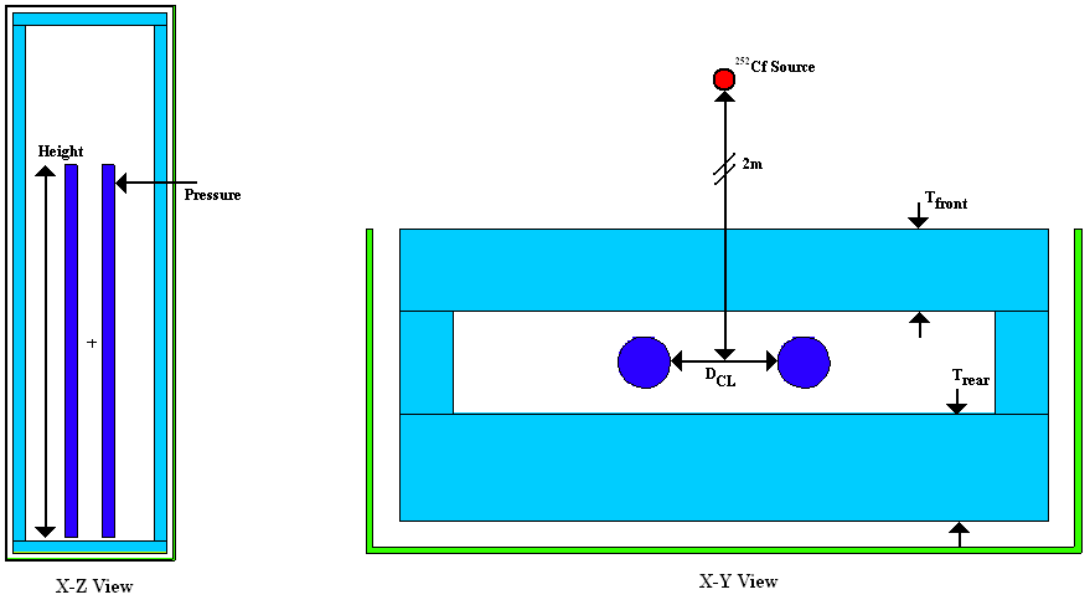

Figure 15. X-Z and X-Y views of the MCNPX ^{3}He RPM Model

4.1.2 RESPONSE VARIABLE OVERVIEW

The four responses used for the RPM analysis are the same as those described in Section 3.3 which are based upon the DHS criteria shown in Table 1. The four response parameters measured are:

1. Absolute neutron detection efficiency (counts per second / ng ^{252}Cf)
2. Intrinsic gamma-neutron detection efficiency
3. Gamma absolute rejection ratio for neutrons, GARRn
4. Cost

The first three responses are calculated using the methodology outlined in Section 3.5 for a non-scintillating detector. The cost response function was calculated using a modified version of Equation 3.3-5 specific to ^{3}He detection systems as shown below:

$$Cost_{\,^{3}He\ RPM} = \left(\frac{manufacturing\ cost}{materials\ cost}\right) * \left\{\left(Volume\ \ ^{3}He@STP\right)\left(\$\ \ ^{3}He\ @STP/liter\right) + (Volume\ HDPE)(\$\ HDPE/liter)\right\}$$

Where the ratio of manufacturing cost to materials cost was taken to be equal to 2, the price of ^{3}He per liter at STP was taken to be \$930 based on recent reports, and the price of HDPE was assumed to be \$100 per ft^3 [33].

4.1.3 FACTORIAL DESIGN ANALYSIS

After determining the factors (explanatory variables), factor levels, and responses, the factorial design analysis can be performed to identify the relationships between the explanatory and response variables. Table 5 shows the factorial design matrix generated using SAS for the ^{3}He RPM system. This design is a 2^5 design (five factors with two levels each), with no replication, which results in 32 MCNPX cases. This table was used to build MCNPX input files to calculate the response variables for each treatment combination.

Table 5. ^{3}He RPM Factorial Design Matrix

Filename	Tube Height (ft)	Front Poly Thickness (cm)	Rear Poly Thickness (cm)	^{3}He Pressure (atm)	Tube separation distance (in)
3He_1	3	5	7.2	1	3
3He_2	3	5	7.2	1	5.25
3He_3	3	5	7.2	3	3
3He_4	3	5	7.2	3	5.25
3He_5	3	5	10.4	1	3
3He_6	3	5	10.4	1	5.25
3He_7	3	5	10.4	3	3
3He_8	3	5	10.4	3	5.25
3He_9	3	8	7.2	1	3
3He_10	3	8	7.2	1	5.25
3He_11	3	8	7.2	3	3
3He_12	3	8	7.2	3	5.25
3He_13	3	8	10.4	1	3
3He_14	3	8	10.4	1	5.25
3He_15	3	8	10.4	3	3
3He_16	3	8	10.4	3	5.25
3He_17	5	5	7.2	1	3
3He_18	5	5	7.2	1	5.25
3He_19	5	5	7.2	3	3
3He_20	5	5	7.2	3	5.25
3He_21	5	5	10.4	1	3
3He_22	5	5	10.4	1	5.25
3He_23	5	5	10.4	3	3
3He_24	5	5	10.4	3	5.25
3He_25	5	8	7.2	1	3
3He_26	5	8	7.2	1	5.25
3He_27	5	8	7.2	3	3
3He_28	5	8	7.2	3	5.25
3He_29	5	8	10.4	1	3
3He_30	5	8	10.4	1	5.25
3He_31	5	8	10.4	3	3
3He_32	5	8	10.4	3	5.25

The results for each of the four response variables calculated using MCNPX tallies for all 32 simulations are presented in Table 36 of Appendix A. At this point, the SAS software package was used to analyze the results. Recall that each of the response variables must first be analyzed independently to determine statistically significant factors. Each of the four response variables are analyzed in the following sub-sections.

4.1.3.1 Absolute Neutron Detection Efficiency Response Analysis

Results of the factorial Analysis of Variance for the absolute neutron detection efficiency (n_abs_eff) response variable are presented below:

Dependent Variable: n_abs_eff n_abs_eff

R-Square	Coeff Var	Root MSE	n_abs_eff Mean
0.999440	1.198117	0.032046	2.674677

Source	DF	Type I SS	Mean Square	F Value	Pr > F
height	1	14.67541553	14.67541553	14290.6	**<.0001**
front_th	1	3.30424398	3.30424398	3217.59	**<.0001**
height*front_th	1	0.18332864	0.18332864	178.52	**<.0001**
rear_th	1	0.14455789	0.14455789	140.77	**<.0001**
height*rear_th	1	0.01104210	0.01104210	10.75	**0.0047**
front_th*rear_th	1	0.00549428	0.00549428	5.35	**0.0344**
pressure	1	10.20334294	10.20334294	9935.77	**<.0001**
height*pressure	1	0.53976819	0.53976819	525.61	**<.0001**
front_th*pressure	1	0.18258334	0.18258334	177.80	**<.0001**
rear_th*pressure	1	0.00708150	0.00708150	6.90	**0.0183**
cl_distance	1	0.01427267	0.01427267	13.90	**0.0018**
height*cl_distance	1	0.00000019	0.00000019	0.00	0.9893
front_th*cl_distance	1	0.02630805	0.02630805	25.62	**0.0001**
rear_th*cl_distance	1	0.00080318	0.00080318	0.78	0.3896
pressure*cl_distance	1	0.00367304	0.00367304	3.58	0.0768

These results show that 99.94% of the variability in the absolute neutron detection efficiency can be explained by main effects and two-way interactions. This confirms that higher order interactions (e.g., pressure*height^2, etc.) do not contribute to the variability of the response and that the assumption of not requiring case replication was justified. Statistically significant effects are identified from the ANOVA output when a "Pr > F" term (which is the probability of obtaining an F-statistic this large if the null hypothesis were true) for an effect is less than the α-level of 0.05. When this occurs, we can reject

the null hypothesis and conclude that the effects are statistically significant. The results show that the all of the main effects and the majority of the two-way interactions have a statistically significant impact (shown in red bold) on the absolute neutron detection efficiency.

4.1.3.2 Intrinsic γ/n Detection Efficiency Response Analysis

Results of the factorial Analysis of Variance for the intrinsic γ detection efficiency (g_int_eff) response variable are presented below:

Dependent Variable: g_int_eff g_int_eff

R-Square	Coeff Var	Root MSE	g_int_eff Mean
0.957024	31.07413	8.4262E-6	0.000027

Source	DF	Type I SS	Mean Square	F Value	Pr > F
height	1	3.204679E-11	3.204679E-11	0.45	0.5113
front_th	1	3.172334E-11	3.172334E-11	0.45	0.5134
height*front_th	1	2.903723E-10	2.903723E-10	4.09	0.0602
rear_th	1	2.760483E-13	2.760483E-13	0.00	0.9511
height*rear_th	1	1.001543E-11	1.001543E-11	0.14	0.7122
front_th*rear_th	1	1.170746E-13	1.170746E-13	0.00	0.9681
pressure	1	2.3529669E-8	2.3529669E-8	331.40	**<.0001**
height*pressure	1	3.204679E-11	3.204679E-11	0.45	0.5113
front_th*pressure	1	3.172334E-11	3.172334E-11	0.45	0.5134
rear_th*pressure	1	2.760483E-13	2.760483E-13	0.00	0.9511
cl_distance	1	2.718975E-10	2.718975E-10	3.83	0.0680
height*cl_distance	1	1.659383E-10	1.659383E-10	2.34	0.1458
front_th*cl_distance	1	6.212797E-10	6.212797E-10	8.75	**0.0093**
rear_th*cl_distance	1	8.127683E-12	8.127683E-12	0.11	0.7395
pressure*cl_distance	1	2.718975E-10	2.718975E-10	3.83	0.0680

These results show that 95.70% of the variability in the intrinsic γ detection efficiency can be explained by main effects and two-way interactions. The results also show that the following main effects and two-way interactions have a statistically significant impact (shown in red bold) on the intrinsic γ detection efficiency at an α-value of 0.05: pressure, and the two-way interaction between the thickness of the polyethylene in the front and tube separation distance. Two-way interactions can be further examined to reveal the nature of their relationship. For example, the two-way interaction between the thickness of the polyethylene in the front and tube separation distance can be

explained as the intrinsic γ/n detection efficiency as a function of the thickness of the polyethylene in the front of the ^{3}He tube differs depending on the tube separation distance. In order to elucidate this effect, the Least Squares Means (LSM) procedure in SAS was performed. The results of the LSM procedure for are presented below.

The GLM Procedure
Least Squares Means

front_th	cl_distance	g_int_eff LSMEAN	LSMEAN Number
5	3	0.00002761	1
5	5.25	0.00002463	2
8	3	0.00002079	3
8	5.25	0.00003543	4

Least Squares Means for effect front_th*cl_distance
Pr > |t| for H0: LSMean(i)=LSMean(j)

Dependent Variable: g_int_eff

i/j	1	2	3	4
1		0.4892	0.1250	0.0819
2	0.4892		0.3758	**0.0208**
3	0.1250	0.3758		**0.0031**
4	0.0819	**0.0208**	**0.0031**	

These results show that the means of the intrinsic γ detection efficiency are not statistically significantly different for the cases where the thickness of the polyethylene in the front is 5 cm and the tube distance is varied (p-value of 0.4892), but the means of the intrinsic γ detection efficiency are significantly different for the cases where the thickness of the polyethylene in the front is 8 cm and the tube distance is varied (p-value of 0.0031). This effect can be summarized by noting that for models where the thickness of the polyethylene in the front is 5 cm, varying the tube distance does not impact the intrinsic γ detection efficiency, but the same cannot be said for cases where the thickness of the polyethylene in the front is 8 cm.

4.1.3.3 Gamma Absolute Rejection Ratio for Neutrons Response Analysis

Results of the factorial Analysis of Variance for the gamma absolute rejection ratio for neutrons (GARRn) response variable are presented below:

Dependent Variable: GARRn GARRn

R-Square	Coeff Var	Root MSE	GARRn Mean
0.960179	0.094274	0.000945	1.002568

Source	DF	Type I SS	Mean Square	F Value	Pr > F
height	1	0.00005640	0.00005640	63.14	**<.0001**
front_th	1	0.00000255	0.00000255	2.86	0.1103
height*front_th	1	0.00000039	0.00000039	0.44	0.5175
rear_th	1	0.00000000	0.00000000	0.00	0.9605
height*rear_th	1	0.00000004	0.00000004	0.05	0.8283
front_th*rear_th	1	0.00000000	0.00000000	0.00	0.9924
pressure	1	0.00021097	0.00021097	236.17	**<.0001**
height*pressure	1	0.00005640	0.00005640	63.14	**<.0001**
front_th*pressure	1	0.00000255	0.00000255	2.86	0.1103
rear_th*pressure	1	0.00000000	0.00000000	0.00	0.9605
cl_distance	1	0.00000139	0.00000139	1.56	0.2303
height*cl_distance	1	0.00000710	0.00000710	7.95	**0.0123**
front_th*cl_distance	1	0.00000526	0.00000526	5.89	**0.0275**
rear_th*cl_distance	1	0.00000018	0.00000018	0.20	0.6606
pressure*cl_distance	1	0.00000139	0.00000139	1.56	0.2303

These results show that 96.02% of the variability in the gamma absolute rejection ratio for neutrons can be explained by main effects and two-way interactions. The results also show that two following main effects (height and pressure) have a statistically significant impact (shown in red bold) on the gamma absolute rejection ratio for neutrons at an α-value of 0.05. There are also several significant two-way interactions.

4.1.3.4 Cost Response Analysis

Results of the factorial Analysis of Variance for the cost (cost) response variable are presented below:

Dependent Variable: Cost Cost

R-Square	Coeff Var	Root MSE	Cost Mean
1.000000	0	0	19723.02

Source	DF	Type I SS	Mean Square	F Value	Pr > F
height	1	651356542	651356542	Infty	<.0001
front_th	1	674327	674327	Infty	<.0001
height*front_th	1	0	0	.	.
rear_th	1	767234	767234	Infty	<.0001
height*rear_th	1	0	0	.	.
front_th*rear_th	1	0	0	.	.
pressure	1	2605426169	2605426169	Infty	<.0001
height*pressure	1	162839136	162839136	Infty	<.0001
front_th*pressure	1	0	0	.	.
rear_th*pressure	1	0	0	.	.
cl_distance	1	0	0	.	.
height*cl_distance	1	0	0	.	.
front_th*cl_distance	1	0	0	.	.
rear_th*cl_distance	1	0	0	.	.
pressure*cl_distance	1	0	0	.	.

These results show that 100% of the variability in the cost can be explained by main effects and two-way interactions. This is due to the simple linear equation used to calculate the cost of the RPM system as discussed in Section 4.1.2.

4.1.3.5 ^{3}He RPM Factorial Design Analysis Results Summary

Table 6 presents a summary of the parameters which were identified as being statistically significant for each of the response variables by the factorial design analysis. Note that the each of the main effects was identified as being statistically significant for at least one of the response variables. Therefore, none of the factors can be screened out of the following central composite design analysis.

4.1.4 RESPONSE SURFACE DESIGN ANALYSIS

The next step in the optimization methodology is to expand the factorial design analysis to a central composite design, to estimate second-degree polynomial models for each of the response variables. Using Equation 2.4-5, the α value required for rotatability is calculated as $\alpha = (2^k)^{1/4} = (2^5)^{1/4} = 2.378$. Table 7 presents the natural and coded variables for the ^{3}He RPM central composite design. These design levels are used by SAS to construct the ^{3}He RPM CCD Matrix as presented in Table 8. The results for each of the four response variables generated by MCNPX simulations for all 36 cases are presented in Table 37 of Appendix A.

Table 6. ^{3}He RPM Factorial Design Analysis Results Summary

	Absolute neutron detection efficiency	Intrinsic gamma-neutron detection efficiency	GARRn	Cost
R^2	0.9994	0.9570	0.9637	1.00
height	X		X	X
front_th	X			X
rear_th	X			X
pressure	X	X	X	X
cl_distance	X			
front_th*height	X			
rear_th*height	X			
rear_th*front_th	X			
pressure*height	X		X	X
pressure*front_th	X			
pressure*rear_th	X			
cl_distance*height			X	
cl_distance*front_th	X	X	X	
cl_distance*rear_th				
cl_distance*pressure				

Table 7. ^{3}He RPM Central Composite Design Levels

Design Factors	-2.378	-1	0	1	2.378
X1 = Tube Height (feet)	1.62	3.00	4.00	5.00	6.38
X2 = Front Thickness (cm)	2.93	5.00	6.50	8.00	10.07
X3 = Rear Thickness (cm)	5.00	7.20	8.80	10.40	12.60
X4 = Pressure (atm)	0.50	1.00	2.00	3.00	3.50
X5 = CL Distance (in)	1.45	3.00	4.13	5.25	6.80

Table 8. ^{3}He RPM Central Composite Design Matrix (Coded Variables)

Filename	Tube Height (ft)	Front Poly Thickness (cm)	Rear Poly Thickness (cm)	^{3}He Pressure (atm)	Tube separation distance (in)
3He_1	-1	-1	-1	-1	1
3He_2	-1	-1	-1	1	-1
3He_3	-1	-1	1	-1	-1
3He_4	-1	-1	1	1	1
3He_5	-1	1	-1	-1	-1
3He_6	-1	1	-1	1	1
3He_7	-1	1	1	-1	1
3He_8	-1	1	1	1	-1
3He_9	1	-1	-1	-1	-1
3He_10	1	-1	-1	1	1
3He_11	1	-1	1	-1	1
3He_12	1	-1	1	1	-1
3He_13	1	1	-1	-1	1
3He_14	1	1	-1	1	-1
3He_15	1	1	1	-1	-1
3He_16	1	1	1	1	1
3He_17	-2.378	0	0	0	0
3He_18	2.378	0	0	0	0
3He_19	0	-2.378	0	0	0
3He_20	0	2.378	0	0	0
3He_21	0	0	-2.378	0	0
3He_22	0	0	2.378	0	0
3He_23	0	0	0	-2.378	0
3He_24	0	0	0	2.378	0
3He_25	0	0	0	0	-2.378
3He_26	0	0	0	0	2.378
3He_27	0	0	0	0	0
3He_28	0	0	0	0	0
3He_29	0	0	0	0	0
3He_30	0	0	0	0	0
3He_31	0	0	0	0	0
3He_32	0	0	0	0	0
3He_33	0	0	0	0	0
3He_34	0	0	0	0	0
3He_35	0	0	0	0	0
3He_36	0	0	0	0	0

At this point, the SAS software package was used to perform least squares regression analysis of the data and to fit quadratic equations for each of the response variables. Table 9 presents the results of the regression analysis, and shows that the total R^2 values for the four different response variables are close to 1 indicatign that the quadratic models are able to predict the variability in the simulated responses very well.

A surface plot generated using the quadratic models of the absolute neutron detection efficiency response as a function of the ^{3}He pressure and the thickness of the polyethylene in the front of the detector is presented in Figure 16.

As shown in Figure 16, the absolute neutron detection efficiency increases with increasing ^{3}He pressure as expected due to the increase in the amount of the neutron absorber per unit volume, but also has an optimal value depending on the thickness of the polyethylene in the front of the detector. This plot is consistent with the results presented in Table 6, which showed that these two factors were significant to this response.

Table 9. ^{3}He RPM Central Composite Design Quadratic Model Fit

	Absolute Neutron Detection Efficiency	**Intrinsic γ Detection Efficiency**	**GARRn**	**Cost**
Linear	0.9488	0.7601	0.6802	0.9595
Quadratic	0.0207	0.0676	0.0383	0.0000
Cross-Product	0.0250	0.0455	0.1730	0.0405
Total	0.9945	0.8732	0.8915	1.0000

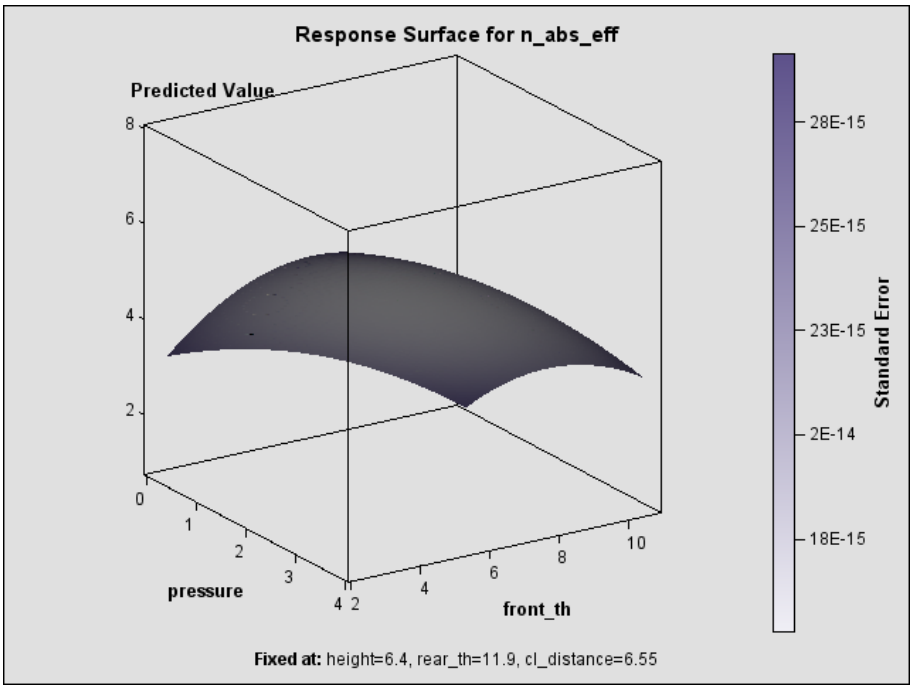

Figure 16. Example Surface Plot Generated from the ^{3}He CCD Analysis

4.1.5 CONSTRAINED MULTIVARIATE OPTIMIZATION

The final step in the optimization methodology is to use the models developed by the CCD analysis to search for an optimal design configuration which satisfies the DNDO performance criteria. From Table 1, the optimized detector must satisfy the following constraints:

1. Absolute neutron detection efficiency $\geq$ 2.5 cps/ng of ^{252}Cf
2. Intrinsic gamma-neutron detection efficiency $\leq 10^{-6}$
3. $0.9 \leq$ GARRn ≤ 1.1 at 10 mR/h exposure
4. Cost $\leq$ \$30,000

These constraints were programmed into SAS, and a list of satisfactory detector combinations was generated and sorted by minimum cost as shown in Table 10.

The system may also be optimized with regard to the highest priority being placed on neutron sensitivity. Table 11 presents the optimized results sorted by descending absolute neutron detection efficiency.

Table 10. ^{3}He RPM Optimized Results by Minimum Cost

Obs	height	front_th	rear_th	Press.	cl_dist.	n_abs_eff	g_int_eff	GARRn	Cost
1	5.4	2.9	5.6	0.5	4.75	2.5076	6.70E-8	0.9961	$7,109
2	5.4	3.2	5.3	0.5	4.75	2.5010	9.30E-7	0.9964	$7,109
3	5.4	3.2	5.6	0.5	4.75	2.5146	5.11E-7	0.9964	$7,138
4	5.2	2.9	8.3	0.5	4.45	2.5023	3.44E-7	0.9969	$7,144

Table 11. ^{3}He RPM Optimized Results by Maximum Neutron Sensitivity

Obs	height	front_th	rear_th	Press.	cl_dist.	n_abs_eff	g_int_eff	GARRn	Cost
1	6.4	2.9	11.9	1.5	6.55	5.2206	7.49E-7	0.9960	$23,283
2	6.4	2.9	11.6	1.5	6.55	5.1874	2.04E-7	0.9961	$23,254
3	6.2	2.9	10.1	1.7	6.55	5.1013	7.89E-7	0.9972	$25,230
4	6.4	3.2	11	1.5	6.55	5.0815	6.69E-7	0.9966	$23,225

In order to gain a better understand of the behavior of the detector, two-dimensional overlaid contour plots can be generated which show how the defined constraints on the response parameters are satisfied as a function of two factors. Figure 17 presents an overlaid contour plot as a function of ^{3}He pressure and the thickness of the polyethylene in the front of the detector at a fixed ^{3}He tube height of 5.4 feet. Analysis of this contour plot shows that at a ^{3}He pressure of 1.8 atmospheres and a front polyethylene thickness of 3 cm, increasing the pressure beyond ~2 atmospheres results in the system no longer satisfying the constraint on the intrinsic gamma efficiency. This is intuitive since the probability for photon interaction within the detector should increase with increasing ^{3}He density. Other inferences can also be made by review of this plot. Finally, Figure 17 shows the complex nature of the performance of the detector where the correlations between the factors results in the levels at which the response constraints are satisfied varying over the ranges analyzed. This complexity in the overall performance of the detection system is primary basis of why a multivariate statistical analysis is required to properly optimize these systems.

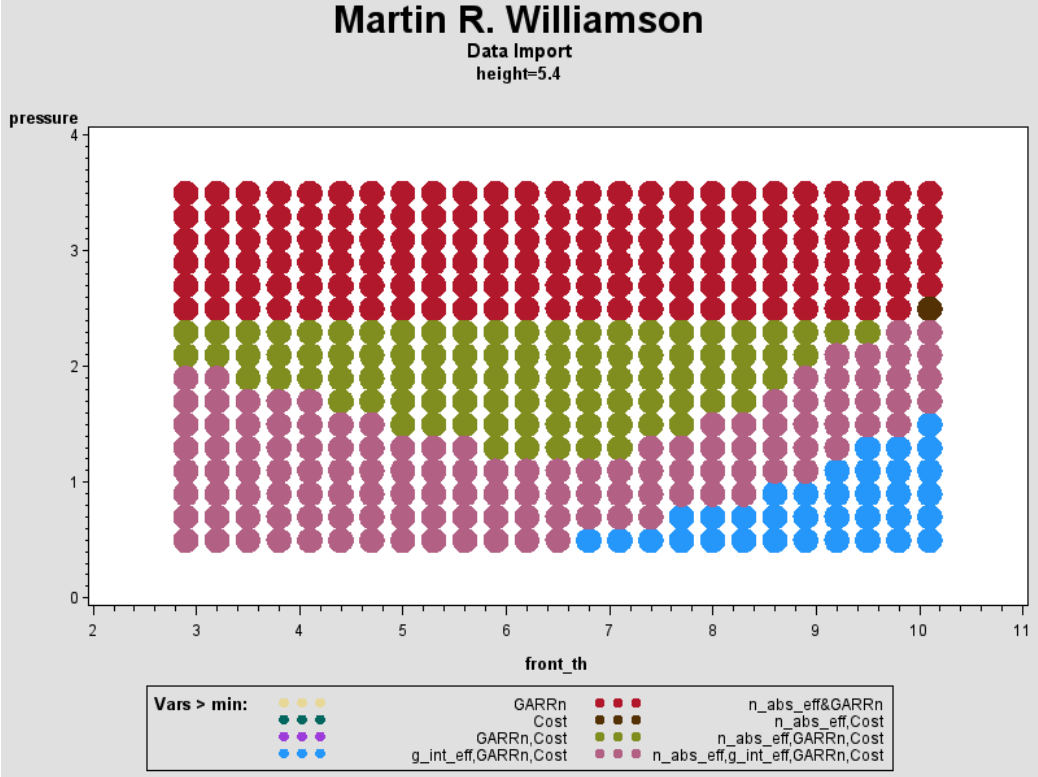

Figure 17. ^{3}He RPM Two-Dimensional Overlaid Contour Plot

4.1.6 ^{3}HE RADIATION PORTAL MONITOR MODEL VALIDATION

The performance of ^{3}He proportional counters in the SAIC RPM8 detector has been measured and documented as a function of gas pressure and the number of tubes in PNNL-19110 [34]. Although the exact dimensional specifications of the SAIC RPM8 detector are proprietary, much of the information required for a detailed model is either included in the text of the report, or can be inferred from a visual inspection of the images within the report. Figure 18 presents a comparison of measured results documented in PNNL-19910 for a two-tube PRM8 system at 1 and 3 atmospheres compared to the MCNPX simulated results generated as a part of the multivariate optimization analysis documented in this section of the dissertation.

As shown in Figure 18, the measured and simulated RPM absolute neutron detection efficiency show good agreement, with a maximum bias of <10%. The majority of this difference is most likely due to the lack of the exact specifications of the RPM8 system; however, simulations presented in PNNL-19910 also show a slight discrepancy between measurements and simulations. The Case IDs for the two simulated MCNPX

calculations presented in Figure 18 are *3He_25.i* and *3He_10.i* for ^{3}He pressures of 1 and 3 atmospheres, respectively.

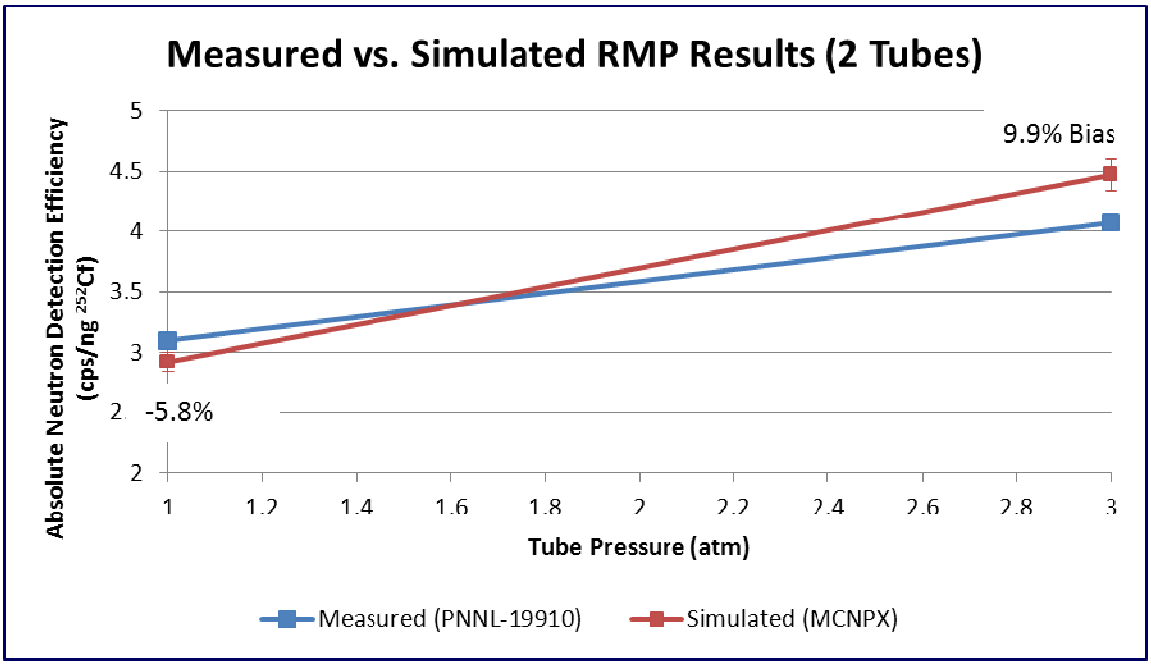

Figure 18. Validation of the Simulated ^{3}He RPM Results

4.1.7 ^{3}HE RADIATION PORTAL MONITOR SUMMARY AND CONCLUSIONS

Multivariate optimization of the SAIC RPM8 generic model was successfully performed utilizing the methodology outlined in this dissertation. The analysis was performed using five factors (^{3}He tube height, the thickness of polyethylene in the front of the detector, the thickness of polyethylene in the back of the detector, the ^{3}He tube pressure, and the separation distance between the two ^{3}He tubes from the center of the RPM) and four response parameters (the absolute neutron detection efficiency, the intrinsic gamma-neutron detection efficiency, the gamma absolute rejection ratio for neutrons, and cost). All five factors were shown to have a statistically significant impact on at least one of the response variables; therefore none of the factors screened out of the RSM analysis. Results for the optimization analysis presented in Table 10 and Table 11 show that there are multiple combinations of the design factors which result in all four of the DNDO performance constraints being satisfied, with the optimized conditions varying significantly depending on which response parameter the results are sorted by (e.g., minimum cost or maximum neutron sensitivity). For the minimum cost design, the optimized factors are: height = 5.4 feet; front polyethylene thickness = 2.9 cm; rear polyethylene thickness = 5.6 cm; ^{3}He pressure = 0.5 atmospheres; and ^{3}He tube separation distance = 4.75 inches. Table 12 presents a comparison of the simulated performance of the optimized ^{3}He RPM system (for the minimum cost design) compared to DNDO requirements. Finally, a validation of the SAIC RPM8 model was performed by comparison of measured and MCNPX simulated results of the absolute neutron detection efficiency. The measured and simulated results show excellent agreement, with a maximum bias of <10%).

Table 12. Optimized ^{3}He RPM System Performance Summary

Response Parameter	Optimized Performance	DNDO Requirement
Absolute efficiency	2.51 cps/ng of ^{252}Cf	$\epsilon_{abs\ n} \geq 2.5$ cps/ng of ^{252}Cf
Intrinsic gamma-neutron detection efficiency	6.70E-8	$\epsilon_{int\ \gamma n} \leq 10^{-6}$
Gamma absolute rejection ratio for neutrons (GARRn)	0.9961	$0.9 \leq$ GARRn ≤ 1.1
Cost	$7,109	$30,000 per system

4.2 ^{6}LI-SAL/P2VN HOMOGENEOUS SCINTILLATION DETECTOR OPTIMIZATION ANALYSIS

Multivariate optimization analysis was performed on ^{6}Li-loaded polymer composite scintillators in the form of thin films which were developed at the University of Tennessee. Lithium-salicylate (enriched to 95% ^{6}Li) was used as the neutron capture reagent for the polymeric composite detectors, and the matrix polymer used to carry the Li-salicylate (Li-Sal) was poly(2-vinylnaphthalene) (P2VN). The detectors also contained a wavelength-shifting fluor (available under the trade name of ADS038FO) which harvests the excitations from surrounding P2VN molecules and then emit light intensely [35].

The purpose of the optimization analysis is to determine optimal values for the detector thickness and weight percent of Li-Sal in the system with respect to the four DNDO response parameters outlined in Table 1. Results from the analysis will not only provide optimal levels for the factors, but will also elucidate the relationship between these factors and the response parameters. Finally, results from this optimization analysis can be used to simulate a large-scale version of an optimized Li-Sal/P2VN detector in a RPM configuration to determine if a large-scale fabricated detector would satisfy the DNDO constraints. In order to perform this optimization analysis, the Birks/Chou equations must be solved for so that the effectiveness of PHD can be simulated and the DNDO response parameters can be calculated. The sample identifications numbers for these four detectors are NN-09-08-10A, NN-09-08-10B, NN-09-08-10C, and NN-09-08-10D. A picture of the four detector films is presented in Figure 19.

Figure 19. Li-Sal/P2VN Film Detectors

Dr. Indraneel Sen, who designed and fabricated the films, has provided the following details regarding the composition of the detectors [36]. The four detectors were prepared using an identical mixture of 650mg P2VN (chemical formula: $C_{12}H_{10}$, ρ=1.45 g/cm^3), 200mg Li-Sal (chemical formula: $HOC_6H_4CO_2Li$, ρ=1.5 g/cm^3) and 60mg ADS038FO for each thin film. However, due to the use of a syringe dropper during the fabrication process, there are slight variations between the total masses (and subsequent thicknesses) of the films. For the purposes of simulation with MCNPX, ADS038FO is modeled as P2VN due to the chemical formula and density of the materials being comparable. The bulk density of the detector material has been calculated by Dr. Sen as 1.5 g/cm^3. The diameter of each detector is approximately 4.5 cm, with varying masses and thicknesses as shown in Table 13.

4.2.1 LIGHT YIELD RESPONSE

In order to fit the parameters for the semi-empirical Birks/Chou equations described in Section 2.2.4.1, several measurements were performed on the fabricated detectors. These measurements include the response of the detectors to beta, alpha, and neutron (combined alpha and triton) sources. The light yield as a function of increasing

detector thickness was also studied. While detector degradation issues made it impossible to fabricate significantly thicker films than those presented in Table 13, the performance of thicker detectors was measured by stacking multiple layers of the thin films. Films were stacked and measured in the following configurations: one layer (film A), two layers (films A+B), three layers (films A+B+C), and four layers (films A+B+C+D). Beta and alpha measurements were performed with the source placed directly on top of the detector(s), and the source and detector(s) being sandwiched between two 2-inch diameter quartz disks to minimize air gaps between the films when stacked. The sandwiched system was then placed directly on top of the PMT (#30584). Teflon tape and a light tight plastic cap were placed over the detector, source, and quartz disk assembly. The light yield response of all of the Li-Sal/P2VN detector systems was measured using a high voltage power supply (HVPS) set at 1000 Volts and an amplifier gain of 120. The beta sources used to irradiate the films are presented in Table 14.

An example of the measured beta response as well as the fitted linear equation relating the measured channel number to the average energy of the beta sources from Table 14 for the three layer system is presented in Figure 20. This equation allows the measured light output (in terms of the channel number) from other particles to be converted into terms of electron equivalent energy (MeVee). The alpha sources used to irradiate the film combinations are presented in Table 15. The films were stacked for the alpha response measurements in an identical manner as was done for the beta sources. An example of the measured alpha response for the two layer (films A+B) system is presented in Figure 21.

Table 13. Lithium-salicylate Film Detector Parameters

	A	B	C	D
Detector Mass (mg)	235	270	300	235
Approx. Thickness (μm)	140	140	160	140

Table 14. Measured Beta Sources

Nuclide	Avg. Energy (MeV)	Activity (μCi)
^{14}C	0.0495	0.58
$^{90}Sr/^{90}Y$	0.1958	0.1
^{36}Cl	0.2513	0.1

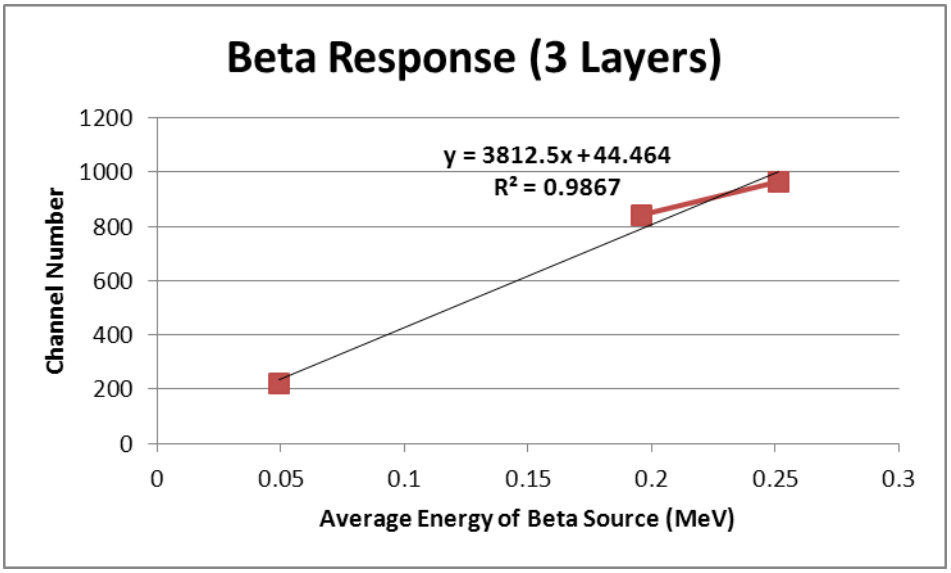

Figure 20. Measured Beta Response for Li-Sal/P2VN Films (Three Layers)

Table 15. Measured Alpha Sources

Nuclide	Energy (MeV)	Activity (nCi)
^{230}Th	4.687	2370
^{241}Am	5.4857	10
^{244}Cm	5.805	10

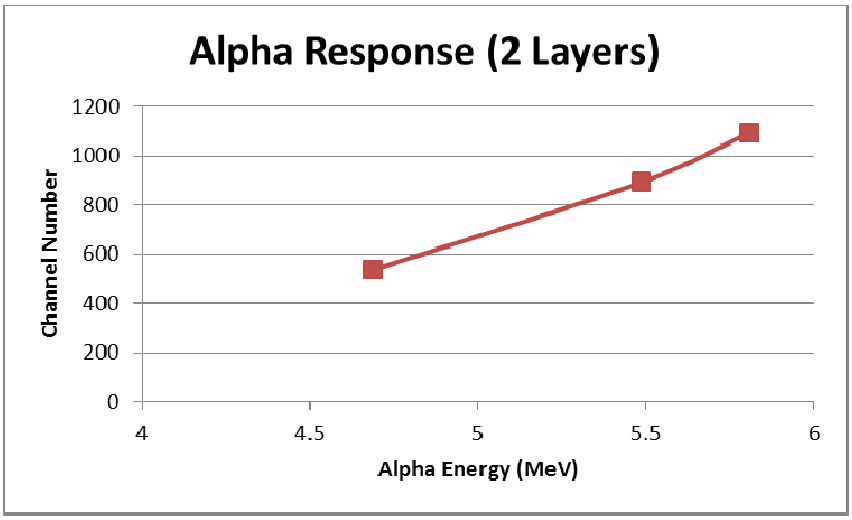

Figure 21. Measured Alpha Response for Li-Sal/P2VN Films (Two Layers)

The neutron response was measured for each of the film combinations using the neutron irradiator described in Section 3.1. The net thermal neutron response was calculated by subtracting the measured results from the cadmium shielded well from the measured results of the plastic well. The measured net thermal neutron response for the three layer system (films A+B+C) is presented in Figure 22.

Using the measured responses of the layer combinations to beta, alpha, and neutron (combined alpha and triton) as well as the stopping power tables from MCNPX for the Li-Sal/P2VN material, the fitting parameters for the Birks/Chou equations are determined for each type of charged particle. In order to accomplish this, an equation for the relationship between electron energy and channel number is generated for each detector film combination by fitting a linear function to the measured beta response (as shown in Figure 20). This equation is then used to convert the measured alpha and neutron response from channel number to equivalent electron energy (MeVee). This allows both the direct comparison of the quantum efficiency for each of the charged particle types and the fitting of the Birks parameters as shown in Figure 23 for the 1 layer detector system.

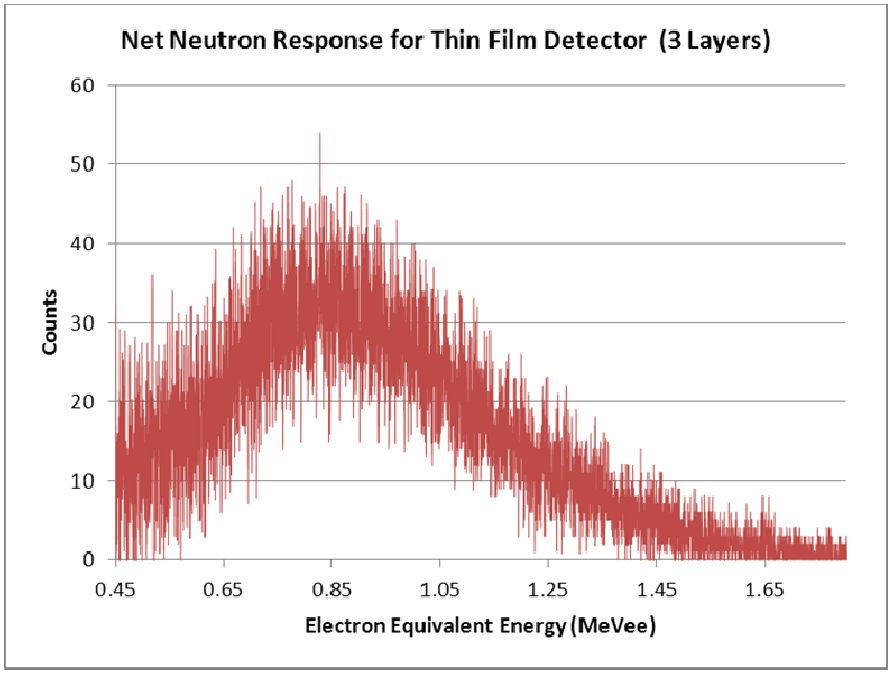

Figure 22. Measured Net Thermal Neutron Response for Three Layer Li-Sal/P2VN Films

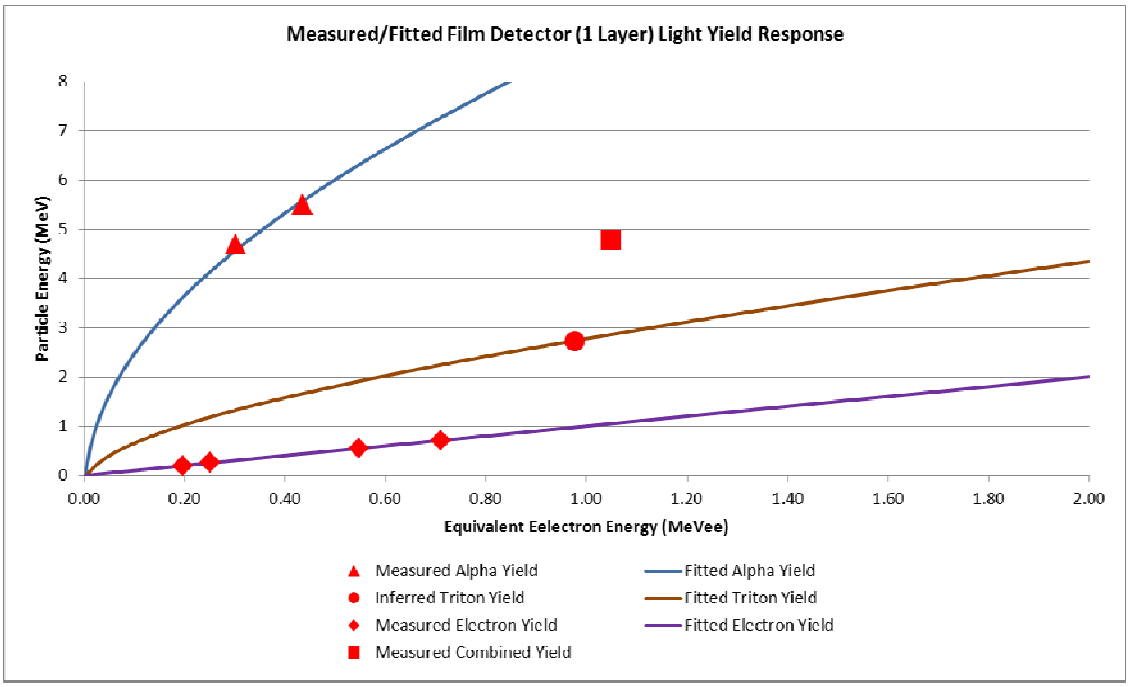

Figure 23. Li-Sal/P2VN Relative Response to Several Charged Particles

The fitting parameters for the Birks equation for each type of charged particle were solved for by fitting the Birks equation to the measured data and minimizing the SSE using the nonlinear Generalized Reduced Gradient (GRG) method within the Microsoft Excel solver. As shown in Figure 23, the fitted Birks/Chou equations for each of the charged particles corresponds very well to the measured responses. As expected, the relative light output of the triton is much greater than that of the alpha particle in accordance with Birks Saturation Law as described in Section 2.2.4.1. The fitting parameters for each of the detector film combinations are presented in Table 16.

Table 16. Birks Parameters for Li-Sal/P2VN Film Detectors

	Alpha Particle Parameters		Triton Particle Parameters		SSE
	kB	C	kB	C	
A	1.08E-02	5.28E-06	4.81E-03	5.82E-06	3.59E-04
A+B	1.30E-02	1.24E-05	4.74E-03	7.82E-06	2.00E-05
A+B+C	1.97E-02	3.05E-07	6.65E-03	8.28E-06	3.32E-03
A+B+C+D	4.57E-02	8.15E-06	7.63E-03	2.38E-05	7.29E-13

The Birks/Chou equations along with these parameters are used in the Matlab post-processing program to calculate the amount of light output (in MeVee) for a given charged particle energy deposition (in MeV from MCNPX simulations). For example, for a one layer detector, the Birks/Chou equations would be:

$$(dL)_{1\ layer,alpha} = (dE)_{alpha}\left\{1 + 1.08E-2\left(\frac{dE}{dx}\right)_{alpha} + 5.28E-6\left(\frac{dE}{dx}\right)^{2}_{alpha}\right\}^{-1}$$

$$(dL)_{1\ layer,triton} = (dE)_{triton}\left\{1 + 4.81E-3\left(\frac{dE}{dx}\right)_{triton} + 5.82E-6\left(\frac{dE}{dx}\right)^{2}_{triton}\right\}^{-1}$$

The optical clarity of the films decreases with increasing detector thickness due to problems in the fabrication process which caused phase separation of the components and agglomeration of molecules [36]. This agglomeration subsequently decreases the quantum efficiency due to increased light scattering and quenching of the scintillation response to thermal neutrons. This effect can be demonstrated by plotting the measured light output (in MeVee) as a function of detector thickness as presented in Figure 24. The impact of the decrease in light output with increasing detector thickness on the Birks fitting parameter (kB) for both alpha and triton particles is presented in Figure 25.

Light output of a scintillator is often expressed in terms of the number of photons produced by 1 MeV gamma rays (photons/MeV). The relative light output in terms of photons/MeV was determined by comparison to a known commercial scintillator (GS20), which emits approximately 3500 photons/MeV [7]. For example, using the same equipment settings of 1000 volts and a gain of 120, the peak net neutron channel number of the reference GS20 detector was measured to be 3,708. For the one layer Li-Sal film, the peak net neutron channel number was measured to be 4,657. Therefore, the relative

light output of the one layer Li-Sal film is calculated to be (3,500*4,657)/3,708 = 4,396 photons/MeV. Figure 26 shows the relative light output of the four Li-Sal detector thicknesses measured compared to that of GS20, again demonstrating the decrease in light output with increasing detector thickness.

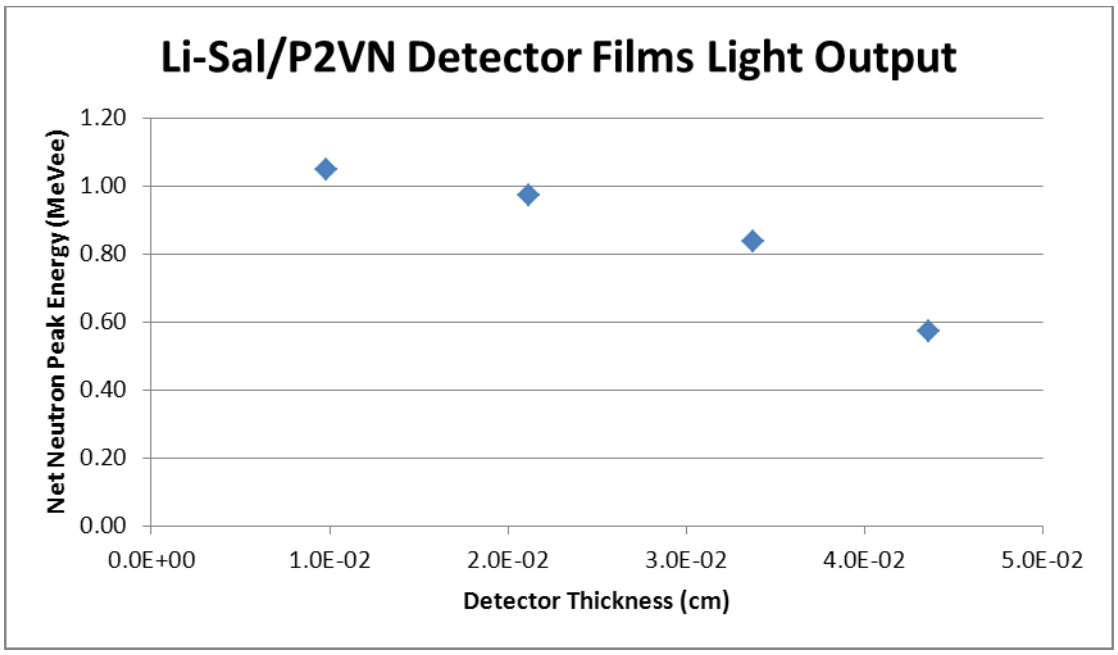

Figure 24. Light Output vs. Li-Sal/P2VN Detector Thickness

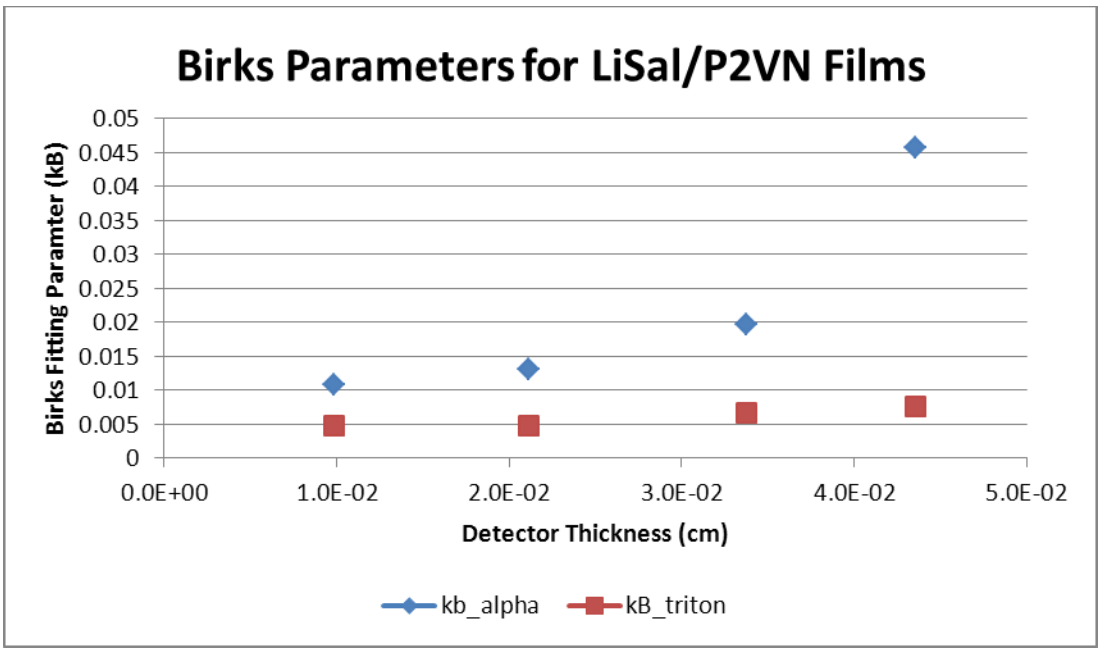

Figure 25. Birks Parameters vs. Li-Sal/P2VN Detector Thickness

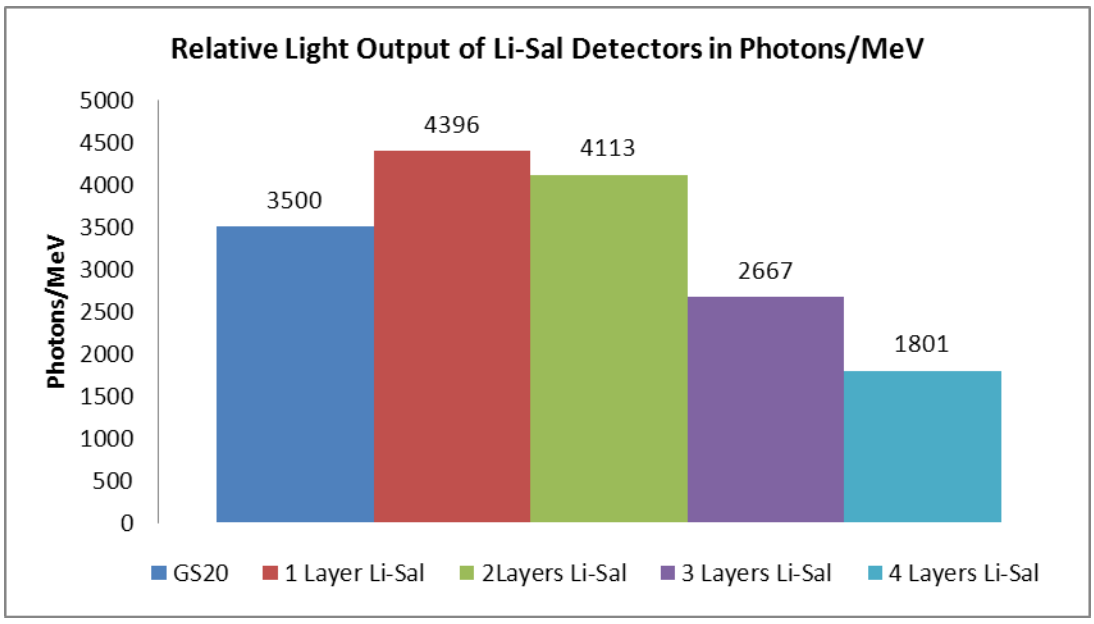

Figure 26. Relative Light Output of Li-Sal Detectors in Photons/MeV

The empirically fit Birks equations allow the conversion of energy deposited (in MeV from MCNPX) into light output (in MeVee) as a function of detector thickness. Previous studies have also shown that the quantum efficiency is also dependent on the mass fraction of Li-Sal in the system [35]. The weight percent of Li-Sal in the NN-09-08-10A, B, C, and D detectors was 21.89 % (200 mg / 910 mg). Table 17 presents the measured results for seven Li-Sal/P2VN thin film detectors with varying amounts of Li-Sal. These results show that the maximum light output occurs at a weight percent of Li-Sal in the Li-Sal/P2VN mixture of ~25%. The multivariate optimization analysis of Li-Sal/P2VN detectors includes weight percent of Li-Sal as an explanatory variable (or factor). Therefore, a 3rd order polynomial was fit to this measured data to provide a relationship between the weight percent of Li-Sal and the relative light output. This equation was used to scale the energy of the pulse generated by the neutron absorption event in the Matlab post-processing program. The equation used to fit this data is presented in Figure 27.

Table 17. Li-Sal/P2VN Detector Relative Light Output vs. Weight Percent Li-Sal (Source: Sen et al, 2010 [35])

Sample #	Weight % Li-Sal	Relative Light Output (to sample 3)
1	10	0.70
2	15	0.70
3	25	1.00
4	40	0.70
5	50	0.60
6	60	0.30
7	75	0.25

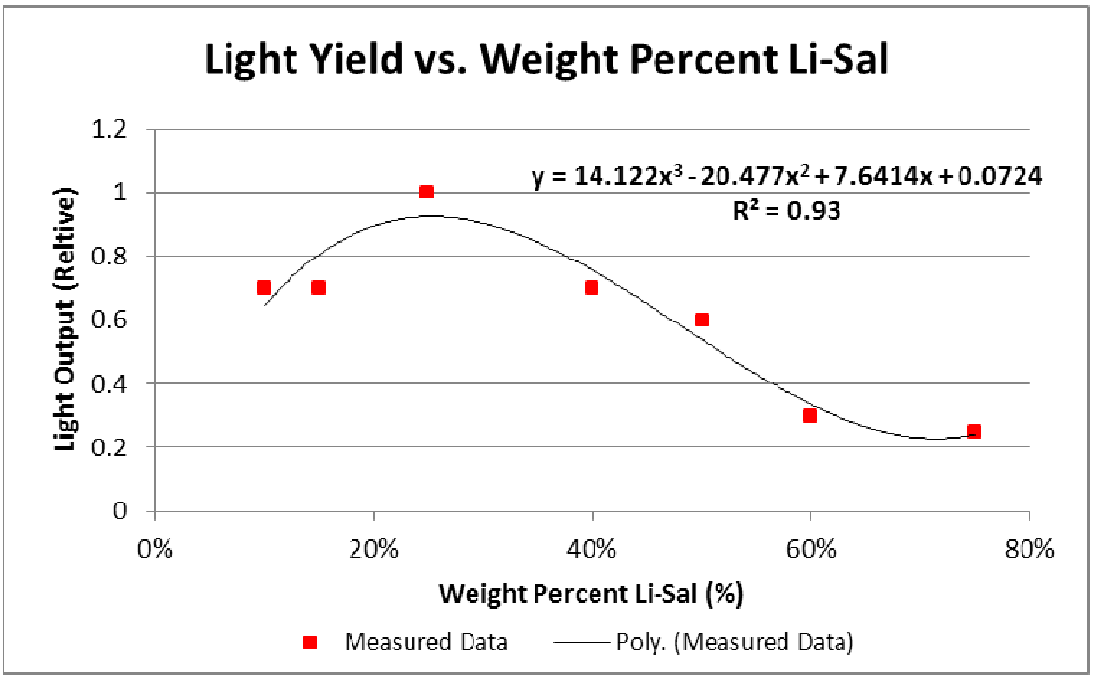

Figure 27. Li-Sal/P2VN Relative Light Output vs. Weight Percent Li-Sal

4.2.2 EXPLANATORY VARIABLE OVERVIEW

As noted previously, the goal of this optimization analysis is to determine optimal levels for the detector thickness and the weight percent of Li-Sal in the detector. The levels at which to vary these factors were determined though discussions with Dr. Sen, and are based on fabrication limitations. The two factors and associated ranges are:

1. The Li-Sal/P2VN detector thickness
    a. 150 µm
    b. 350 µm

2. The weight percent of Li-Sal in the detector
    a. 20 %
    b. 60%

4.2.3 RESPONSE VARIABLE OVERVIEW

The four responses used for the Li-Sal/P2VN optimization analysis are the same as those described in Section 3.3 and are based upon the DNDO criteria shown in Table 1. In order to compare experimental results to those which are simulated, this optimization

analysis is simulated with the detector being placed in the neutron irradiator described in Section 3.1. Therefore, the first response parameter measuring neutron sensitivity is not in terms of counts per second per ng of ^{252}Cf per the DNDO specified configuration (as it was for the ^{3}He RPM optimization analysis), but rather in the fraction form of the absolute neutron detection efficiency. Therefore, the four response parameters are:

1. Absolute neutron detection efficiency
2. Intrinsic gamma-neutron detection efficiency
3. Gamma absolute rejection ratio for neutrons, GARRn
4. Cost

The first three responses were calculated using the methodology outline in Section 3.5 for a scintillator. The cost response function was calculated using a specific version of Equation 3.3-5 modified for Li-Sal/P2VN detectors as shown below:

$$Cost = \left(\frac{fabrication\ cost}{materials\ cost}\right)\left[\left(Mass\ of\ P2VN * {}^{\$200}/_{gram\ P2VN}\right) + \left(Mass\ of\ Li-Sal * {}^{\$2.04}/_{gram\ Li-Sal}\right) + \left(Mass\ of\ \text{ADS038FO} * {}^{\$600}/_{gram\ \text{ADS038FO}}\right)\right]$$

Prices for each the components are taken directly from various vendors, including: P2VN from Polymer Source™ (http://www.polymersource.com), Li-Sal from Sigma-Aldrich® (http://www.sigmaaldrich.com), and ADS038FO from American Dye Source, Inc. (http://www.adsdyes.com). The ratio of the fabrication cost to materials cost was assumed to be 2.

4.2.4 FACTORIAL DESIGN ANALYSIS

Table 18 shows the factorial design matrix generated using SAS for the Li-Sal/P2VN detector system. This design is a 2^2 design (two factors with two levels each), with no replication, which results in four MCNPX cases. This table was used to build MCNPX input files to calculate the response variables for each treatment combination.

The results for each of the four response variables generated by MCNPX simulations (with the simulated LLD set to 0.35 MeVee) are presented in Table 19.

Table 18. Li-Sal/P2VN Factorial Design Matrix

Filename	Thickness (μm)	Weight Percent Li-Sal (%)
LiSal_1	150	20
LiSal _2	150	60
LiSal _3	350	20
LiSal _4	350	60

Table 19. Li-Sal/P2VN Factorial Design Results

Filename	Absolute neutron detection efficiency	Intrinsic γ Detection Efficiency	GARRn	Cost
LiSal_1	9.688E-05	6.844E-06	1.0211	$167.65
LiSal_2	1.970E-05	6.176E-06	1.0668	$84.56
LiSal_3	2.166E-04	1.708E-04	1.2386	$391.19
LiSal_4	1.650E-05	1.680E-04	3.2499	$197.30

Visual analysis of the results presented in Table 19 show two expected results. First, the intrinsic gamma-neutron detection efficiency increases significantly due to the increase in detector thickness (see cases 1 and 2 compared to cases 3 and 4). Also, the absolute neutron detection efficiency increased with increasing thickness.

At this point, the SAS software package was used to analyze the results. Recall that each of the response variables must first be analyzed independently to determine statistically significant factors. Rather than reporting the detailed results of the factorial ANOVA for each of the four response variables, Table 20 shows a summary of the main effects and two-way interactions which were identified as being statistically significant for each of the response variables. Note that the R^2 values for each of the response variables are all close to 1, indicating that the majority of the variability in the response parameters can be explained with main effects and two-way interactions between those effects. These results showed that both factors have a statistically significant impact on multiple response parameters. Therefore, neither of the factors can be screened out of the following response surface design analysis.

4.2.5 RESPONSE SURFACE DESIGN ANALYSIS

The next step in the optimization methodology is to expand the factorial design analysis to a central composite design, to estimate second-degree polynomial models for each of the response variables. Using Equation 2.4-5 from Section 2.4, the α value required for rotatability is calculated as $\alpha = (2^k)^{1/4} = (2^2)^{1/4} = 1.4142$. Table 21 presents the natural and coded variables for the Li-Sal/P2VN central composite design.

These design levels are used by SAS to construct the Li-Sal/P2VN CCD Matrix as presented in Table 22. The results for each of the four response variables generated by all 16 MCNPX simulations are presented in Table 38 of Appendix A.

Table 20. Li-Sal/P2VN Factorial Design Analysis Results Summary

	Absolute neutron detection efficiency	Intrinsic gamma-neutron detection efficiency	GARRn	Cost
R^2	0.8897	0.9982	0.6565	1.00
thickness	X	X		X
wt_percent	X	X	X	
thickness*thickness		X		X
wt_percent* thickness			X	
wt_percent* wt_percent	X		X	

Table 21. Li-Sal/P2VN Central Composite Design Levels

Design Factors	-1.4142	-1	0	1	1.4142
X1 = Detector Thickness (μm)	108.58	150.00	250.00	350.0	391.42
X2 = Weight % Li-Sal (%)	11.72	20.00	40.00	60.00	68.28

Table 22. Li-Sal/P2VN Central Composite Design Matrix (Coded Variables)

Filename	Detector Thickness (µm)	Weight % Li-Sal (%)
LiSal_1	-1	-1
LiSal_2	-1	1
LiSal_3	1	-1
LiSal_4	1	1
LiSal_5	-1.4142	0
LiSal_6	1.4142	0
LiSal_7	0	-1.4142
LiSal_8	0	1.4142
LiSal_9	0	0
LiSal_10	0	0
LiSal_11	0	0
LiSal_12	0	0
LiSal_13	0	0
LiSal_14	0	0
LiSal_15	0	0
LiSal_16	0	0

At this point, the SAS software package was used to perform least squares regression analysis of the data and to fit quadratic equations for each of the response variables. Table 23 presents the results of the regression analysis, and shows that the total R^2 values for the four different response variables are very close to 1 indicating that the quadratic models are able to predict the simulated responses very well.

A surface plot generated using the quadratic models of the neutron count rate response as a function of Li-Sal weight percent and the thickness of the detector is presented in Figure 28. As shown in Figure 28, the neutron count rate increases with increasing Li-Sal weight percent up to approximately 33% where the effects of quenching begin to shift the peak pulse height below the LLD cutoff, thus decreasing the count rate. Figure 28 also shows that as the thickness of the detector increases, the count rate initially increases due to the additional absorbing material but then decreases due to self-absorption within the detector. These results are expected due to the detector clarity decreasing with increasing detector thickness from the phase separation of the components as discussed in Section 4.2.1.

Table 23. Li-Sal/P2VN Central Composite Design Quadratic Model Fit

	Absolute Neutron Detection Efficiency	Intrinsic γ/n Detection Efficiency	GARRn	Cost
Linear	0.2265	0.7911	0.4262	0.9687
Quadratic	0.6474	0.2069	0.1838	0.0000
Cross-Product	0.0157	0.0002	0.2032	0.0313
Total	0.8897	0.9982	0.8131	1.0000

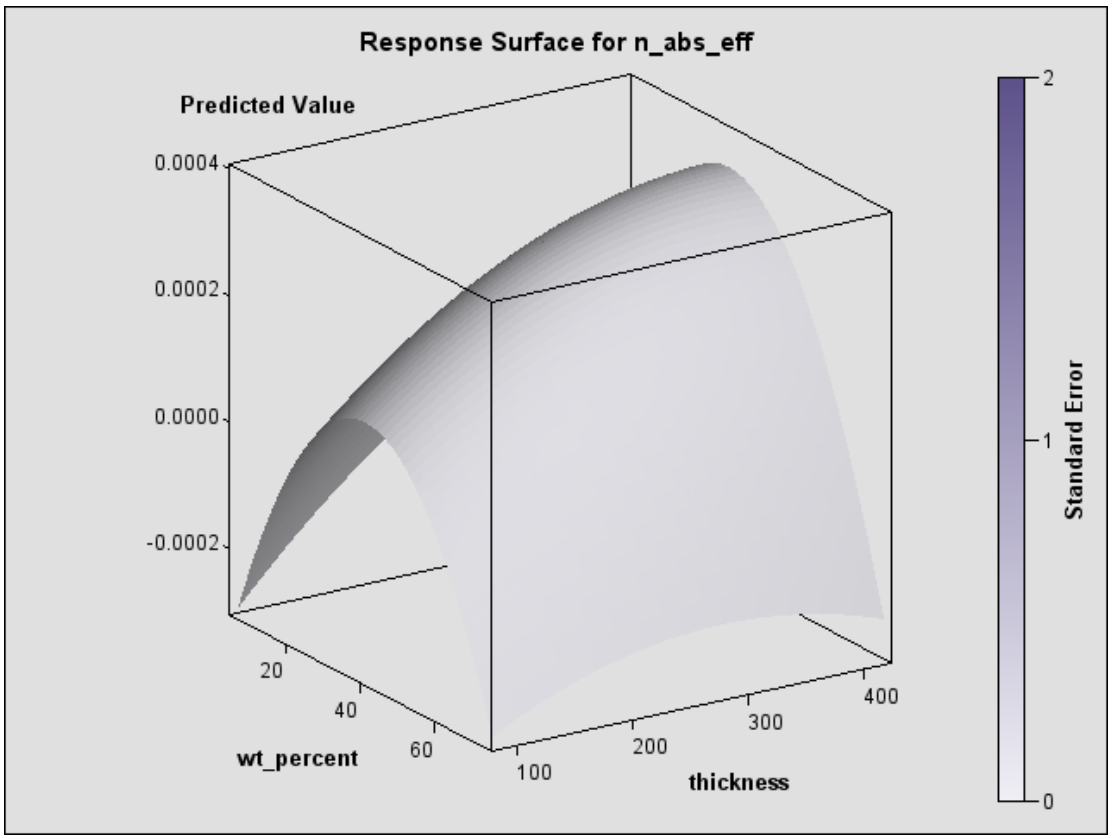

Figure 28. Example Surface Plot Generated from the Li-Sal/P2VN CCD Analysis

4.2.6 CONSTRAINED MULTIVARIATE OPTIMIZATION

The final step in the optimization methodology is to use the quadratic models developed by the RSM analysis to search for an optimal design configuration which satisfies our performance criteria. From Table 1, the optimized detector must satisfy the following constraints:

1. Absolute neutron detection efficiency ≥ 0.0012
2. Intrinsic gamma-neutron detection efficiency $\leq 10^{-6}$
3. $0.9 \leq$ GARRn ≤ 1.1 at 10 mR/h exposure
4. Cost $\leq$ \$30,000

These constraints were programmed into SAS; however, no satisfactory factor combinations were generated that satisfied all of the response constraints. Therefore, the constraint on the absolute neutron detection efficiency was relaxed to ≥ 0.0002. A list of satisfactory detector combinations was generated and sorted by maximum absolute neutron detection efficiency as shown in Table 24.

Table 24. Li-Sal/P2VN Optimized Results by Maximum Neutron Sensitivity

Obs	Detector Thickness (μm)	Weight % Li-Sal (%)	n_abs_eff	g_int_eff	GARRn	Detector Film Cost
1	185	38	2.357E-04	9.360E-7	0.9450	\$160.66
2	185	36	2.345E-04	9.580E-7	0.9457	\$165.78
3	185	40	2.342E-04	9.250E-7	0.9469	\$155.53
4	180	38	2.306E-04	5.420E-7	0.9424	\$156.31
5	185	34	2.306E-04	9.920E-7	0.9490	\$170.90

4.2.7 ^{6}LI-SAL/P2VN HOMOGENEOUS SCINTILLATION DETECTOR RPM SYSTEM RESULTS

In order to determine if a large-scale version of an optimized ^{6}Li-Sal/P2VN detector would satisfy DNDO constraints, the detector conditions resulting the best performance from Table 24 (observation 1) were modeled in a RPM-type system similar to the SAIC RPM8-system described in Section 4.1. The Li-Sal/P2VN detector was modeled with dimensions of ~20 inches wide, 72 inches tall (6 feet), and 7.28E-3 inches (185 μm) thick at 38% by weight of Li-Sal. The Li-Sal/P2VN RPM detection system was modeled with a ^{252}Cf source at 2 meters per the DNDO guidelines specified in Section 3.3, and all four DNDO detector response parameter were calculated. The performance of the Li-Sal/P2VN RPM system is presented in Table 25.

As shown in Table 25, the performance of the detector is not sufficient to satisfy the DNDO requirements. The high cost of the system is dominated by the price of ADS, which at $600 per gram, is significant at this size of a detector. However, this price would likely be significantly less if bought in bulk for this application. The neutron sensitivity could be improved by increasing the detector thickness or weight fraction of Li-Sal; however, this would come at a sacrifice of light output and discrimination ability. The increase of the intrinsic gamma-neutron detection efficiency compared to that presented in Table 24 is most likely due to the significant increase in detector volume which allows a larger portion of the energy from secondary electrons generated from photon interactions to be deposited within the detector. Additional issues associated with Li-Sal/P2VN detectors are that the material is hygroscopic and brittle, thus field deployment of these detectors would be challenging. In order to address these issues, current research at UT related to detector development for DNDO applications has shifted towards the use of Lithium Fluoride (LiF) as a neutron capture reagent. Lithium Fluoride is not hygroscopic and has a much higher intrinsic ^{6}Li weight fraction. The higher weight fraction of ^{6}Li in LiF would provide greater neutron sensitivity at a decreased thickness, thus addressing both the issue of neutron sensitivity and discrimination ability.

Table 25. Optimized Li-Sal/P2VN RPM System Performance Summary

Response Parameter	Optimized Performance	DNDO Requirement
Absolute neutron detection efficiency	1.31 cps/ng of ^{252}Cf	$\epsilon_{abs\ n} \geq 2.5$ cps/ng of ^{252}Cf
Intrinsic gamma-neutron detection efficiency	2.75E-5	$\epsilon_{int\ \gamma n} \leq 10^{-6}$
Gamma absolute rejection ratio for neutrons (GARRn)	1.035	$0.9 \leq$ GARRn ≤ 1.1
Cost	$94,978.89	$30,000 per system

4.2.8 ^{6}LI-SAL/P2VN HOMOGENEOUS SCINTILLATION DETECTOR MODEL VALIDATION

Table 26 presents a comparison of the results of the measured detector performance of the Li-Sal/P2VN films and the simulated results using MCNPX and the fitted Birks/Chou equations.

The results presented in Table 26 show that the simulated neutron absorption rate is significantly greater than the measured net neutron count rate. This discrepancy is mainly due to the simulated results being a measurement of the number of ^{6}Li absorption events within the detector while the measured results are a measurement of scintillation light which reaches the PMT as a result of neutron absorption events. Therefore, the MCNPX simulated result does not take self-absorption of the scintillation photons generated within the detector into consideration or light losses between the detector and the PMT. Table 26 shows that the measured and MCNPX simulated PHS peak energy show excellent agreement, with a maximum bias of <6%. This close agreement shows that the calculated Birks/Chou parameters fit the data well throughout the range of detector thicknesses analyzed.

4.2.9 ^{6}LI-SAL/P2VN HOMOGENEOUS SCINTILLATION DETECTOR RESULTS SUMMARY AND CONCLUSIONS

Multivariate optimization of Li-Sal/P2VN detectors was successfully performed utilizing the methodology outlined in this dissertation. The analysis was performed using two factors (detector thickness and weight percent Li-Sal) and four response parameters (the absolute neutron detection efficiency, the intrinsic gamma-neutron detection

efficiency, the gamma absolute rejection ratio for neutrons, and cost). The Birks/Chou equations were successfully solved for allowing the calculation of the discrimination ability from PHD. Both of the factors analyzed were shown to have a statistically significant impact on at least one of the response variables; therefore neither of the factors screened out of the RSM analysis. For the minimum cost design, the optimized factors are a detector thickness of 185 μm and 38% Li-Sal by weight. Results for the optimization analysis presented in Table 25 show that the optimized Li-Sal/P2VN detector in a RPM-type configuration does not satisfy the DNDO requirements for neutron sensitivity, discrimination ability, or cost. Also, due to the Li-Sal/P2VN detectors being hygroscopic and brittle, field deployment of these detectors would be challenging. Therefore, current research at UT related to detector development for DNDO applications has shifted towards LiF-based systems, which are not hygroscopic and have a higher intrinsic ^{6}Li weight fraction. The higher weight fraction of ^{6}Li in LiF would provide greater neutron sensitivity at a decreased thickness, thus addressing both the issue of neutron sensitivity and discrimination ability.

A comparison of measured and MCNPX simulated results for the detector within the neutron irradiator show that while the bias in the net neutron count rate was large (~100%) due to the simulated count rate not including detector self-absorption and light losses between the detector and PMT, excellent agreement was shown for the PHS peak position (which utilized the calculated Birks/Chou equations).

Table 26. Li-Sal/P2VN Validation Results

	Net Neutron Count Rate			PHS Peak Energy (MeVee)		
	Measured	**Simulated**	**% Diff**	**Measured**	**Simulated**	**% Diff**
A	36.75	79.77	117.04%	1.05	1.02	-2.76%
A+B	92.18	164.23	78.16%	0.98	0.94	-3.61%
A+B+C	124.79	253.79	103.38%	0.84	0.82	-2.21%
A+B+C+D	196.84	320.59	62.87%	0.57	0.54	-5.54%

4.3 ^{10}B-BASED DETECTOR OPTIMIZATION ANALYSIS

In order to explore the possibility of utilizing ^{10}B-based plastic scintillation detectors to satisfy DNDO requirements, three commercially available detectors in the form of 2-inch diameter disks of varying thicknesses were analyzed for multivariate optimization analysis. These organic scintillators were procured from Eljen Technology and had either 5% or 1 % natural boron by weight (where the isotopic fraction of ^{10}B in natural boron is 19.9%). A picture of the ¾-inch thick Eljen detector with 5% natural boron by weight is presented in Figure 29. Relevant parameters for each of the three detectors measured for light output is presented in Table 27.

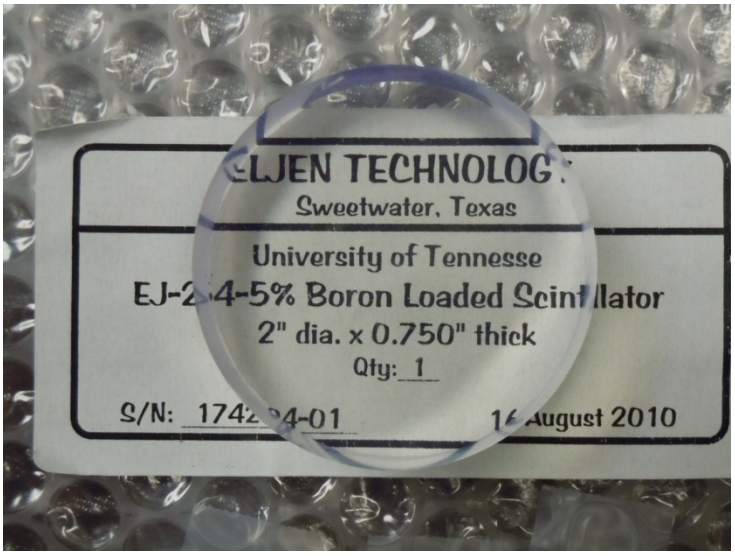

Figure 29. Eljen ^{10}B-Based Plastic Scintillation Detector

Table 27. Eljen ^{10}B-Based Plastic Scintillation Detector Parameters (Source: Eljen Technology, 2010 [37])

Eljen Product ID	Thickness (inches)	Weight Percent B (natural)	Density (g/cm^3)	Carbon Atom Density (atoms/cm^3)	Hydrogen Atom Density (atoms/cm^3)	^{10}B Atom Density (atoms/cm^3)
EJ-254	0.75	5%	1.026	4.44E22	5.18E22	5.68E22
EJ-254	0.25	5%	1.026	4.44E22	5.18E22	5.68E22
EJ-254	0.25	1%	1.021	4.62E22	5.16E22	1.14E20

Two methods of n/γ discrimination were studied for the ^{10}B-based plastic scintillation detectors. The first discrimination method tested is based upon the use of the pulse height, and the second discrimination method is based on coincidence counting. Coincidence counting is possible by counting the simultaneous detection of the charged particle reaction products from the ^{10}B neutron absorption event (alpha and ^{7}Li) and the 478 keV prompt gamma that is emitted by the excited ^{7}Li nucleus in 94% of the thermal neutron absorption reactions. Analysis of the potential use of pulse height as a discrimination method is presented in the following section.

4.3.1 LIGHT YIELD RESPONSE

The light yield response of the detectors presented in Table 27 was measured to determine the feasibility of utilizing pulse height for n/γ discrimination. In order to accomplish this, the parameters for the semi-empirical Birks/Chou equations for both of the neutron absorption reaction products (alpha and ^{7}Li) were solved for using beta, alpha, and neutron (combined alpha and ^{7}Li) sources. The sources utilized for these measurements are the same as those used in the Li-Sal/P2VN analysis presented in Section 4.2.1.

The fitted Birks/Chou equations allow for the simulation of the detector PHS as well as the calculation of the DNDO response parameters when utilizing PHD. Due to the similarities in the methodology for measuring the light yield response and the fitting of the Birks parameters, only a summary of the results of this analysis for the B-loaded Eljen detectors is presented here and the reader is directed to Section 4.2.1 for a detailed discussion of this procedure. The neutron response was measured for each of the Eljen detectors using the neutron irradiator described in Section 3.1, with the HVPS set at 1000 Volts and the amplifier set to a gain of 75. The net thermal neutron response was calculated by subtracting the measured results from the cadmium shielded well from the measured results of the plastic well. The measured net thermal neutron response for the 0.75-inch thick Eljen detector at 5% boron is presented in Figure 30.

Using the measured responses of the detectors to beta, alpha, and neutron (combined alpha and ^{7}Li) as well as the stopping power tables from MCNPX for the EJ-254 material, the fitting parameters for the Birks equations are fitted for each type of

charged particle. Figure 31 shows the fitted Birks/Chou equations to the 0.25-inch thick Eljen detector at 1 percent natural boron. It is interesting to note the from the figure dominance of the alpha particle in the relative light output as compared to the ^{7}Li particle. This is due to the larger mass and stopping power of the ^{7}Li particle, which results in a greater ionization potential and less light output as discussed in Section 2.2.4.1.

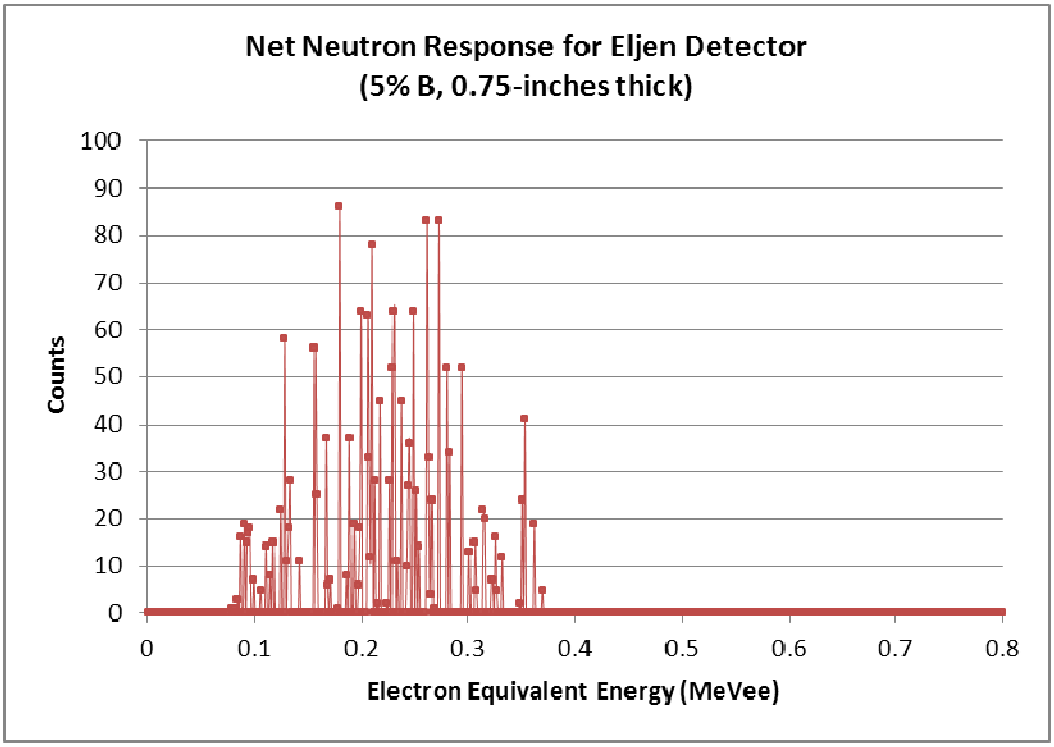

Figure 30. Measured Net Thermal Neutron Response for Eljen Detector (5%B, 0.75-in Thick)

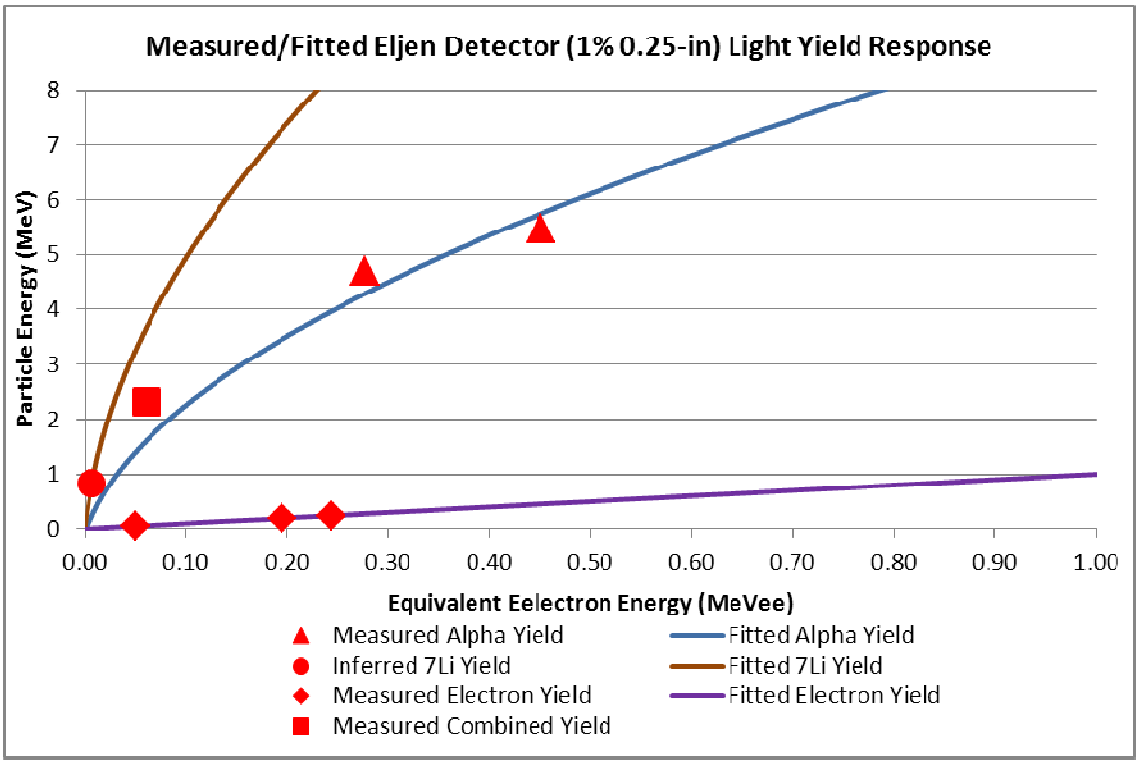

Figure 31. Eljen Detector Relative Response to Several Charged Particles

Preliminary calculations using the fitted Birks/Chou equations showed that due to the low net neutron peak energy, PHD is an ineffective method of discriminating between neutrons and photons. For example, approximately 95% of the neutron pulses are rejected using a LLD setting of 200 keV, and only ~50% of the photon pulses are rejected. This result is expected for several reasons. First, the lower Q-value of the $^{10}B(n,\alpha)$ reaction compared to that of the $^{7}Li(n,\alpha)$ reaction (2.3 MeV vs. 4.78 MeV, respectively) results in less energy being deposited in the scintillating material and thus a lower energy pulse. Secondly, due to the heavier neutron absorption reaction products of the $^{10}B(n,\alpha)$ reaction compared to that of the $^{7}Li(n,\alpha)$ reaction (alpha and ^{7}Li vs. alpha and triton, respectively), greater ionization quenching in the boron event results in a much lower light output. Finally, the thickness of these detectors is such that a significant portion of the incident photons interact within the detector producing an incorrectly categorized neutron pulse. Therefore, the optimization analysis was performed using coincidence counting of the 478 keV prompt gamma that is emitted by the excited ^{7}Li nucleus in 94% of the thermal neutron absorption reactions by ^{10}B.

In order to increase the probability of the coincidence counts, the system was analyzed in a sandwich-type configuration where the boron loaded detector (Model IDL EJ-254) is placed between two Eljen plastic scintillators (Model ID: EJ-200). The purpose of the optimization analysis is to determine optimal values for the EJ-254 detector thickness, the front EJ-200 detector thickness, and the thickness of the EJ-200 detector in the rear with respect to the four DNDO response parameters outlined in Table 1. Results from the analysis will not only provide optimal levels for the factors, but will also elucidate the relationship between these factors and the response parameters.

The efficiency of the coincidence counting was simulated using MCNPX coincidence tallies where a coincidence count is registered when both the boron loaded detector and one of the plastic scintillation detectors generate a pulse from the same neutron absorption event. The pulse in the boron loaded detector originates from a minimum energy deposition from the alpha and ^{7}Li neutron absorption reaction products, while the pulse from the plastic scintillator originates from the energy deposition from an electron generated by the interaction of the 478 keV photon. In order to increase the neutron sensitivity and decrease the probability for photon interactions, the boron-loaded detector was modeled with 10% boron by weight at 100% ^{10}B. The sandwiched detector system was modeled in a RPM-type configuration similar to the SAIC RPM8 system described in Section 4.1. The neutron detector was modeled with dimensions of ~20-inches wide, 72 inches tall (6 feet), and a varying thickness. The neutron sensor was surrounded by a ¼-inch thick steel shield around the back and sides and a ½-inch thick steel shield in the front. A ^{252}Cf source surrounded by 0.5 cm of lead and 2.5 cm of polyethylene was modeled at 2 meters perpendicular to the geometric midpoint of the RPM in accordance with the DNDO test configuration specifications.

4.3.2 EXPLANATORY VARIABLE OVERVIEW

For this detector system, the following explanatory detector parameters and ranges were chosen:

1. The EJ-254 (boron loaded) detector thickness
    a. 0.3 inches
    b. 0.6 inches
2. The front EJ-200 (no boron) detector thickness
    a. 0.55 inches
    b. 1.45 inches
3. The rear EJ-200 (no boron) detector thickness
    a. 1 inch
    b. 2 inches

Figure 32 shows X-Z and X-Y views of the MCNPX Eljen RPM model with the explanatory variables outlined, respectively.

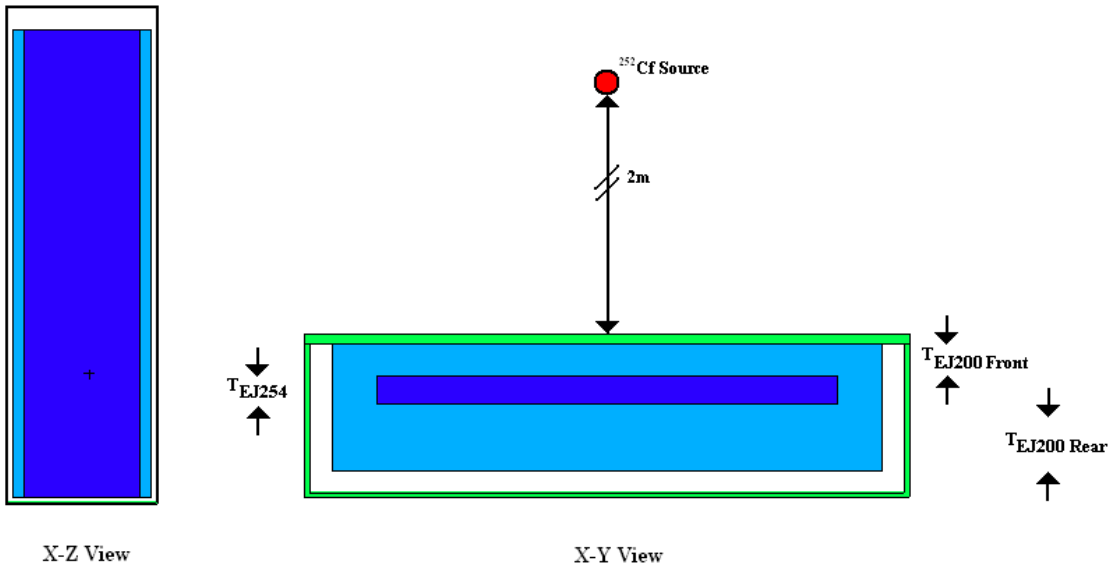

Figure 32. X-Z and X-Y Views of the MCNPX ^{10}B-Based RPM Model

4.3.3 RESPONSE VARIABLE OVERVIEW

The three responses used for the RPM analysis are the same as those described in Section 3.3 (with the exception of cost) which are based upon the DHS criteria shown in Table 1.

1. Absolute neutron detection efficiency (counts per second / ng ^{252}Cf)
2. Intrinsic gamma-neutron detection efficiency
3. Gamma absolute rejection ratio for neutrons, GARRn

Cost was excluded as a response parameter due to the lack of information related to large scale plastic scintillators such as those used in this analysis. However, discussions with Eljen Technology representatives suggest that the boron loaded detector alone would cost in the tens of thousands of dollars [38]. The three response parameters were calculated using the methodology outline in Section 3.5 for a non-scintillator.

4.3.4 FACTORIAL DESIGN ANALYSIS

Table 28 shows the factorial design matrix generated using SAS for the Eljen detector system. This design is a 2^3 design (three factors with two levels each), with no replication, which results in eight MCNPX cases. This table was used to build MCNPX input files to calculate the response variables for each treatment combination.

The results for each of the three response variables generated by MCNPX simulations are presented in Table 29.

Table 28. ^{10}B-Based Detector Factorial Design Matrix

Filename	EJ-254 thickness (inches)	EJ-200 Front Thickness (inches)	EJ-200 Rear Thickness (inches)
Eljen_1	0.30	0.55	1.00
Eljen_2	0.30	0.55	2.00
Eljen_3	0.30	1.45	1.00
Eljen_4	0.30	1.45	2.00
Eljen_5	0.60	0.55	1.00
Eljen_6	0.60	0.55	2.00
Eljen_7	0.60	1.45	1.00
Eljen_8	0.60	1.45	2.00

Table 29. ^{10}B-Based Detector Factorial Design Results

Filename	Neutron Sensitivity (cps/ng ^{252}Cf)	Intrinsic γ Detection Efficiency	GARRn
Eljen_1	1.3155	2.132E-03	3.7113
Eljen_2	1.9640	2.279E-03	2.9907
Eljen_3	1.8530	2.246E-03	2.9499
Eljen_4	2.3648	2.264E-03	2.5867
Eljen_5	1.6002	3.623E-03	4.7807
Eljen_6	2.3309	3.945E-03	3.8976
Eljen_7	2.0842	3.906E-03	4.0138
Eljen_8	2.8026	4.097E-03	3.4198

Next, the SAS software package was used to analyze the results. Recall that each of the response variables must first be analyzed independently to determine statistically significant factors. Rather than reporting the detailed results of the factorial ANOVA for each of the four response variables, Table 30 shows a summary of the main effects and two-way interactions which were identified as being statistically significant for each of the response variables. Note that the R^2 values for each of the response variables are all close to 1, indicating that the majority of the variability in the response parameters can be explained with main effects and two-way interactions between those effects. These results showed that all three factors have a statistically significant impact on multiple response parameters. Therefore, none of the factors can be screened out of the following response surface design analysis.

Table 30. ^{10}B-Based Detector Factorial Design Analysis Results Summary

	Absolute neutron detection efficiency	Intrinsic gamma-neutron detection efficiency	GARRn
R^2	0.9872	0.9893	0.9888
detector_th	X	X	X
front_th	X		X
rear_th	X		X
detector_th*detector_th			X
front_th*detector_th			
front_th*front_th	X		X
rear_th*detector_th			
rear_th*front_th			X
rear_th*rear_th	X		X

4.3.5 RESPONSE SURFACE DESIGN ANALYSIS

The next step in the optimization methodology is to expand the factorial design analysis to a central composite design, to estimate second-degree polynomial models for each of the response variables. Using Equation 2.4-5 from Section 2.4, the α value required for rotatability is calculated as $\alpha = (2^k)^{1/4} = (2^3)^{1/4} = 1.6818$. Table 31 presents the natural and coded variables for the Eljen detector central composite design. These design levels are used by SAS to construct the Eljen detector CCD Matrix as presented in Table 32. The results for each of the three response variables generated by MCNPX simulations for all 24 cases are presented in Table 39 of Appendix A.

Table 31. ^{10}B-Based Detector Central Composite Design Levels

Design Factors	-1.6818	-1	0	1	1.6818
X1 = EJ-254 thickness (inches)	0.20	0.30	0.45	0.60	0.70
X2 = EJ-200 front th. (inches)	0.24	0.55	1.00	1.45	1.76
X3 = EJ-200 rear th. (inches)	0.66	1.00	1.50	2.00	2.34

Table 32. ^{10}B-Based Detector Central Composite Design Matrix (Coded Variables)

Filename	EJ-254 thickness (inches)	EJ-200 Front Thickness (inches)	EJ-200 Rear Thickness (inches)
Eljen_1	-1	-1	-1
Eljen_2	-1	-1	1
Eljen_3	-1	1	-1
Eljen_4	-1	1	1
Eljen_5	1	-1	-1
Eljen_6	1	-1	1
Eljen_7	1	1	-1
Eljen_8	1	1	1
Eljen_9	-1.6818	0	0
Eljen_10	1.6818	0	0
Eljen_11	0	-1.6818	0
Eljen_12	0	1.6818	0
Eljen_13	0	0	-1.6818
Eljen_14	0	0	1.6818
Eljen_15	0	0	0
Eljen_16	0	0	0
Eljen_17	0	0	0
Eljen_18	0	0	0
Eljen_19	0	0	0
Eljen_20	0	0	0
Eljen_21	0	0	0
Eljen_22	0	0	0
Eljen_23	0	0	0
Eljen_24	0	0	0

The SAS software package was used to perform least squares regression analysis of the data and to fit quadratic equations for each of the response variables. Table 33 presents the results of the regression analysis, and shows that the total R^2 values for the three different response variables are very close to 1 indicating that the quadratic models are able to predict the simulated responses very well.

A surface plot generated using the quadratic models of the absolute neutron detection efficiency as a function of the front and rear EJ-200 thicknesses is presented in Figure 33.

Table 33. ^{10}B-Based Detector Central Composite Design Quadratic Model Fit

	Absolute Neutron Detection Efficiency	**Intrinsic γ/n Detection Efficiency**	**GARRn**
Linear	0.9079	0.9754	0.9099
Quadratic	0.0752	0.0104	0.0680
Cross-Product	0.0042	0.0035	0.0108
Total	0.9872	0.9893	0.9888

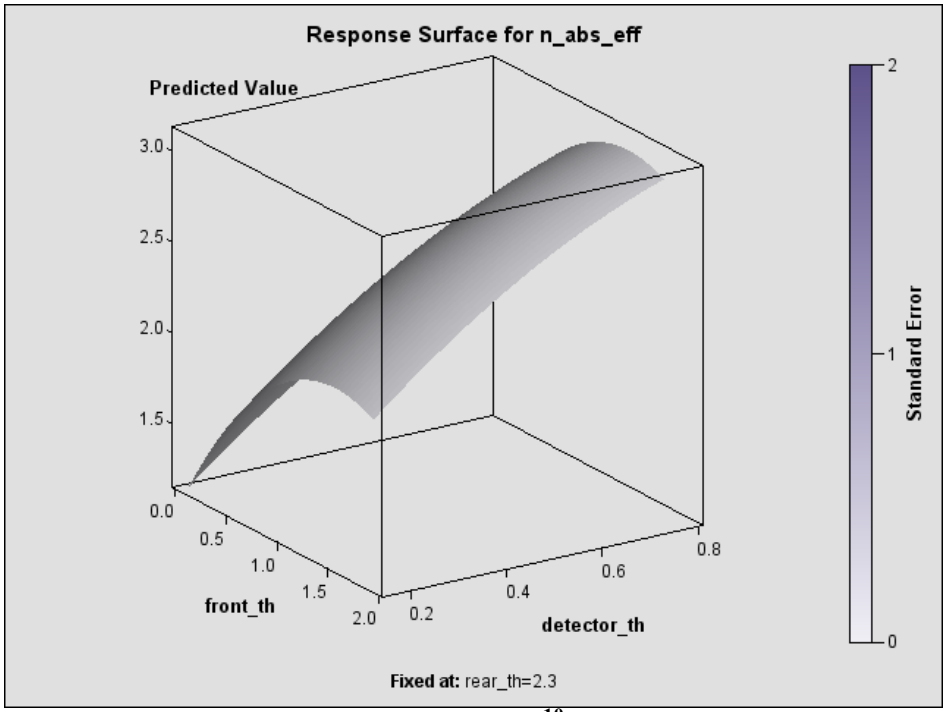

Figure 33. Surface Plot Generated from the ^{10}B-Based Detector CCD Analysis

As shown in Figure 33, the absolute neutron detection efficiency increases with increasing front EJ-200 thickness up to approximately 1.38 inches where the effects of neutron shielding begin to result in the decrease in the neutron sensitivity. Figure 33 also shows that as the rear EJ-200 thickness of the increases, the absolute neutron detection efficiency increases in a linear manner with increasing thickness due to this detector also acting as a reflector of neutrons back towards the EJ-254 detector.

4.3.6 CONSTRAINED MULTIVARIATE OPTIMIZATION

The next step in the optimization methodology is to use the models developed by the CCD analysis to search for an optimal design configuration which satisfies our performance criteria. From Table 1, the optimized detector must satisfy the following constraints:

1. Absolute neutron detection efficiency $\geq$ 2.5 cps/ng of ^{252}Cf
2. Intrinsic gamma-neutron detection efficiency $\leq 10^{-6}$
3. $0.9 \leq$ GARRn ≤ 1.1 at 10 mR/h exposure

These constraints were programmed into SAS; however, no satisfactory factor combinations were generated that satisfied all of the response constraints. Therefore, the constraints were relaxed to the following levels to find an optimal configuration:

1. Absolute neutron detection efficiency $\geq$ 2.5 cps/ng of ^{252}Cf
2. Intrinsic gamma-neutron detection efficiency $\leq 3x10^{-3}$
3. $0.9 \leq$ GARRn ≤ 2.8 at 10 mR/h exposure

A list of satisfactory detector combinations was generated and sorted by descending absolute neutron detection efficiency as shown in Table 34.

Table 34. Optimized ^{10}B-Based Detector Results by Maximum Neutron Sensitivity

Obs	EJ254_th	front_th	rear_th	n_abs_eff	g_int_eff	GARRn
1	0.35	1.55	2.30	2.5601	2.568E-03	2.7956
2	0.35	1.50	2.30	2.5592	2.582E-03	2.7858
3	0.35	1.45	2.30	2.5560	2.594E-03	2.7789
4	0.35	1.55	2.25	2.5530	2.577E-03	2.7821
5	0.35	1.50	2.25	2.5519	2.590E-03	2.7731

In order to gain a better understand of the behavior of the detector, a two-dimensional overlaid contour plots was generated which shows how the defined constraints on the response parameters are satisfied as a function of two factors. Figure 34 presents an overlaid contour plot as a function of the thickness of the front and rear EJ-200 detector thicknesses at a fixed EJ-254 thickness of 0.35 inches. Analysis of this contour plot shows that at only a very small region satisfies the constraints on all three of the reduced response parameters. A decrease in the optimal rear detector thickness initially results in the loss of neutron sensitivity, and further decrease results in exceeding the constraint on GARRn. This result is expected since a decrease in the rear thickness results in fewer neutrons being reflected back to the boron-loaded detector. Further decreases in the rear thickness lowers the neutron count rate to the point that mis-categorized photons dominate the count rate and increase the GARRn. Increasing or decreasing the optimal front detector thickness also results in exceeding constraints on different response parameters. This complexity in the overall performance of the detection system is primary basis of why a multivariate statistical analysis is required to properly optimize these systems.

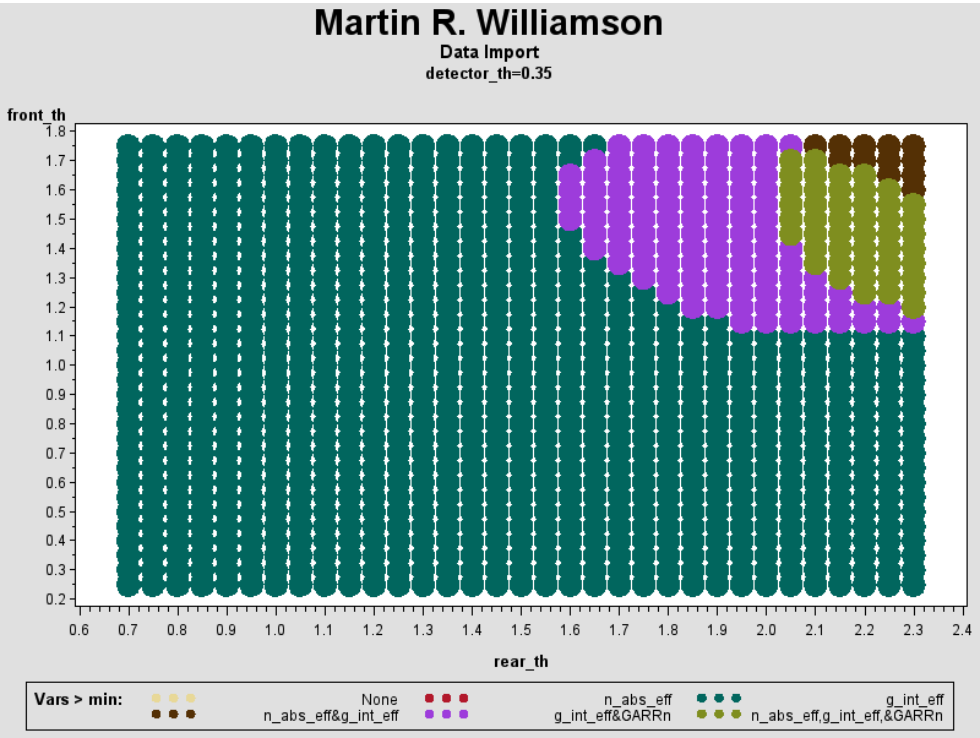

Figure 34. ^{10}B-Based Detector Two-Dimensional Overlaid Contour Plot

4.3.7 ^{10}B-BASED DETECTOR RESULTS SUMMARY AND CONCLUSIONS

Multivariate optimization of a ^{10}B-based detector in a RPM-type configuration was successfully performed utilizing the methodology outlined in this dissertation. The analysis was performed using three factors (the boron-loaded detector thickness and the front and rear plastic scintillation (no boron) detector thicknesses) and three response parameters (the absolute neutron detection efficiency, the intrinsic gamma-neutron detection efficiency, and the gamma absolute rejection ratio for neutrons). The Birks/Chou equations were successfully solved for allowing the calculation of the discrimination ability from PHD. While it was shown that due to the low net neutron peak energy, PHD is an ineffective method of discriminating between neutrons and photons, discrimination using coincidence counting of the 478 keV prompt gamma that is emitted by the excited ^{7}Li nucleus in 94% of the thermal neutron absorption is feasible.

Each of the three factors analyzed were shown to have a statistically significant impact on at least one of the response variables; therefore none of the factors screened out of the RSM analysis. For the maximum neutron sensitivity design, the optimized factors are a boron-loaded detector thickness of 0.35 inches, a front detector thickness of 1.55 inches, and a rear detector thickness of 2.30 inches. A summary of the results for the optimized ^{10}B-based RPM system (maximum neutron sensitivity) is presented in Table 35 and show that while the detector does satisfy the DNDO requirement for neutron sensitivity, it does not satisfy the requirements on the intrinsic gamma-neutron detection efficiency or GARRn. Due to the total thickness of the detector, it is somewhat expected that the discrimination ability would be relatively high. However, as shown in Table 30, the intrinsic gamma-neutron detection efficiency is most strongly correlated to the boron-loaded detector thickness. Therefore, one possible improvement to this system would be to increase the boron content in the detector while decreasing the thickness accordingly. While this modification would certainly improve the discrimination ability without a loss of neutron sensitivity, it may not be possible to perform this to the extent required to reduce these parameters to within the DNDO limits.

Table 35. Optimized ^{10}B-Based RPM System Performance Summary

Response Parameter	Optimized Performance	DNDO Requirement
Absolute neutron detection efficiency	2.56 cps/ng of ^{252}Cf	$\epsilon_{abs\ n} \geq 2.5$ cps/ng of ^{252}Cf
Intrinsic gamma-neutron detection efficiency	2.568E-3	$\epsilon_{int\ \gamma n} \leq 10^{-6}$
Gamma absolute rejection ratio for neutrons (GARRn)	2.796	$0.9 \leq$ GARRn ≤ 1.1

5 CONCLUSIONS AND RECOMMENDATIONS FOR FUTURE WORK

The functionality of the developed multivariate optimization methodology was demonstrated on the successful optimization of three neutron detection systems which utilize varied approaches to satisfying the DNDO criteria for an acceptable alternative neutron detector. The first neutron detection system optimized is a ^{3}He-based radiation portal monitor (RPM) based on a generalized version a currently deployed system. The second system is ^{6}Li-loaded polymer composite scintillator in the form of a thin film. The final system optimized is a ^{10}B-based plastic scintillator sandwiched between two standard plastic scintillators. Results show that only the ^{3}He-based system performed at levels which satisfy all four of the DNDO performance constraints on detection and performance capabilities. Validation results show that the fitted Birks equations performed well in simulating the PHS peak position with a maximum bias of <6% for the ^{6}Li-based composite scintillator.

While only the ^{3}He-based systems satisfied all four of the DNDO constraints, the ^{6}Li-loaded scintillator in the form of a thin film showed the most promise for satisfying all of the constraints given some modifications. Potential improvements for this type of neutron sensor are the use of Lithium Fluoride as a neutron capture reagent rather than Lithium Salicylate. Lithium Fluoride is not hygroscopic and has a much higher intrinsic ^{6}Li weight fraction which would provide greater neutron sensitivity at a decreased thickness, thus addressing both the issue of neutron sensitivity and discrimination ability. Another potential improvement is to utilize neutron absorbing nanoparticles or columns to maximize the fraction of energy from the charged particle reaction products deposited into the scintillating medium.

The results in this dissertation also showed that PHD is an ineffective method of discriminating between neutrons and photons for DNDO applications in ^{10}B-based scintillation detectors due to both the lower Q-value and greater ionization quenching effects in the ^{10}B-based scintillator compared to the ^{6}Li based scintillator. While coincidence counting of the 478 keV prompt gamma that is emitted by the excited ^{7}Li nucleus in 94% of the thermal neutron absorption reactions by ^{10}B proved to be feasible,

the large thickness of the detector necessary to achieve the neutron sensitivity required by DNDO results in poor n/γ discrimination ability.

Possibilities for future work include the incorporation of the measured full width half maximum (FWHM) into the simulated PHS. Inclusion of the FWHM would result in additional broadening of the simulated peaks, thus resulting in the potential loss of detector counts due to shifting a portion of the peak below the LLD cutoff. Based on the demonstrated functionality of the developed multivariate optimization methodology, application of the methodology in the development process of new candidate neutron detector designs is warranted. Results from the multivariate optimization analysis include not only the identification of which factors significantly affect detector performance, but also the determination of optimum levels for those factors with simultaneous consideration of multiple detector performance responses.

BIBLIOGRAPHY

1. Klann, R. T., Shergur, J., & Mattesich, G. (2008), Current State of Commercial Radiation Detection Equipment for Homeland Security Applications. *15th Topical Meeting of the Radiation Protection and Shielding Division (RPSD) of the American Nuclear Society (ANS).* Pine Mountain, Georgia.

2. Van Ginhoven, R. M., Kouzes, R. T., & Stephens, D. L., (2009). *Alternative Neutron Detector Technologies for Homeland Security.* PNNL-18471. Pacific Northwest National Laboratory.

3. Kouzes, R. T. (2009). *The ^{3}He Supply Problem*. PNNL-18388. Pacific Northwest National Laboratory.

4. Domestic Nuclear Detection Office Award Number 003387891.

5. Office of the General Council (2005). *The Atomic Energy Act of 1954*, NUREG-0980, Volume 1, Number 7, Washington, DC. U.S. Nuclear Regulatory Commission.

6. Korea Atomic Energy Research Institute. (2000). Cross Section Plotter. Retrieved November 19, 2009, from Table of Nuclides: http://atom.kaeri.re.kr/.

7. Knoll, G. F. (2000). *Radiation Detection and Measurement* (3rd Edition). Hoboken, New Jersey. John Wiley & Sons, Inc.

8. Tsoulfanidis, N. (1995). *Measurement and Detection of Radiation* (2nd Edition). Washington, D.C.: Taylor & Francis.

9. Bedding, D. H., Johnson, N. H., & Menlove, H. O. (2000). ^{3}He neutron proportional counter performance in high gamma-ray dose environments. *Nuclear Instruments and Methods in Physics Research*, Volume 455, Issue 3, pp. 670-682.

10. ICRU Report 51 (1993), *Quantities and Units in Radiation Protection Dosimetry*, International Commission on Radiation Units and Measurements.

11. Turner, J. E. (1995). *Atoms, Radiation, and Radiation Protection* (2nd Edition). New York, NY: John Wiley & Sons, Inc.

12. Ahmed, S. N. (2007). *Physics & Engineering of Radiation Detection,* (1st Edition). San Diego, CA. Academic Press, Inc.

13. Birks, J. B. (1951), Scintillations from organic crystals: specific fluorescence and relative response to different radiations, *Proceedings Physical Society*. Section A, Volume 64, pp. 874-877.

14. Craun, R. L., & Smith, D. L. (1970). Analysis of Response Data for Several Organic Scintillators. *Nuclear Instruments and Methods*. Volume 80, pp. 239-244.

15. Mouatassim, S., Costa, G. J., Guillaume, G., Heusch, B., Huck, A., & Moszyfiski, M. (1995). The light yield response of NE213 organic scintillators to charged particles resulting from neutron interactions. *Nuclear Instruments and Methods in Physics Research*. Volume 359, pp. 530-536.

16. Kouzes, R. T., Ely, J. R., Lintereur, A. T., & Stephens, D. L. (2009). *Neutron Detector Gamma Insensitivity Criteria*. PNNL-18903. Pacific Northwest National Laboratory.

17. Siciliano, E. R., Private Communication.

18. Delwiche L., & Slaughter S. (2003). *The Little SAS Book: A Primer* (3rd Edition). Cary, NC. SAS Institute, Inc.

19. Mee, R. W. (2009). *A Comprehensive Guide to Factorial Two-Level Experimentation* (1st Edition). Springer Science + Business Media, LLC.

20. Anderson, M. J., & Whitcomb, P. J. (2007). *DOE Simplified, Practical Tools for Effective Experimentation* (2nd Edition). Productivity Press.

21. Yang. K, & El-Haik. B. (2003). *Design for Six Sigma: A Roadmap for Product Development* (1st Edition). McGraw-Hill.

22. Strohmeyer, D. C., & Charlton, W. S. (2009). Feasibility Study of a Portable Coupled ^{3}He Neutron Detector with $LaBr_3$ Gamma Scintillator for the Purpose of Plutonium Identification and Quantification, *Proceedings of 31st Annual Meeting of ESARDA*, May 26-28, 2009, Vilnius, Lithuania.

23. Patronis, N., Kokkoris, M., Giantsoudi, D., Perdikakis, G., Papadopoulos, C. T., & Vlastou, R. (2007). Aspects of GEANT4 Monte-Carlo Calculations of the BC501A Neutron Detector. *Nuclear Instruments and Methods in Physics Research*, Volume 578, Issue 1, pp. 351-355.

24. Dingley, J., LiCausi, N., Danon, Y., Lu, J., & Bhat, I. (2009). Optimization of a Novel Self-Powered Solid-State Neutron Detector. *2009 International Conference on Advances in Mathematics, Computational Methods, and Reactor Physics*.

25. Childress, N. L. & Miller, W. H. (2002). MCNP Analysis and Optimization of a Triple Crystal Phoswich Detector. *Nuclear Instruments and Methods*, Section A, Volume 490, Issues 1-2, pp. 263-270.

26. Gomis, D. B., Velasco, C. B., Sánchez, I. H., Gutiérrez Álvarez M. D. (2009). Optimization by Factorial Design of a Capillary Electrophoresis Method for the Chiral Resolution and Determination of Zopiclone and Its Synthesis Precursor, *Journal of Liquid Chromatography & Related Technologies*, Volume 32, Issue 18, pp. 2654 – 2668.

27. Ng, S. Xu, K. & Wong, W. K. (2007). Optimization of Multiple Response Surfaces with Secondary Constraints for Improving a Radiography Inspection Process, *Quality Engineering*, Volume 19, Issue 1, pp. 53 - 65.

28. Axton, E. J., & Bardell, A. G. (1985). Neutron Yield from the Spontaneous Fission of ^{252}Cf ($\bar{\nu}$). *Metrologia*, Volume 21, Issue 2, pp. 59-74.

29. Martin, R. C., & Kos, S. E. (2000), Applications and Availability of Californium-252 Neutron Sources for Waste Characterization. *Spectrum 2000 International Conference on Nuclear and Hazardous Waste Management*. Chattanooga, Tennessee.

30. Pelowitz, D.B. (2008). *MCNPX™ User's Manual, Version 2.6.0*, LA-CP-07-1473. Los Alamos National Laboratory.

31. PNNL-14716, Revision 6.7 (2003), *Specifications for Radiation Portal Monitor Systems*, Pacific Northwest National Laboratory, Richland, Washington.

32. The MathWorks Inc. (2010), *Matlab® 7: Getting Started Guide*. The MathWorks Inc., Natlick, Massachusetts.

33. Bentz, Col. J. A. (2010), The Helium-3 Shortage and the Future of Neutron Detection, *Transactions of the American Nuclear Society,* Vol. 102, pg. 477.

34. Kouzes, R. T., Ely, J. H., Lintereur, A. T., Siciliano, E. R., Stromswold, D. C., & Woodring, M. L. (2010). *^{3}He Neutron Detector Pressure Effect and Comparison to Models*. PNNL-19110. Pacific Northwest National Laboratory.

35. Sen, I., Green, A. D., Mabe, A. N., Penumadu, D., Schweitzer, G. K., Miller, L. F., & Thomas, K. (2010), *Neutron Scintillator Detectors Based on Light Emitting Polymer Composite Films*, Institute of Electrical and Electronics Engineers (IEEE) Transactions (Submitted).

36. Sen, I., Private Communication.

37. EJ-254 Boron-Loaded Plastic Scintillator Data Sheet. Retrieved Sept. 19, 2010, from http://www.eljentechnology.com/images/stories/Data_Sheets/Loaded_Scintillators/EJ254%20data%20sheet.pdf.

38. Hurlbut, C., Private Communication.

APPENDICES

APPENDIX A – MCNPX DESIGN MATRIX RESULTS

Table 36. ^{3}He RPM Factorial Design Results

Filename	Absolute Neutron Detection Efficiency (cps/ng ^{252}Cf)	Intrinsic γ/n Detection Efficiency	GARRn	Cost
3He_1	1.7204	0.000E+00	1.0000	$8,143.92
3He_2	2.6219	2.257E-04	1.0088	$21,678.84
3He_3	1.7709	0.000E+00	1.0000	$8,453.60
3He_4	2.8685	1.738E-04	1.0065	$21,988.52
3He_5	1.3381	0.000E+00	1.0000	$8,434.25
3He_6	2.0805	2.481E-04	1.0134	$21,969.17
3He_7	1.3985	3.943E-05	1.0033	$8,743.93
3He_8	2.1582	1.159E-04	1.0064	$22,278.85
3He_9	2.8500	0.000E+00	1.0000	$12,655.56
3He_10	4.4717	1.866E-04	1.0176	$35,213.76
3He_11	3.0868	1.065E-05	1.0015	$12,965.24
3He_12	4.5581	1.385E-04	1.0203	$35,523.44
3He_13	2.2815	2.066E-05	1.0041	$12,945.89
3He_14	3.4814	1.354E-04	1.0266	$35,504.09
3He_15	2.4320	0.000E+00	1.0000	$13,255.57
3He_16	3.6504	1.699E-04	1.0216	$35,813.77
3He_17	1.6747	0.000E+00	1.0000	$8,143.92
3He_18	2.7144	4.548E-05	1.0017	$21,678.84
3He_19	1.8301	0.000E+00	1.0000	$8,453.60
3He_20	2.7452	4.280E-05	1.0017	$21,988.52
3He_21	1.3566	0.000E+00	1.0000	$8,434.25
3He_22	2.0879	4.083E-05	1.0022	$21,969.17
3He_23	1.4145	0.000E+00	1.0000	$8,743.93
3He_24	2.1828	7.885E-05	1.0042	$22,278.85
3He_25	2.9203	0.000E+00	1.0000	$12,655.56
3He_26	4.3546	6.372E-05	1.0096	$35,213.76
3He_27	2.9956	0.000E+00	1.0000	$12,965.24
3He_28	4.7554	5.323E-05	1.0049	$35,523.44
3He_29	2.3247	0.000E+00	1.0000	$12,945.89
3He_30	3.4469	6.198E-05	1.0081	$35,504.09
3He_31	2.3715	0.000E+00	1.0000	$13,255.57
3He_32	3.6529	4.625E-05	1.0089	$35,813.77

Table 37. ^{3}He RPM Central Composite Design Results

Filename	Absolute Neutron Detection Efficiency (cps/ng ^{252}Cf)	Intrinsic γ Detection Efficiency	GARRn	Cost
3He_1	1.7204	0.000E+00	1.0000	$8,143.92
3He_2	2.6219	2.257E-04	1.0088	$21,678.84
3He_3	1.7709	0.000E+00	1.0000	$8,453.60
3He_4	2.8685	1.738E-04	1.0065	$21,988.52
3He_5	1.3381	0.000E+00	1.0000	$8,434.25
3He_6	2.0805	2.481E-04	1.0134	$21,969.17
3He_7	1.3985	3.943E-05	1.0033	$8,743.93
3He_8	2.1582	1.159E-04	1.0064	$22,278.85
3He_9	2.8500	0.000E+00	1.0000	$12,655.56
3He_10	4.4717	1.866E-04	1.0176	$35,213.76
3He_11	3.0868	1.065E-05	1.0015	$12,965.24
3He_12	4.5581	1.385E-04	1.0203	$35,523.44
3He_13	2.2815	2.066E-05	1.0041	$12,945.89
3He_14	3.4814	1.354E-04	1.0266	$35,504.09
3He_15	2.4320	0.000E+00	1.0000	$13,255.57
3He_16	3.6504	1.699E-04	1.0216	$35,813.77
3He_17	1.2135	3.013E-04	1.0038	$8,994.35
3He_18	4.5618	5.952E-05	1.0071	$30,451.70
3He_19	2.9931	2.062E-05	1.0031	$19,377.82
3He_20	1.9152	2.740E-05	1.0073	$20,068.23
3He_21	2.7070	4.949E-05	1.0086	$19,354.81
3He_22	3.0621	2.799E-05	1.0045	$20,091.24
3He_23	1.4034	0.000E+00	1.0000	$6,188.11
3He_24	3.3766	1.242E-04	1.0178	$33,257.94
3He_25	2.6638	2.934E-05	1.0139	$19,723.02
3He_26	2.8932	1.458E-05	1.0016	$19,723.02
3He_27	2.9031	2.866E-05	1.0048	$19,723.02
3He_28	2.9083	2.864E-05	1.0048	$19,723.02
3He_29	2.9123	3.818E-05	1.0064	$19,723.02
3He_30	2.9440	6.669E-05	1.0110	$19,723.02
3He_31	2.9043	2.866E-05	1.0048	$19,723.02
3He_32	2.7918	5.729E-05	1.0100	$19,723.02
3He_33	2.9133	2.863E-05	1.0048	$19,723.02
3He_34	2.9031	2.866E-05	1.0048	$19,723.02
3He_35	2.8803	9.543E-06	1.0016	$19,723.02
3He_36	2.9056	2.867E-05	1.0048	$19,723.02

Table 38. Li-Sal/P2VN Central Composite Design Results

Filename	Absolute Neutron Detection Efficiency (cps/ng ^{252}Cf)	Intrinsic γ/n Detection Efficiency	GARRn	Cost
LiSal_1	1.328E+02	6.844E-06	1.0211	$167.65
LiSal_2	3.783E+01	6.176E-06	1.0668	$84.56
LiSal_3	2.964E+02	1.708E-04	1.2386	$391.19
LiSal_4	3.092E+01	1.680E-04	3.2499	$197.30
LiSal_5	1.822E+02	1.673E-06	1.0037	$91.28
LiSal_6	5.830E+02	2.404E-04	1.1711	$329.07
LiSal_7	1.269E+02	5.511E-05	1.1787	$308.11
LiSal_8	2.728E+01	5.561E-05	1.8391	$112.25
LiSal_9	4.044E+02	5.478E-05	1.0558	$210.18
LiSal_10	3.812E+02	5.308E-05	1.0574	$210.18
LiSal_11	4.044E+02	5.478E-05	1.0558	$210.18
LiSal_12	3.735E+02	4.898E-05	1.0540	$210.18
LiSal_13	4.014E+02	5.494E-05	1.0563	$210.18
LiSal_14	4.044E+02	5.478E-05	1.0558	$210.18
LiSal_15	3.903E+02	5.594E-05	1.0590	$210.18
LiSal_16	4.044E+02	5.478E-05	1.0558	$210.18

Table 39. ^{10}B-Based Detector Central Composite Design Results

Filename	Absolute Neutron Detection Efficiency (cps/ng ^{252}Cf)	Intrinsic γ/n Detection Efficiency	GARRn
Eljen_1	1.3155	2.132E-03	3.7113
Eljen_2	1.9640	2.279E-03	2.9907
Eljen_3	1.8530	2.246E-03	2.9499
Eljen_4	2.3648	2.264E-03	2.5867
Eljen_5	1.6002	3.623E-03	4.7807
Eljen_6	2.3309	3.945E-03	3.8976
Eljen_7	2.0842	3.906E-03	4.0138
Eljen_8	2.8026	4.097E-03	3.4198
Eljen_9	1.8407	1.587E-03	2.4345
Eljen_10	2.4974	4.639E-03	4.0828
Eljen_11	1.4923	2.922E-03	4.3526
Eljen_12	2.4604	3.269E-03	3.1426
Eljen_13	1.4553	2.907E-03	4.2404
Eljen_14	2.6299	3.364E-03	3.1700
Eljen_15	2.2507	3.176E-03	3.3463
Eljen_16	2.2417	3.223E-03	3.3764
Eljen_17	2.2257	3.273E-03	3.4310
Eljen_18	2.2635	3.190E-03	3.3413
Eljen_19	2.2140	3.121E-03	3.3433
Eljen_20	2.2291	3.149E-03	3.3483
Eljen_21	2.2145	3.425E-03	3.5520
Eljen_22	2.3466	3.275E-03	3.3175
Eljen_23	2.2165	3.127E-03	3.3240
Eljen_24	2.1365	3.235E-03	3.5020

APPENDIX B – SELECT MCNPX INPUTS

MCNPX Case ID: 3He_1.i

```
Settings, -1, -1, -1, -1, 1  SAIC RPM8 "Generic Model" from PNNL-18471,-19050
C    Tube Ht (feet), Ft Th (cm), Rr Th (cm), P (atm), CL Dist (in)
C    3.00             5.00           7.20      1.00      5.25
1    3  -7.82       (1 -2 5 -6 8 -9) (-3:4:-7:6:-10:11)    $ Steel shield
50   2  -0.92       -50                                    $ Poly Bottom
51   2  -0.92       -51                                    $ Poly Top
52   2  -0.92       -52                                    $ Poly Left
53   2  -0.92       -53                                    $ Poly Right
54   2  -0.92       -54                                    $ Poly Front
55   2  -0.92       -55                                    $ Poly Back
60   1  -1.2259E-4  -60                                    $ Left 3He Tube
61   1  -1.2259E-4  -61                                    $ Right 3He Tube
70   5  -15.1       -70                                    $ 252Cf source
71   6  -11.34      -71 70                                 $ Lead around source
500  4  -1.205e-3   -500 #1 #50 #51 #52 #53 #54 #55
                    #60 #61 #70 #71                        $ Atmosphere
501  0              500

c  Surface Cards
1    px  0.0
2    px  68.35
3    px  0.635
4    px  67.715
5    py  0.0
6    py  25.375
7    py  0.635
8    pz  0.0
9    pz  227.35
10   pz  0.635
11   pz  226.715
50   rpp 3.175  65.175    10.375  20.375    3.175   8.255      $ Poly Bottom
51   rpp 3.175  65.175    10.375  20.375    219.095 224.175    $ Poly Top
52   rpp 3.175  8.255     10.375  20.375    8.255   219.095    $ Poly Left
53   rpp 60.095 65.175    10.375  20.375    8.255   219.095    $ Poly Right
54   rpp 3.175  65.175    20.375 25.375    3.175   224.175     $ Poly Front
55   rpp 3.175  65.175    3.175  10.375     3.175   224.175    $ Poly Rear
60   rcc 20.84  15.38  9.525   0 0 91.4     2.5                $ Left 3He Tube
61   rcc 47.51  15.38  9.525   0 0 91.4     2.5                $ Right 3He Tube
70   s   34.175 220.675 113.675    2.510E-04                   $ Source
71   s   34.175 220.675 113.675    5.0025E-01                    $ 0.5 cm lead surrounding
source
500  so  300

MODE N P T D H E                    $ Type of particles to transport: neutrons, photons,
tritons, deuterons, protons, & electrons
PHYS:N 100 4j -1 2                $ Turned on fission multiplicity "FISM" (-1) and light
ion recoil "NCIA" (2)
PHYS:P 3j -1                     $ Turn on photonuclear particle production - 4th entry
CUT:N  2j 0 0                    $ Analog Capture for Neutrons - 4th entry
CUT:P,T,H,E  j  0                    $ Set  low KE cutoff to 0 Mev for photons, tritons,
protons, & electrons - 2nd entry
IMP:N,P,T,D,H,E   1 11R 0        $ Particle Importances within cells
nps  500000
c     1 nanogram Cf-252 source = 1E-9 grams = 6.623E-11 cc - modeled as sphere in SS
sdef  pos=34.175 220.675 113.675  cel=70  par=SF  rad=d1
si1  0 2.510E-04
sp1 -21 1
c  Material Cards
C     Material 1 is 3He Gas (Note that the .66c library includes 2ndary charged particle
data)
m1    2003.66c   1 gas=1
```

```
C    Material 2 is Polyethylene - CH2 - rho=0.92g/cc - MCNP Primer
m2    6000   3.950E-02
      1001   7.899E-02
mt2   poly.01t
C    Material 3 is Carbon Steel (99.5% wt% Iron) - rho=7.82g/cc - MCNP Primer
m3    6000   -0.005
      26000  -0.995
C    Material 4 is Atmosphere
m4    1001     -0.00070
      6000     -0.00015
      7014     -0.76060
      8016     -0.23860
C    Material 5 is Cf-252 - rho = 15.1 g/cc - Wiki
m5    98252.66c  1
C    Material 6 is lead - rho = 11.34 g/cc - Wiki
m6    82204    -0.014
      82206    -0.241
      82207    -0.221
      82208    -0.524
FC4  F4 = N Flux avg over cells 60 (left) and 61 (right) detectors (#/cm2)
F4:n  60 61 T
c     FM4 - 1) Atom density in cell (atom/barn-cm), 2) Material 1 - detector, 3)-2 = Abs
x-sec (barns)
c     The output from this is absorptions/cm3/source particle - Need to multiply this by
the source strength
c     Requirment is >= 2.5 cps/ng 252Cf, so multiply by 2.316E3 nps (1ng 252Cf) & see if
>= 2.5.
FM4  (-1 1 -2)
sd4   1  1 1       $ segment divisor - equiv. to mult. the tally by the cell volume, now
output=abs/source particle
FC6  F6 tallies to set up the pulse height tallies
F6:H  60 61
F16:T 60 61
FC8  F8 Pulse height tally for cell 60 - Left 3He (H+T) - Q-val=0.764 MeV
F8:H  60
E8   0 1E-3 1200I 1
FT8  PHL 2 6 1 16 1 0
FC18  F18 Pulse height tally for cell 61 - Right 3He (H+T) - Q-val=0.764 MeV
F18:H  61
E18   0 1E-3 1200I 1
FT18  PHL 2 6 2 16 2 0
print
```

MCNPX Case ID: LiSal_1.i

```
Settings, -1, -1 --> Detector Dim = 4.5 cm Diameter
C    Detector Thickness (microns), Li-Sal Weight Percent (%)
C          150                          20
1    2  -0.92         -1               $ Bottom Center
2    2  -0.92         -2               $ Right Side
3    2  -0.92         -3               $ Left Side
4    2  -0.92         -4               $ Front
5    2  -0.92         -5               $ Back
6    2  -0.92         -6               $ Source Cover Front
7    2  -0.92         -7               $ Source Cover Back
8    2  -0.92         -8               $ Source Cover Top
9    2  -0.92         -9               $ Source Cover Bottom
10   2  -0.92         -10              $ Source Cover Left
11   2  -0.92         -11              $ Source Cover Right
12   2  -0.92         -12              $ Detector Well Base
13   2  -0.92         -13              $ Wall Behind Channels
14   2  -0.92         -14              $ Block on top of top 1
15   2  -0.92         -15              $ Block on top of top 2
16   2  -0.92         -16              $ Block on top of top 2(a)
17   2  -0.92         -17              $ Block on top of top 2(b)
18   2  -0.92         -18              $ Block on top of top 2(c)
19   2  -0.92         -19 27           $ Block holding source
20   2  -0.92         -20              $ Block above source
24   7  -15.1         -100             $ Cf-252 Source
25   8  -7.92          100 -25         $ SS316 source container
26   4  -1.205e-3      25 -26         $ Inside lead source container
27   6  -11.34         26 -27         $ Lead source container
30   3  -1.18         -31 30 40 -45    $ Bare Channel Plexi
31   3  -1.18         -33 32 40 -45    $ Covered Channel Plexi
32   5  -8.65         -34 33           $ Covered Channel Cd
40   1  -1.5          -101             $ Detector - Bare Channel
41   1  -1.5          -102             $ Detector - Shielded Channel
50   4  -1.205e-3     -50 27           $ Air surrounding source
51   4  -1.205e-3     -51 #30 #31 #32
                          #40 #41      $ Air surrounding tubes
52   4  -1.205e-3     -52              $ Air behind tubes
53   4  -1.205e-3      53 -54 #14 #15 #16 #17
                           #18 #30 #31 #32 $ Air around box
54   0                 54

c  Surface Cards
1    rpp   5.3975   45.72     0        30.48     0        5.3975  $ Bottom Center
2    rpp   45.72    51.1175   0        30.48     0        35.56   $ Right Side
3    rpp   0        5.3975    0        30.48     0        35.56   $ Left Side
4    rpp   5.3975   45.72     0        5.3975    5.3975   35.56   $ Front
5    rpp   5.3975   45.72     25.0825  30.48     5.3975   35.56   $ Back
6    rpp   5.3975   25.7175   5.3975   10.795    10.795   35.56   $ Source Cover Front
7    rpp   5.3975   25.7175   19.685   25.0825   10.795   35.56   $ Source Cover Back
8    rpp   5.3975   25.7175   10.795   19.685    30.1625  35.56   $ Source Cover Top
9    rpp   5.3975   25.7175   5.3975   25.0825   5.3975   10.795  $ Source Cover Bottom
10   rpp   5.3975   10.795    10.795   19.685    10.795   30.1625 $ Source Cover Left
11   rpp   20.32    25.7175   10.795   19.685    10.795   30.1625 $ Source Cover Right
12   rpp   25.7175  36.5125   5.3975   25.0825   5.3975   10.795  $ Detector/Channel Base
13   rpp   36.5125  39.0525   5.3975   25.0825   5.3975   35.56   $ Wall behind channels
14   rpp   5.08     22.2251   0        30.48     35.56    40.64   $ Block on top of top 1
15   rpp   33.9727  51.1175   0        30.48     35.56    38.1    $ Block on top of top 2
16   rpp    22.2251  33.9727   0         5.08      35.56    38.1    $ Block on top of top
2(a)
17   rpp    22.2251  33.9727   13.97     16.51     35.56    38.1    $ Block on top of top
2(b)
18   rpp    22.2251  33.9727   25.4      30.48     35.56    38.1    $ Block on top of top
2(c)
19   rpp   10.795   20.32     10.795   19.685    10.795   15.875  $ Block holding source
20   rpp   10.795   20.32     10.795   19.685    24.13    30.1625 $ Block above source
25   rcc   15.5575  15.24     13.305   0 0 3.81      0.3175       $ Source (SS outer)
```

```
26    rcc    15.5575   15.24      13.305    0 0 9.525      1.27          $ Source container
inner (lead)
27    rcc    15.5575   15.24      10.795    0 0 13.335     2.54          $ Source container
outer (lead)
30    c/z    29.8451   9.68375  3.81                                  $ Bare Channel ID
31    rcc    29.8451    9.68375   10.795    0 0 27.94    3.96875         $ Bare Channel OD
(1/16"-thick wall)
32    c/z    29.8451   20.79625 3.81                                  $ Cd Channel ID
33    rcc    29.8451   20.79625 10.795   0 0 27.94   3.96875        $ Cd Channel OD (1/16"-
thick wall)
34    rcc    29.8451   20.79625 10.795   0 0 27.94   4.1275         $ Cd Channel OD (1/16"-
thick Cd)
40    pz     10.795                                                 $ Channel Bottom
41    pz     16.383                                                 $ Channel (Base + H/5)
42    pz      21.971                                                       $ Channel (Base +
2*(H/5))
43    pz      27.559                                                       $ Channel (Base +
3*(H/5))
44    pz      33.147                                                       $ Channel (Base +
4*(H/5))
45    pz     38.735                                                 $ Channel Top
50     rpp    10.795     20.32      10.795   19.685      15.875   24.13    $ Air surrounding
source
51    rpp    25.7175   36.5125   5.3975  25.0825    10.795  35.56   $ Air surrounding tubes
52    rpp    39.0525   45.72     5.3975  25.0825    5.3975  35.56   $ Air behind tubes
53    rpp    0         51.1175   0       30.48      0       35.56   $ Box dimensions
54    rpp    -5.3975   55.88    -5.3975  35.56     -5.3975  45.72   $ Outside world
100   s      15.5575 15.24  15.21  2.5914E-04                       $ Source
101   rcc    29.8451    9.68375     10.795     0 0 1.500E-2 2.25         $ Detector - Bare
Channel
102   rcc    29.8451    20.79625   10.795     0 0 1.500E-2 2.25        $ Detector - Shielded
Channel

c  Material Cards
c  Material 1 ND13 (LiSal - PVN mix) - (20% Li-Sal)
m1    3006.60c  1.1292E-03
      3007      5.9433E-05
      1001      5.3484E-02
      1002      6.1514E-06
      8016      3.5646E-03
      8017      1.3551E-06
      6012      6.4677E-02
      6013      6.9953E-04
m2    6000   3.9499E-02     $ Polyethylene - CH2 - rho=0.92 - MCNP Primer
      1001   7.8998E-02
m3    6000   3.549E-02      $ Plexiglas - C5H8O2 - rho=1.18 - MCNP Primer
      1001   5.678E-02
      8016   1.420E-02
m4    1001   -0.00070       $ Atmosphere
      6000   -0.00015
      7014   -0.76060
      8016   -0.23860
m5    48106  -0.0125        $ Cadmium
      48108  -0.0089
      48110  -0.1249
      48111  -0.128
      48112  -0.2413
      48113  -0.1222
      48114  -0.2873
      48116  -0.0749
m6    82204  -0.014         $ Lead - rho = 11.34 g/cc - MCNP primer
      82206  -0.241
      82207  -0.221
      82208  -0.524
m7    98252  1              $ Cf-252 - rho = 15.1 g/cc - Wiki
m8    26000  -0.655         $ SS-316 -rho = 7.92 g/cc - MCNP primer
      24000  -0.170
      28000  -0.120
      42000  -0.025
```

```
      25055  -0.020
      14000  -0.010
MODE N P A T D E                    $ Type of particles to transport: neutrons, photons,
alphas, tritons, deuterons, & electrons
PHYS:N 100 4j -1 2                 $ Turned on fission multiplicity "FISM" (-1) and light
ion recoil "NCIA" (2)
PHYS:P 3j -1                      $ Turn on photonuclear particle production - 4th entry
CUT:N  2j 0 0                     $ Analog Capture for Neutrons - 4th entry
CUT:P,T,A,E  j 0                     $ Set low KE cutoff to 0 Mev for photons, tritons,
alphas, and electrons - 2nd entry
IMP:N,P,A,T,D,E   1 32R 0         $ Particle Importances within cells
c      0.59 uCi (5.9E-7 Ci) Cf-252 source = 1.1008E-9 grams = 7.2898E-11 cc - modeled as
sphere in SS
sdef  pos=15.5575 15.24  15.21  cel=24  par=SF  rad=d1
si1  0 2.5914E-04
sp1 -21 1
nps  1000000
c       Need to multiply all tallies by the calculated source strength of 1.367E6
neutrons/second
FC1  F1 = Neutron current int. over tube surface (30=ID Bare) (par/sf n)
F1:n  30
FM1   1 0
E1    0 1E-3 3000I 15
FC11  F11 = Neutron current int. over tube surface (32=ID Shielded) (par/sf n)
F11:n  32
FM11   1 0
E11    0 1E-3 3000I 15
FC21  F21 = Photon current int. over tube surface (30=ID Bare) (par/sf n)
F21:p  30
FM21   1 0
E21    0 1E-3 3000I 15
FC31  F31 = Photon current int.over tube surface (32=ID Shielded) (par/sf n)
F31:p  32
FM31   1 0
E31    0 1E-3 3000I 15
FC4  F4 = N Flux avg over cell 40 (bare) and 41 (shielded) detectors (#/cm2)
F4:n  40 41
E4    0 1E-3 3000I 15
c     FM4 - 1) Atom density in cell (atom/barn-cm), 2) Material 1 - detector, 3)-2 = Abs
x-sec (barns)
c     The output from this is absorptions/cm3/source particle - Need to multiply this by
the source strength
FM4  (-1 1 -2)
sd4   1  1        $ segment divisor - equiv. to mult. the tally by the cell volume, now
output=abs/source particle
FC14  F14 = Neutron Flux avg over cell 40 (bare) detector (#/cm2)
F14:n 40
E14   0 1E-3 3000I 15
FC24  F24 = Neutron Flux avg over cell 41 (shielded) detector (#/cm2)
F24:n 41
E24   0 1E-3 3000I 15
FC34  F34 = Photon Flux avg over cell 40 (bare) detector (#/cm2)
F34:p 40
E34   0 1E-3 3000I 15
FC44  F44 = Photon Flux avg over cell 41 (shielded) detector (#/cm2)
F44:p 41
E44   0 1E-3 3000I 15
FC6  F6 tallies to set up the pulse height tallies
F6:A  40 41
F16:T 40 41
F26:E 40 41
F36:P 40 41
FC8  F8 Pulse height tally for cell 40 - bare (alpha+triton)
F8:A  40
E8   0 1E-3 500I 5
FT8  PHL 2 6 1 16 1 0
FC18  F18 Pulse height tally for cell 40 - bare (triton+alpha+electron)
F18:T  40
E18   0 1E-3 500I 5
```

```
FT18  PHL 3 6 1 16 1 26 1 0
FC28  F28 Pulse height tally for cell 40 - bare (triton+alpha+electron+photon)
F28:T  40
E28   0 1E-3 500I 5
FT28  PHL 4 6 1 16 1 26 1 36 1 0
FC38  F38 Pulse height tally for cell 41 - shielded (alpha+triton)
F38:A  41
E38    0 1E-3 500I 5
FT38  PHL 2 6 2 16 2 0
FC48  F48 Pulse height tally for cell 41 - shielded (triton+alpha+electron)
F48:T  41
E48    0 1E-3 500I 5
FT48  PHL 3 6 2 16 2 26 2 0
FC58  F58 Pulse height tally for cell 41 - shielded (t+a+e+p)
F58:T  41
E58    0 1E-3 500I 5
FT58  PHL 4 6 2 16 2 26 2 36 2 0
FC108  F108 Pulse height tally for cell 40 - bare (alpha)
F108:A  40
E108   0 1E-3 500I 3
FC118  F118 Pulse height tally for cell 40 - bare (triton)
F118:T  40
E118   0 1E-3 500I 3
FC114   F114 = Photon Flux tally avg over cell 40 (b) and 41 (s) detrs (#/cm2)
F114:p  40 41
FM114   (-1 1 -1)     $ 1) Atom density (atom/barn-cm), 2) Mat. 1, 3) -1 = Incoherent
(Compton) x-sec (barns)
       (-1 1 -2)      $ 1) Atom density (atom/barn-cm), 2) Mat. 1, 3) -2 = Coherent
(Rayleigh) x-sec (barns)
       (-1 1 -3)    $ 1) Atom density (atom/barn-cm), 2) Mat. 1, 3) -3 = Photoelectric x-
sec (barns)
       (-1 1 -4)    $ 1) Atom density (atom/barn-cm), 2) Mat. 1, 3) -4 = Pair Production
x-sec (barns)
       (-1 1 -5)    $ 1) Atom density (atom/barn-cm), 2) Mat. 1, 3) -5 = Total Photon x-
sec (barns)
sd114   1 1         $ segment divisor - equiv. to mult. the tally by the cell volume
E114   0 1E-3 8000I 15
FC121  F121 = Neutron Flux avg over surface 100 (source) (#/cm2)
F121:n 100
E121   0 1E-3 8000I 15
FC131  F131 = Photon Flux avg over surface 100 (source) (#/cm2)
F131:p 100
E131   0 1E-3 8000I 15
FC134  F134 = Photon Flux avg over cell 24 (source) (#/cm2)
F134:p 24
E134   0 1E-3 8000I 15
FC144  F144 = Neutron Flux avg over cell 24 (source) (#/cm2)
F144:n 24
E144   0 1E-3 8000I 15
FC154  F154 = Photon Flux avg over cell 27 (lead around source) (#/cm2)
F154:p 27
E154   0 1E-3 8000I 15
FC208 - Scintillation Efficiency (alpha+triton)
F208:T  1
E208   0 0.01 100
FT208  PHL 2 6 1 16 1 0
c        From  PTRAC  output,  1=neutron,  2=photon,  3=electron,  9=proton,  31=deuteron,
32=triton, 34=alpha (pg 4-11 MCNPX)
ptrac BUFFER=1000 TYPE=A,T CELL=40,41 FILE=ASC WRITE=ALL
print
```

MCNPX Case ID: Eljen_1.i

```
Settings (-1,-1,-1), PNNL generic RPM model with
C    EJ-200 and BC-454 panel detector inside
1    3  -7.82       (1 -2 5 -6 8 -9) (-3:4:-7:6:-10:11)    $ Steel shield
50   1  -1.026      -50                                    $ BC-254 (boron)
60   2  -1.023      -60 #50                                $ EJ-400
61   3  -7.82       -61                                    $ 1/2-in steel face
70   5  -15.1       -70                                    $ 252Cf source
71   6  -11.34      -71 70                                 $ Lead around source
72   7  -0.92       -72 71                                 $ Poly around source
500  4  -1.205e-3   -500 #1 #50 #60 #61 #70 #71 #72        $ Atmosphere
501  0              500

c  Surface Cards
1    px  0.0
2    px  68.35
3    px  0.635
4    px  67.715
5    py  0.0
6    py  7.874
7    py  0.635
8    pz  0.0
9    pz  227.35
10   pz  0.635
11   pz  226.715
50   rpp 8.255  60.095    5.715    6.477    3.176 216.535      $ BC-454 (20.41" wide, 7'
tall)
60   rpp 3.175  65.175    3.175    7.874    3.175 216.535      $ EJ-400 (24.41" wide, 7'
tall)
61   rpp 0      68.35     7.874    9.144    3.175 216.535      $ 1/2-in steel face
70   s   34.175 209.144 109.855    2.510E-04                   $ Source
71   s   34.175 209.144 109.855    5.0025E-01                    $ 0.5 cm lead surrounding
source
72   s   34.175 209.144 109.855    3.00025                     $ 2.5 cm poly surrounding
source
500  so  300

MODE N P A D E #                    $ Type of particles to transport: neutrons, photons,
alphas, deuterons, electrons, & heavy
PHYS:N 100 4j -1 2                $ Turned on fission multiplicity "FISM" (-1) and light
ion recoil "NCIA" (2)
PHYS:P 3j -1                    $ Turn on photonuclear particle production - 4th entry
CUT:N  2j 0 0                   $ Analog Capture for Neutrons - 4th entry
CUT:P,A,E,#  j 0                    $ Set low KE cutoff to 0 Mev for photons, tritons,
alphas, electrons, & heavy - 2nd entry
IMP:N,P,A,D,E,# 1 7R 0          $ Particle Importances within cells
nps  100000
c     1 nanogram Cf-252 source = 1E-9 grams = 6.623E-11 cc - modeled as sphere in SS
sdef  pos=34.175 209.144 109.855  cel=70  par=SF  rad=d1
si1  0 2.510E-04
sp1 -21 1
c  Material Cards
C    Material 1 is BC-454 - 10% Natural Boron - rho = 1.026 g/cc
m1    6012   4.1353E-02
      6013   4.4726E-04
      1001   5.1794E-02
      1002   5.9570E-06
      5010   1.1250E-03
mt1   poly.01t
C    Material 2 is EJ-200 - rho = 1.023 g/cc
m2    6012   4.6398E-02
      6013   5.0183E-04
      1001   5.1694E-02
      1002   5.9455E-06
mt2   poly.01t
C    Material 3 is Carbon Steel (99.5% wt% Iron) - rho=7.82g/cc - MCNP Primer
m3    6000   -0.005
```

```
      26000  -0.995
C    Material 4 is Atmosphere
m4    1001     -0.00070
      6000     -0.00015
      7014     -0.76060
      8016     -0.23860
C    Material 5 is Cf-252 - rho = 15.1 g/cc - Wiki
m5    98252.66c  1
C    Material 6 is lead - rho = 11.34 g/cc - Wiki
m6    82204    -0.014
      82206    -0.241
      82207    -0.221
      82208    -0.524
C    Material 7 is Polyethylene - CH2 - rho=0.92g/cc - MCNP Primer
m7    6000   3.950E-02
      1001   7.899E-02
mt7   poly.01t
FC4  F4 = N Flux avg over cells 50 (BC-454) and 60 (BC-400) detectors (#/cm2)
F4:n  50 60 T
c     FM4 - 1) Atom density in cell (atom/barn-cm), 2) Material 1 - detector, 3)-2 = Abs
x-sec (barns)
c     The output from this is absorptions/cm3/source particle - Need to multiply this by
the source strength
c     Requirment is >= 2.5 cps/ng 252Cf, so multiply by 2.316E3 nps (1ng 252Cf) & see if
>= 2.5.
FM4  (-1 1 -2)
sd4    1  1 1       $ segment divisor - equiv. to mult. the tally by the cell volume, now
output=abs/source particle
FC6  F6 tallies to set up the pulse height tallies
F6:A  50 60
F16:# 50 60
F26:E 50 60
FC8  F8 Pulse height tally for cell 50 - BC-454 (alpha+7Li - Q=2.31MeV)
F8:A  50
E8    0 1E-3 500I 3
FT8  PHL 2 6 1 16 1 0
FC208 - Coincidence Counting Fraction (alpha in 50, gamma in 60)
F208:N  1
E208   0 100
FT208  PHL 2 6 1 26 2 0
FC508 - Coincidence -Alpha in 50 (F6@1.4662MeV), Electron in 60 (F26@0.3115 MeV)
F508:N 1
FT508 PHL 1 6 1 1 26 2
E508 0 1.0 1.467
FU508 0 0.1 0.312
c     From PTRAC output, 1=neutron, 2=photon, 3=electron, 9=proton, 31=deuteron, #=heavy,
34=alpha (pg 4-11 MCNPX)
c    Alpha = 1.4664 MeV, 7Li = 0.83623 MeV
ptrac BUFFER=1000 TYPE=A,# CELL=50,60 FILE=ASC WRITE=ALL MAX=50000
print
```

APPENDIX C – SAS INPUTS

SAS Input ID: 3He_optimization.sas

```
Options NoDate PageNo=1 Pagesize=43;
ODS HTML;
ODS Graphics On;
Title 'Martin R. Williamson';


Title2 'Build the Full Factorial Design Matrix';
proc factex;
      factors height front_th rear_th pressure cl_distance;

      output out=design designrep=1
      height nvals=( 3 5 )                              /* Height of tubes
(feet) */
      front_th nvals=( 5 8 )                            /* Thickness of poly in
front (cm) */
      rear_th nvals=( 7.2 10.4 )                        /* Thickness of poly in
back (cm) */
      pressure nvals=( 1 3 )                            /* Pressure (atm) */
      cl_distance nvals=( 3 5.25 )                      /* Distance from
Centerline */
      ;
      Proc Print;
Run;


Title2 'Build the Half-fraction Factorial Design Matrix';
/* Suppose that all main effects and two-factor interactions are to be
estimated.
     An appropriate design for this situation is a design of resolution 5, in
which no main effect
     or two-factor interaction is aliased with any other main effect or two-
factor interaction but
     in which two-factor interactions are aliased with three-factor
interactions. This design loses
     the ability to estimate interactions between three or more factors, but
this is usually not a
     serious loss. */
proc factex;
      factors height front_th rear_th pressure cl_distance;
         size design=16;
         model resolution=5;

      output out=design designrep=1
      height nvals=( 3 5 )                              /* Height of tubes
(feet) */
      front_th nvals=( 5 8 )                            /* Thickness of poly in
front (cm) */
      rear_th nvals=( 7.2 10.4 )                        /* Thickness of poly in
back (cm) */
      pressure nvals=( 1 3 )                            /* Pressure (atm) */
      cl_distance nvals=( 3 5.25 )                      /* Distance from
Centerline */
```

```
      ;
      Proc Print;
Run;



Title2 'Data Import';
PROC IMPORT OUT= WORK.A
            DATAFILE= "C:\3He_Opt.xlsx"
            DBMS=EXCEL REPLACE;
     RANGE="Factorial Design$";
     GETNAMES=YES;
     MIXED=YES;
     SCANTEXT=YES;
     USEDATE=YES;
     SCANTIME=YES;
RUN;

Proc Print Data=A; Run;


Title2 'ANOVA to determine significant parameters';
proc glm data=A;
       class height front_th rear_th pressure cl_distance;
       model n_abs_eff g_int_eff GARRn Cost=
height|front_th|rear_th|pressure|cl_distance@2 / solution;
       lsmeans height*pressure / slice=height pdiff;
    lsmeans height*front_th / slice=height pdiff;
    lsmeans front_th*pressure / slice=pressure pdiff;
       lsmeans front_th*rear_th / slice=front_th pdiff;
       lsmeans front_th*cl_distance / slice=front_th pdiff;
       run; quit; run;


/*************************************************************************
**/
/*
*/
/*                         Begin CCD Analysis
*/
/*
*/
/*************************************************************************
**/


Title2 'Data Import';
PROC IMPORT OUT= WORK.B
            DATAFILE= "C:\3He_Opt.xlsx"
            DBMS=EXCEL REPLACE;
     RANGE="CCD$";
     GETNAMES=YES;
     MIXED=YES;
     SCANTEXT=YES;
     USEDATE=YES;
     SCANTIME=YES;
RUN;

Proc Print Data=B; Run;
```

```
/*************************************************************************
*****************/
/* Append a grid of factor values to the observed data, with missing values for
the responses  */
/*************************************************************************
*****************/

Data C;
   Set B end=eof;
   Output;
   If eof then do;
      n_abs_eff=.;
      g_int_eff=.;
      GARRn=.;
      Do height=1.6 to 6.4 by .2;
         Do front_th=2.9 to 10.1 by .3;
            Do rear_th=5 to 12.6 by 0.3;
                        Do pressure=0.5 to 3.5 by 0.2;
                               Do cl_distance=1.45 to 6.8 by 0.3;
                               Output;
                               End;
                        End;
            End;
         End;
      End;
   End;
Run;

/* Proc Print Data=C; Run;


/*************************************************************************
*****************/
/*  Use PROC RSREG to fit a response surface model to the data and to compute
predicted values */
/*    for both the observed data and the grid, putting the predicted values in
a data set D.   */
/*************************************************************************
*****************/

Proc RSReg Data=C Out=D plots=all;
   Model n_abs_eff g_int_eff GARRn Cost = height front_th rear_th pressure
cl_distance / nocode Predict;
Run;

/* Proc Print Data=D; Run;



/*************************************************************************
*****************/
/*  Find the subset of predicted values that satisfy the constraints, sort by
the              */
/*     unconstrained variable, and display the top five predictions.
*/
/*     Neutron absorption efficiency - Constrained to a minimum of 2.5 cps/ng
252Cf = 2.5      */
/*     Gamma intrinsic efficiency - Constrained to a maximum of 0.001 = 1E-6
*/
/*     Gamma absolute rejection ratio for neutrons (GARRn) = 0.9 < GARRn < 1.1
*/
```

```
/*     Cost <= 30,000
*/
/*****************************************************************************
*****************/

Data E;
   set D;
   if n_abs_eff >= 2.5;
   if 0 < g_int_eff <= 1.0E-6;
   if 0.9 < GARRn < 1.1;
   if Cost <= 30000;

Proc Sort data=E;
   by Cost;
Run;

data E; set E;
   if (_n_ <= 10);
Proc Print;
Run;


Data M;
   set D;
   if n_abs_eff >= 2.5;
   if 0 < g_int_eff <= 1.0E-6;
   if 0.9 < GARRn < 1.1;
   if Cost <= 30000;

Proc Sort data=M;
   by descending n_abs_eff;
Run;

data M; set M;
   if (_n_ <= 10);
Proc Print;
Run;


/*****************************************************************************
*****************/
/*  To simultaneously optimize the responses, make a visual comparison of the
response         */
/*     surfaces by overlaying their contour plots.
*/
/*****************************************************************************
*****************/

Proc Rsreg Data=B plots=surface(overlaypairs);
   Model n_abs_eff g_int_eff GARRn Cost = height front_th rear_th pressure
cl_distance / nocode;
Run;


/* Create 3D plots */
proc rsreg data=D out=F plots(unpack)=surface(3d at(height=6.4, front_th=2.9,
rear_th=11.9, pressure=1.5, cl_distance=6.55));
       model n_abs_eff = height front_th rear_th pressure cl_distance / predict;
run; quit; run;
```

```
proc rsreg data=D out=G plots(unpack)=surface(3d at(height=6.4, front_th=2.9,
rear_th=11.9, pressure=1.5, cl_distance=6.55));
       model g_int_eff = height front_th rear_th pressure cl_distance / predict;
run; quit; run;

proc rsreg data=D out=H plots(unpack)=surface(3d at(height=6.4, front_th=2.9,
rear_th=11.9, pressure=1.5, cl_distance=6.55));
       model GARRn = height front_th rear_th pressure cl_distance / predict;
run; quit; run;

proc rsreg data=D out=H plots(unpack)=surface(3d at(height=6.4, front_th=2.9,
rear_th=11.9, pressure=1.5, cl_distance=6.55));
       model Cost = height front_th rear_th pressure cl_distance / predict;
run; quit; run;



Data I;
  set D;
  area = (n_abs_eff >= 2.5) + 2*(g_int_eff <= 1.0E-3) + 4*(0.9 < GARRn < 1.1) +
6*(Cost<=30000);
run; *no subsetting if statments... want all of C copied into D;

/*The area variable defines the eight areas that appear on the contour plot.
The terms in parentheses in the expression for area have the value one if the
logical expression is true and the value zero if the logical expression is
false.

You will also need a format to provide labels for the plot legend that
correspond to your definition of area:*/

proc format; value yfmt                  /* n_abs_eff   g_int_eff   GARRn  Cost
Value   */
    0='None'                               /* 1*0       +   2*0   +  4*0  + 6*0
=  0      */
    1='n_abs_eff'                          /* 1*1       +   2*0   +  4*0  + 6*0
=  1      */
    2='g_int_eff'                          /* 1*0       +   2*1   +  4*0  + 6*0
=  2      */
    3='n_abs_eff&g_int_eff'                /* 1*1       +   2*1   +  4*0  + 6*0
=  3      */
    4='GARRn'                              /* 1*0       +   2*0   +  4*1  + 6*0
=  4      */
    5='n_abs_eff&GARRn'                    /* 1*1       +   2*0   +  4*1  + 6*0
=  5      */
    6='Cost'                               /* 1*0       +   2*0   +  4*0  + 6*1
=  6      */
    7='n_abs_eff,Cost'                     /* 1*1       +   2*0   +  4*0  + 6*1
=  7      */
       8='g_int_eff,Cost'                     /* 1*0       +   2*1   +  4*0  +
6*1  =  8      */
       9='n_abs_eff,g_int_eff,Cost'           /* 1*1       +   2*1   +  4*0  +
6*1  =  9      */
       10='GARRn,Cost'                        /* 1*0       +   2*0   +  4*1  +
6*1  =  10     */
       11='n_abs_eff,GARRn,Cost'              /* 1*1       +   2*0   +  4*1  +
6*1  =  11     */
       12='g_int_eff,GARRn,Cost'              /* 1*0       +   2*1   +  4*1  +
6*1  =  12     */
```

```
      13='n_abs_eff,g_int_eff,GARRn,Cost'   /* 1*1       +   2*1   +  4*1  +
6*1  =  13     */
;


proc sort data=I; by height;

proc gplot uniform data=I; by height;
    symbol1 value=dot color=cream h=3;
    symbol2 value=dot repeat=13 h=3;
    legend1 frame label=("Vars > min:");
    format area yfmt.;
    plot front_th*rear_th=area / legend=legend1;
run; quit; run;


proc gplot uniform data=I; by height;
    symbol1 value=dot color=cream h=3;
    symbol2 value=dot repeat=13 h=3;
    legend1 frame label=("Vars > min:");
    format area yfmt.;
    plot pressure*cl_distance=area / legend=legend1;
run; quit; run;

proc gplot uniform data=I; by height;
    symbol1 value=dot color=cream h=3;
    symbol2 value=dot repeat=13 h=3;
    legend1 frame label=("Vars > min:");
    format area yfmt.;
    plot pressure*front_th=area / legend=legend1;
run; quit; run;

proc gplot uniform data=I; by height;
    symbol1 value=dot color=cream h=3;
    symbol2 value=dot repeat=13 h=3;
    legend1 frame label=("Vars > min:");
    format area yfmt.;
    plot pressure*rear_th=area / legend=legend1;
run; quit; run;

proc gplot uniform data=I; by height;
    symbol1 value=dot color=cream h=3;
    symbol2 value=dot repeat=13 h=3;
    legend1 frame label=("Vars > min:");
    format area yfmt.;
    plot cl_distance*rear_th=area / legend=legend1;

proc gplot uniform data=I; by height;
    symbol1 value=dot color=cream h=3;
    symbol2 value=dot repeat=13 h=3;
    legend1 frame label=("Vars > min:");
    format area yfmt.;
    plot cl_distance*front_th=area / legend=legend1;

run; quit; run;

ODS html close;
ODS Graphics off;
```

SAS Input ID: LiSal_P2VN_optimization.sas

```
Options NoDate PageNo=1 Pagesize=43;
ODS HTML;
ODS Graphics On;
Title 'Martin R. Williamson';


Title2 'Build the Full Factorial Design Matrix';
proc factex;
      factors thickness wt_percent;

      output out=design designrep=1
      thickness nvals=( 150 350 )                              /* Detector
thickness (microns) */
      wt_percent nvals=( 20 60 )                               /* Weight fraction
of Li-Sal (%) */
      ;
      Proc Print;
Run;

/*************************************************************************
**/
/*
*/
/*                         Begin Factorial Design Analysis
*/
/*
*/
/*************************************************************************
**/

Title2 'Data Import';
PROC IMPORT OUT= WORK.A
            DATAFILE= "C:\LiSal_P2VN_Opt.xlsx"
            DBMS=EXCEL REPLACE;
     RANGE="Factorial Design$";
     GETNAMES=YES;
     MIXED=YES;
     SCANTEXT=YES;
     USEDATE=YES;
     SCANTIME=YES;
RUN;

Proc Print Data=A; Run;


Title2 'ANOVA to determine significant parameters';
proc glm data=A;
       class thickness wt_percent;
       model n_cr g_int_eff GARRn Cost= thickness|wt_percent@2 / solution;
       lsmeans thickness*wt_percent / slice=thickness pdiff;
    run; quit; run;



/*************************************************************************
**/
```

```
/*
*/
/*                          Begin CCD Analysis
*/
/*
*/
/*************************************************************************
**/


Title2 'Data Import';
PROC IMPORT OUT= WORK.B
            DATAFILE= "C:\LiSal_P2VN_Opt.xlsx"
            DBMS=EXCEL REPLACE;
     RANGE="CCD$";
     GETNAMES=YES;
     MIXED=YES;
     SCANTEXT=YES;
     USEDATE=YES;
     SCANTIME=YES;
RUN;

Proc Print Data=B; Run;



/*************************************************************************
*****************/
/* Append a grid of factor values to the observed data, with missing values for
the responses  */
/*************************************************************************
*****************/

Data C;
   Set B end=eof;
   Output;
   If eof then do;
      n_cr=.;
      g_int_eff=.;
      GARRn=.;
         Cost=.;
      Do thickness=150 to 350 by 5;
         Do wt_percent=20 to 60 by 2;
                     Output;
               End;
      End;
   End;
Run;

/* Proc Print Data=C; Run;


/*************************************************************************
*****************/
/*  Use PROC RSREG to fit a response surface model to the data and to compute
predicted values */
/*    for both the observed data and the grid, putting the predicted values in
a data set D.   */
/*************************************************************************
*****************/
```

```
Proc RSReg Data=C Out=D plots=all;
   Model n_cr g_int_eff GARRn Cost = thickness wt_percent / nocode Predict;
Run;

/* Proc Print Data=D; Run;

/*************************************************************************
*****************/
/*  Find the subset of predicted values that satisfy the constraints, sort by
the              */
/*     unconstrained variable, and display the top five predictions.
*/
/*     Neutron absorption efficiency - Constrained to a minimum of 2.5 cps/ng
252Cf = 2.5      */
/*     g_int_effination ability - Constrained to a maximum of 0.001 = 1E-3
*/
/*     Gamma absolute rejection ratio for neutrons (GARRn) = 0.9 < GARRn < 1.1
*/
/*     Cost <= 30,000
*/
/*************************************************************************
*****************/

Data E;
   set D;
   if n_cr >= 100;
   if 0 < g_int_eff <= 1.0E-6;
   if 0.9 < GARRn < 1.1;
   if Cost <= 30000;

Proc Sort data=E;
   by descending n_cr;
Run;

data E; set E;
   if (_n_ <= 10);
Proc Print;
Run;


/*************************************************************************
*****************/
/*  To simultaneously optimize the responses, make a visual comparison of the
response         */
/*     surfaces by overlaying their contour plots.
*/
/*************************************************************************
*****************/

Proc Rsreg Data=B plots=surface(overlaypairs);
   Model n_cr g_int_eff GARRn Cost = thickness wt_percent / nocode;
Run;


/* Create 3D plots */
proc rsreg data=D out=F plots(unpack)=surface(3d at(thickness=276,
wt_percent=24));
       model n_cr = thickness wt_percent / predict;
run; quit; run;
```

```
proc rsreg data=D out=G plots(unpack)=surface(3d at(thickness=276,
wt_percent=24));
       model g_int_eff = thickness wt_percent / predict;
run; quit; run;

proc rsreg data=D out=H plots(unpack)=surface(3d at(thickness=276,
wt_percent=24));
       model GARRn = thickness wt_percent / predict;
run; quit; run;

proc rsreg data=D out=H plots(unpack)=surface(3d at(thickness=276,
wt_percent=24));
       model Cost = thickness wt_percent / predict;
run; quit; run;



ODS html close;
ODS Graphics off;
```

SAS Input ID: Eljen_optimization.sas

```
Options NoDate PageNo=1 Pagesize=43;
ODS HTML;
ODS Graphics On;
Title 'Martin R. Williamson';


Title2 'Build the Full Factorial Design Matrix';
proc factex;
      factors detector_th front_th rear_th;

      output out=design designrep=1
      detector_th nvals=( 0.3 0.6 )                    /* BC-454 Detector
thickness (inches) */
      front_th nvals=( 0.55 1.45 )                     /* Front EJ-200
thickness (inches) */
      rear_th nvals=( 1 2 )                            /* Rear EJ-200
thickness (inches) */
      ;
      Proc Print;
Run;

/*************************************************************************
**/
/*
*/
/*                        Begin Factorial Design Analysis
*/
/*
*/
/*************************************************************************
**/

Title2 'Data Import';
PROC IMPORT OUT= WORK.A
            DATAFILE= "C:\ELjen_Opt.xlsx"
            DBMS=EXCEL REPLACE;
     RANGE="Factorial Design$";
     GETNAMES=YES;
     MIXED=YES;
     SCANTEXT=YES;
     USEDATE=YES;
     SCANTIME=YES;
RUN;

Proc Print Data=A; Run;


Title2 'ANOVA to determine significant parameters';
proc glm data=A;
       class detector_th front_th rear_th;
       model n_abs_eff g_int_eff GARRn= detector_th|front_th|rear_th@2 /
solution;
       lsmeans detector_th*front_th / slice=detector_th pdiff;
    lsmeans detector_th*rear_th / slice=detector_th pdiff;
       lsmeans front_th*rear_th / slice=front_th pdiff;
       run; quit; run;
```

```
/*************************************************************************
**/
/*
*/
/*                          Begin CCD Analysis
*/
/*
*/
/*************************************************************************
**/


Title2 'Data Import';
PROC IMPORT OUT= WORK.B
            DATAFILE= "C:\ELjen_Opt.xlsx"
            DBMS=EXCEL REPLACE;
     RANGE="CCD$";
     GETNAMES=YES;
     MIXED=YES;
     SCANTEXT=YES;
     USEDATE=YES;
     SCANTIME=YES;
RUN;

Proc Print Data=B; Run;



/*************************************************************************
*****************/
/* Append a grid of factor values to the observed data, with missing values for
the responses  */
/*************************************************************************
*****************/

Data C;
   Set B end=eof;
   Output;
   If eof then do;
      n_abs_eff=.;
      g_int_eff=.;
      GARRn=.;
      Do detector_th=0.2 to 0.7 by .05;
         Do front_th=0.25 to 1.75 by 0.05;
            Do rear_th=0.7 to 2.3 by 0.05;
                           Output;
            End;
         End;
      End;
   End;
Run;

/* Proc Print Data=C; Run;


/*************************************************************************
*****************/
/*  Use PROC RSREG to fit a response surface model to the data and to compute
predicted values */
```

```
/*    for both the observed data and the grid, putting the predicted values in
a data set D.   */
/*************************************************************************
*****************/

Proc RSReg Data=C Out=D plots=all;
   Model n_abs_eff g_int_eff GARRn = detector_th front_th rear_th / nocode
Predict;
Run;

/* Proc Print Data=D; Run;

/*************************************************************************
*****************/
/*  Find the subset of predicted values that satisfy the constraints, sort by
the              */
/*     unconstrained variable, and display the top five predictions.
*/
/*     Neutron absorption efficiency - Constrained to a minimum of 2.5 cps/ng
252Cf = 2.5      */
/*     g_int_effination ability - Constrained to a maximum of 0.001 = 1E-3
*/
/*     Gamma absolute rejection ratio for neutrons (GARRn) = 0.9 < GARRn < 1.1
*/
/*     Cost <= 30,000
*/
/*************************************************************************
*****************/

Data E;
   set D;
   if n_abs_eff >= 2.5;
   if 0 < g_int_eff <= 3.0E-3;
   if 0.9 < GARRn < 2.8;

Proc Sort data=E;
   by descending n_abs_eff;
Run;

data E; set E;
   if (_n_ <= 10);
Proc Print;
Run;


/*************************************************************************
*****************/
/*  To simultaneously optimize the responses, make a visual comparison of the
response         */
/*     surfaces by overlaying their contour plots.
*/
/*************************************************************************
*****************/

Proc Rsreg Data=B plots=surface(overlaypairs);
   Model n_abs_eff g_int_eff GARRn = detector_th front_th rear_th / nocode;
Run;


/* Create 3D plots */
```

```
proc rsreg data=D out=F plots(unpack)=surface(3d at(detector_th=0.35,
front_th=1.5, rear_th=2.3));
      model n_abs_eff = detector_th front_th rear_th / predict;
run; quit; run;

proc rsreg data=D out=G plots(unpack)=surface(3d at(detector_th=0.35,
front_th=1.5, rear_th=2.3));
      model g_int_eff = detector_th front_th rear_th / predict;
run; quit; run;

proc rsreg data=D out=H plots(unpack)=surface(3d at(detector_th=0.35,
front_th=1.5, rear_th=2.3));
      model GARRn = detector_th front_th rear_th / predict;
run; quit; run;



Data I;
  set D;
  area = (n_abs_eff >= 2.5) + 2*(g_int_eff <= 4.0E-3) + 4*(0.9 < GARRn < 2.8);
run; *no subsetting if statments... want all of C copied into D;

/*The area variable defines the eight areas that appear on the contour plot.
The terms in parentheses in the expression for area have the value one if the
logical expression is true and the value zero if the logical expression is
false.

You will also need a format to provide labels for the plot legend that
correspond to your definition of area:*/

proc format; value yfmt                  /* n_abs_eff   g_int_eff   GARRn
Value   */
    0='None'                               /* 1*0       +   2*0   +  4*0    =  0
*/
    1='n_abs_eff'                          /* 1*1       +   2*0   +  4*0    =  1
*/
    2='g_int_eff'                          /* 1*0       +   2*1   +  4*0    =  2
*/
    3='n_abs_eff&g_int_eff'                /* 1*1       +   2*1   +  4*0    =  3
*/
    4='GARRn'                              /* 1*0       +   2*0   +  4*1    =  4
*/
    5='n_abs_eff&GARRn'                    /* 1*1       +   2*0   +  4*1    =  5
*/
    6='g_int_eff&GARRn'                    /* 1*0       +   2*1   +  4*1    =  6
*/
    7='n_abs_eff,g_int_eff,&GARRn'         /* 1*1       +   2*1   +  4*1    =  7
*/
;


proc sort data=I; by detector_th;

proc gplot uniform data=I; by detector_th;
    symbol1 value=dot color=cream h=3;
    symbol2 value=dot repeat=13 h=3;
    legend1 frame label=("Vars > min:");
    format area yfmt.;
    plot front_th*rear_th=area / legend=legend1;
run; quit; run;
```

```
ODS html close;
ODS Graphics off;
```

APPENDIX D – MATLAB®-M-FILES

This appendix contains the Matlab PTRAC post-processing suite of computer codes in the order in which they were discussed in Section 3.4. Comments are included throughout the code in order to help follow the logic. User control of this suite of codes is accomplished using the GUI which is presented after running the main program file (MCNPX_GRABBER.m). While the Birks/Chou fitting parameters and the stopping power tables must be input directly into the main program file (MCNPX_GRABBER.m) for each type of detector configuration, all other program files should not normally be modified.

MCNPX_GRABBER.m

```
%%%%%%%%%%%%%%%%%%%%%%%%%%%%%%%%%%%%%%%%%%%%%%%%%%%%%%%%%%%%%%%%%%%%%%%%%%%%%%%%
%%%%%%%%%%%%%%%%%%%%%%%%%%%%%%%%%%%%%%%%%%%%%%%%%%%%%%%%%%%%%%%%%%%%%%%%%%%%%%%%
%                                                                                 %
%   This m-file (named GRABBER) does the following:                               %
%      - Reads MCNPX output file defined by the user (if applicable),             %
%      - Reads MCNPX ptrac output file defined by the user,                       %
%      - Places all of the PTRAC events in an array (named Data),                 %
%      - Calculated the energy deposited from charged particles within            %
%        each cell,                                                               %
%      - Calculated a simulated pulse height spectra plot based on the            %
%        energy deposited from the charged particles,                             %
%      - Calculates the number and probability of all particle event types%
%      - Compares results from multiple MCNPX outputs for sensitivity             %
%        studies,                                                                 %
%      - Prints the results.                                                      %
%                                                                                 %
%   grabber.m requires the following files:                                       %
%       - A MCNPX generated PTRAC output file                                     %
%       - The following Matlab function files used to analyze the data            %
%         - add_energy.m    (Tracks/tallies the charged particle energy           %
%                            deposition within each cell)                         %
%         - stats.m          (Follows the charged particles, tallying            %
%                             the number of location, energy deposition,          %
%                             and other things)                                   %
%         - scintillation.m  (Calculates final scintillation statistics          %
%                             for each cell)                                      %

%   grabber.m requires the following files if the MCNPX output if the            %
%             MCNPX output file is analyzed also (such as in the case             %
%             where the PTRAC output only shows charged particle results)         %
%       - A MCNPX output file which corresponds to the PTRAC output file          %
%       - num_source_reader.m    (Tallies the number of source                    %
%                                 particles from the MCNPX output file)           %
%       - g_from_brem_reader.m   (Tallies the number of gammas generated          %
%                                 from bremsstrahlung)                            %
%       - g_from_n_reader.m      (Tallies the number of gammas generated          %
%                                 from neutrons)                                  %
%       - n_abs_reader.m         (Tallies the number of neutron abs)              %
%       - n_escape_reader.m      (Tallies the number of neutron escapes)          %
%       - p_capture_reader.m     (Tallies the number of photon captures)          %
%       - p_compt_scatt_reader.m (Tallies the number of photon compton            %
%                                 scattering events)                              %
%       - p_energy_cut_reader.m  (Tallies the number of photons who's             %
%                                 history ended due to the low E cutoff)          %
%       - p_escape_reader.m      (Tallies the number of photon escapes)           %
%       - p_fluorescence_reader.m  (Tallies the number of photons                 %
%                                   generated from fluorescence)                  %
%       - p_pair_prod_reader.m   (Tallies the number of photons                   %
%                                   lost from pair production events)           %
%       - p_photonuclear_abs_reader.m   (Tallies the number of photons            %
%                                        lost from photonuclear_abs events)       %
%                                                                                 %
%    Notice that useful data within the "charged_per_cell_X (X=particle)          %
%           arrays after a run.  Descriptions of column data are provided         %
%           in this code (grabber).                                               %
%                                                                                 %
%%%%%%%%%%%%%%%%%%%%%%%%%%%%%%%%%%%%%%%%%%%%%%%%%%%%%%%%%%%%%%%%%%%%%%%%%%%%%%%%
%%%%%%%%%%%%%%%%%%%%%%%%%%%%%%%%%%%%%%%%%%%%%%%%%%%%%%%%%%%%%%%%%%%%%%%%%%%%%%%%
```

```
%                                                                      %
%   The PTRAC output is described as follows:                          %
%                                                                      %
%   Event Types as described by MCNP Manual Table 1.5 (and also 3-148) %
%     1000 = src = initial source event                                %
%     2000 = bnk = bank event (includes photon production, etc.)       %
%            If you have a bank event, the type is described by Table I.6 %
%     3000 = sur = surface event                                       %
%     4000 = col = collision event                                     %
%     5000 = ter = terminiation event                                  %
%            If you have a ter event, the type is described by Table I.7 %
%                                                                      %
%   Event Type Variable IDs as described by MCNP Manual Table I.4      %
%    1 = NPS = Particle number                                         %
%    2 = --- = Event type for the 1st event                            %
%    7 = --- = Event type for the next event                           %
%    8 = NODE = # of nodes in track from source to here                %
%    9 = NSR = Source type                                             %
%   10 = NXS = Blocks of descriptors of x-section tables               %
%   11 = NTYN = Reaction Type in current collision - see Table I.7     %
%   12 = NSF = Problem names of surfaces (surface #)                   %
%   13 = --- = Angle with surface normal (degrees)                     %
%   14 = NTER = Reaction Type of the termination of the track          %
%               See Table I.7 for details                              %
%   15 = --- = branch number for this history                          %
%   16 = IPT = Type of particle (1=neutron, 2=photon, 3=electron, ...  %
%              9=proton, 32=triton, 34=alpha)                          %
%   17 = NCL = Problem numbers of the cell                             %
%   18 = MAT = Material numbers of the cell                            %
%   19 = NCP = Count of collisions per track                           %
%   20 = XXX = X-coordinate of particle position                       %
%   21 = YYY = Y-coordinate of particle position                       %
%   22 = ZZZ = Z-coordinate of particle position                       %
%   23 = UUU = Particle direction cosine with X-axis                   %
%   24 = VVV = Particle direction cosine with Y-axis                   %
%   25 = WWW = Particle direction cosine with Z-axis                   %
%   26 = ERG = Particle energy (MeV)                                   %
%   27 = WGT = Paricle weight                                          %
%   28 = TME = Time at the particle position - shakes                  %
%                                                                      %
%   Variable Type IDs by Event Type:                                   %
%       NOTE: These may change depending on PTRAC options              %
%             These values are for all with no tallies                 %
%             This can be verified by looking at the 3 lines preceeding %
%             the first event.                                         %
%   1000 (SRC): 1,2,7,8,9,16,17,18,19,20,21,22,23,24,25,26,27,28       %
%   2000 (BNK):   7,8,10,11,16,17,18,19,20,21,22,23,24,25,26,27,28     %
%   3000 (SUR):   7,8,12,13,16,17,18,19,20,21,22,23,24,25,26,27,28     %
%   4000 (COL):   7,8,10,11,16,17,18,19,20,21,22,23,24,25,26,27,28     %
%   5000 (TER):   7,8,14,15,16,17,18,19,20,21,22,23,24,25,26,27,28     %
%                                                                      %
%   1000: NPS,Event_1,Event_n+1--,NODE,NSR,IPT,NCL,MAT,NCP,            %
%         XXX,YYY,ZZZ,UUU,VVV,WWW,ERG,WGT,TME                          %
%   2000: --,NODE,NXS,NTYN,IPT,NCL,MAT,NCP,XXX,YYY,ZZZ,UUU,VVV,WWW,    %
%         ERG,WGT,TME                                                  %
%   3000: --,NODE,NSF,ANGLE,IPT,NCL,MAT,NCP,XXX,YYY,ZZZ,UUU,VVV,WWW,  %
%         ERG,WGT,TME                                                  %
%   4000: --,NODE,NXS,NTYN,IPT,NCL,MAT,NCP,XXX,YYY,ZZZ,UUU,VVV,WWW,    %
%         ERG,WGT,TME                                                  %
%   5000: --,NODE,NTER,Branch#,IPT,NCL,MAT,NCP,XXX,YYY,ZZZ,UUU,VVV,WWW, %
%         ERG,WGT,TME                                                  %
```

```
%%%%%%%%%%%%%%%%%%%%%%%%%%%%%%%%%%%%%%%%%%%%%%%%%%%%%%%%%%%%%%%%%%%%%%%%%%%%
%%%%%%%%%%%%%%%%%%%%%%%%%%%%%%%%%%%%%%%%%%%%%%%%%%%%%%%%%%%%%%%%%%%%%%%%%%%%

 clear all;
 clc;

 % Stopping powers taken from MCNPX v2.7c output for LiSal/P2VN (ND13)
%   Energy       Alpha SP(MeV-cm2/g)  Triton SP(MeV-cm2/g)
stopping_power1 = [
    0                  0                  0
1.08E-03    4.33E+02    1.86E+02
1.18E-03    4.34E+02    1.87E+02
1.28E-03    4.35E+02    1.88E+02
1.40E-03    4.36E+02    1.89E+02
1.53E-03    4.37E+02    1.91E+02
1.66E-03    4.39E+02    1.92E+02
1.81E-03    4.40E+02    1.94E+02
1.98E-03    4.42E+02    1.97E+02
2.16E-03    4.44E+02    1.99E+02
2.35E-03    4.47E+02    2.02E+02
2.57E-03    4.50E+02    2.06E+02
2.80E-03    4.54E+02    2.09E+02
3.05E-03    4.57E+02    2.13E+02
3.33E-03    4.62E+02    2.18E+02
3.63E-03    4.67E+02    2.23E+02
3.96E-03    4.72E+02    2.28E+02
4.32E-03    4.79E+02    2.34E+02
4.71E-03    4.86E+02    2.40E+02
5.13E-03    4.94E+02    2.46E+02
5.60E-03    5.03E+02    2.53E+02
6.10E-03    5.13E+02    2.61E+02
6.66E-03    5.23E+02    2.69E+02
7.26E-03    5.35E+02    2.78E+02
7.92E-03    5.48E+02    2.87E+02
8.63E-03    5.61E+02    2.97E+02
9.41E-03    5.76E+02    3.07E+02
1.03E-02    5.91E+02    3.18E+02
1.12E-02    6.08E+02    3.30E+02
1.22E-02    6.26E+02    3.42E+02
1.33E-02    6.46E+02    3.55E+02
1.45E-02    6.66E+02    3.68E+02
1.58E-02    6.88E+02    3.83E+02
1.73E-02    7.11E+02    3.98E+02
1.88E-02    7.35E+02    4.14E+02
2.05E-02    7.61E+02    4.30E+02
2.24E-02    7.89E+02    4.48E+02
2.44E-02    8.18E+02    4.66E+02
2.66E-02    8.49E+02    4.85E+02
2.90E-02    8.81E+02    5.05E+02
3.17E-02    9.15E+02    5.25E+02
3.45E-02    9.51E+02    5.44E+02
3.77E-02    9.88E+02    5.63E+02
4.11E-02    1.03E+03    5.82E+02
4.48E-02    1.07E+03    6.01E+02
4.88E-02    1.11E+03    6.20E+02
5.32E-02    1.16E+03    6.39E+02
5.81E-02    1.21E+03    6.58E+02
6.33E-02    1.26E+03    6.76E+02
6.91E-02    1.31E+03    6.94E+02
7.53E-02    1.36E+03    7.11E+02
8.21E-02    1.41E+03    7.28E+02
```

8.96E-02	1.46E+03	7.43E+02
9.77E-02	1.51E+03	7.57E+02
1.06E-01	1.57E+03	7.71E+02
1.16E-01	1.62E+03	7.82E+02
1.27E-01	1.67E+03	7.93E+02
1.38E-01	1.72E+03	8.02E+02
1.51E-01	1.77E+03	8.09E+02
1.64E-01	1.81E+03	8.14E+02
1.79E-01	1.86E+03	8.17E+02
1.95E-01	1.90E+03	8.19E+02
2.13E-01	1.94E+03	8.19E+02
2.32E-01	1.98E+03	8.17E+02
2.53E-01	2.01E+03	8.12E+02
2.76E-01	2.04E+03	8.06E+02
3.01E-01	2.07E+03	7.98E+02
3.28E-01	2.09E+03	7.88E+02
3.58E-01	2.11E+03	7.76E+02
3.91E-01	2.12E+03	7.62E+02
4.26E-01	2.13E+03	7.46E+02
4.65E-01	2.13E+03	7.29E+02
5.07E-01	2.13E+03	7.10E+02
5.52E-01	2.12E+03	6.90E+02
6.02E-01	2.11E+03	6.69E+02
6.57E-01	2.09E+03	6.48E+02
7.16E-01	2.06E+03	6.25E+02
7.81E-01	2.04E+03	6.02E+02
8.52E-01	2.00E+03	5.78E+02
9.29E-01	1.96E+03	5.54E+02
1.01E+00	1.92E+03	5.30E+02
1.10E+00	1.88E+03	5.05E+02
1.20E+00	1.83E+03	4.81E+02
1.31E+00	1.77E+03	4.57E+02
1.43E+00	1.72E+03	4.34E+02
1.56E+00	1.66E+03	4.11E+02
1.70E+00	1.60E+03	3.89E+02
1.86E+00	1.54E+03	3.67E+02
2.03E+00	1.48E+03	3.46E+02
2.21E+00	1.41E+03	3.26E+02
2.41E+00	1.35E+03	3.06E+02
2.63E+00	1.29E+03	2.88E+02
2.87E+00	1.22E+03	2.70E+02
3.13E+00	1.16E+03	2.53E+02
3.41E+00	1.10E+03	2.37E+02
3.72E+00	1.04E+03	2.22E+02
4.05E+00	9.84E+02	2.08E+02
4.42E+00	9.28E+02	1.94E+02
4.82E+00	8.74E+02	1.81E+02
5.26E+00	8.22E+02	1.69E+02
5.73E+00	7.72E+02	1.58E+02
6.25E+00	7.25E+02	1.48E+02
6.82E+00	6.80E+02	1.38E+02
7.43E+00	6.37E+02	1.29E+02
8.11E+00	5.97E+02	1.21E+02
8.84E+00	5.59E+02	1.13E+02
9.64E+00	5.23E+02	1.06E+02
1.05E+01	4.90E+02	9.92E+01
1.15E+01	4.59E+02	9.29E+01
1.25E+01	4.30E+02	8.71E+01
1.36E+01	4.03E+02	8.17E+01
1.49E+01	3.78E+02	7.66E+01
1.62E+01	3.54E+02	7.17E+01

```
1.77E+01    3.32E+02    6.70E+01
1.93E+01    3.12E+02    6.26E+01
2.10E+01    2.92E+02    5.84E+01
2.29E+01    2.73E+02    5.45E+01
2.50E+01    2.55E+02    5.09E+01
2.73E+01    2.38E+02    4.75E+01
2.97E+01    2.22E+02    4.43E+01
3.24E+01    2.07E+02    4.13E+01
3.54E+01    1.94E+02    3.85E+01
3.86E+01    1.80E+02    3.59E+01
4.20E+01    1.68E+02    3.35E+01
4.59E+01    1.57E+02    3.12E+01
5.00E+01    1.46E+02    2.91E+01
5.45E+01    1.36E+02    2.71E+01
5.95E+01    1.27E+02    2.53E+01
6.48E+01    1.19E+02    2.35E+01
7.07E+01    1.10E+02    2.19E+01
7.71E+01    1.03E+02    2.04E+01
8.41E+01    9.59E+01    1.91E+01
9.17E+01    8.94E+01    1.78E+01
1.00E+02    8.33E+01    1.66E+01];

kB_alpha = 0.045659688;
C_alpha = 8.15139E-06;
kB_triton = 0.007630933;
C_triton = 2.37676E-05;

argout = {};
argout = selection_gui();

if ischar(argout{1})==1
    mxfilename = argout{1};
    mx=1;
else
    mx=0;
end

if ischar(argout{2})==1
    filename = argout{2};
else
    error('Please enter a PTRAC filename.');
end

if argout{3}=='y'
    filter = 'y';
else
    filter = 'n';
end

if argout{4}==1
    run_electron = 1;
else
    run_electron = 0;
end

if argout{5}==1
    run_proton = 1;
else
    run_proton = 0;
end
```

```
if argout{6} == 1
    run_triton = 1;
else
    run_triton = 0;
end

% if argout{7} == 1
%     run_he3 = 1;
% else
%     run_he3 = 0;
% end

if argout{7} == 1
    run_alpha = 1;
else
    run_alpha = 0;
end

if argout{8} <=2
    multiplier = argout{8};
else
    disp('Invalid multiplier value; resetting multiplier to 1.');
    multiplier = 1;
end

if argout{9}=='y'
    pfilter = 'y';
else
    pfilter = 'n';
end

if argout{10} == 1
    run_heavy = 1;
else
    run_heavy = 0;
end


%Read data from file into Data matrix
index=1;

fid = fopen(filename);

%Scans numbers from the open file int a cell array after skipping first ten
%lines. Change the header lines variable if the input file is formatted
%differently than ptrac_all.o
C = textscan(fid,'%n',2, 'HeaderLines', 10);

%Convert cell array into readable Data array
while(true)

    %Quit if nothing was read (size of cell == 0)
    d=C{1};
    if(size(d)==[0,1])break;
    end

    %Read event number and source event type
    Data(index,1) = d(1,1);
    index=index+1;
    Data(index,1) =d(2,1);
```

```
    if filter == 'y'
        C = textscan(fid,'%n',1);
    end

    %Continue to end of file
    while(true)
        %Store next event type in event variable and set number of columns
        %appropriate to event type
        event=Data(index,1);
        if(event==1000) && pfilter == 'n'
            x=16;
        else
            x=17;
        end

        if pfilter == 'y' && event == 1000
            C = textscan(fid,'%n',4);
            d=C{1};
            Data(index,2:4) = d(2:4,1);
            nextevent = d(1,1);

            Data(index,5) = 0;

            C = textscan(fid,'%n',x-5);
            d=C{1};
            Data(index,6:x) = d(1:x-5,1);
        else%Read in all columns for current event
            C = textscan(fid,'%n',x);
            d=C{1};
            Data(index,2:x) = d(2:x,1);
            nextevent = d(1,1);
        end


        %Increment pointer to next row
        index=index+1;
        %Read next event type and exit if event == 9000 (end)
        Data(index,1)=nextevent;

        if Data(index,1)==9000
            break;
        end;
    end;

    %Since events are out of order, one row of variables is left to match
    %with stored event type. Read those in now.
    C = textscan(fid,'%n',2);
end

fclose(fid);

%%%%%%%%%%%%%%%%%%%%%%%%%%%%%%%%%%%%%%%%%%%%%%%%%%%%%%%%%%%%%%%%%%%%%%%%%%%%%%%
%                                                                              %
%  Source Events (EVENT=1000)                                                  %
%                                                                              %
%%%%%%%%%%%%%%%%%%%%%%%%%%%%%%%%%%%%%%%%%%%%%%%%%%%%%%%%%%%%%%%%%%%%%%%%%%%%%%%

if mx == 1
    num_source = num_source_reader(mxfilename);
else
    num_source = length(find(Data(:,1)==1000));
```

```
end


%%%%%%%%%%%%%%%%%%%%%%%%%%%%%%%%%%%%%%%%%%%%%%%%%%%%%%%%%%%%%%%%%%%%%%%%%%%%%%%%
%                                                                               %
%  Bank Events (EVENT=2000)                                                     %
%                                                                               %
%%%%%%%%%%%%%%%%%%%%%%%%%%%%%%%%%%%%%%%%%%%%%%%%%%%%%%%%%%%%%%%%%%%%%%%%%%%%%%%%

% Initialize Tallies
bnk_t_created = 0;
bnk_a_created = 0;
bnk_h_created = 0;
bnk_e_created = 0;
% bnk_s_created = 0;
bnk_g_from_n_created = 0;
bnk_g_from_brem_created = 0;
other_bank_events = 0;
triton_stats=zeros(8,1);
alpha_stats=zeros(8,1);
heavy_stats=zeros(8,1);
% he3_stats=zeros(8,1);
proton_stats=zeros(8,1);
electron_stats=zeros(8,1);

% Stats matrix row labels
% 1 = Total energy difference
% 2 = Birth cell
% 3 = Death cell
% 4 = Distance traveled
% 5 = Birth cell energy deposited
% 6 = Death cell energy deposited
% 7 = Event number
% 8 = Number of additional cells particle passed through
% 9-n = Pairs of values indicating cell number and energy deposited in cell

% Filter out only bank event types (EVENT=20xx)
bnk_eventtype = find(2000 <= Data(:,1) & Data(:,1) <= 2034);
for i=1:length(bnk_eventtype)

    % What type of bank event occured (2030 = light ions from neutron)
    if(Data(bnk_eventtype(i,1),1)==2030)
        % What type of light ions were generated (32 = triton)
        if(Data(bnk_eventtype(i,1),5)==32) && run_triton==1
            bnk_t_created = bnk_t_created + 1;
            triton_stats =
stats(Data,bnk_eventtype,triton_stats,i,stopping_power1,kB_triton,C_triton,32);

%         % What type of light ions were generated (33 = helium3)
%         elseif(Data(bnk_eventtype(i,1),5)==33) && run_he3==1
%             bnk_s_created = bnk_s_created + 1;
%             he3_stats = stats(Data,bnk_eventtype,he3_stats,i);

        % What type of light ions were generated (34 = alpha)
        elseif(Data(bnk_eventtype(i,1),5)==34) && run_alpha==1
            bnk_a_created = bnk_a_created + 1;
            alpha_stats =
stats(Data,bnk_eventtype,alpha_stats,i,stopping_power1,kB_alpha,C_alpha,34);

        % What type of light ions were generated (35 = heavy)
        elseif(Data(bnk_eventtype(i,1),5)==35) && run_heavy==1
```

```
            bnk_h_created = bnk_h_created + 1;
            heavy_stats =
stats(Data,bnk_eventtype,heavy_stats,i,stopping_power1,kB_triton,C_triton,35);


        % What type of light ions were generated (9 = proton)
        elseif(Data(bnk_eventtype(i,1),5)==9)&& run_proton == 1
            bnk_h_created = bnk_h_created + 1;
            proton_stats =
stats(Data,bnk_eventtype,proton_stats,i,stopping_power1,1,1,9);

        end
    % What type of bank event occured (2008 = photon from neutron)
    elseif(Data(bnk_eventtype(i,1),1)==2008)
        bnk_g_from_n_created = bnk_g_from_n_created + 1;

    % What type of bank event occured (2016 = Bremsstrahlung from Electron)
    elseif(Data(bnk_eventtype(i,1),1)==2016)
        bnk_g_from_brem_created = bnk_g_from_brem_created + 1;

    elseif( (Data(bnk_eventtype(i,1),1)==2011 ||
Data(bnk_eventtype(i,1),1)==2012 ||...
            Data(bnk_eventtype(i,1),1)==2013 ||
Data(bnk_eventtype(i,1),1)==2014 ||...
            Data(bnk_eventtype(i,1),1)==2017) && Data(bnk_eventtype(i,1),5)==3
) && run_electron == 1
            % What type of light ions were generated (3 = electron)
            bnk_e_created = bnk_e_created + 1;
            electron_stats =
stats(Data,bnk_eventtype,electron_stats,i,stopping_power1);

    end

end


%%%%%%%%%%%%%%%%%%%%%%%%%%%%%%%%%%%%%%%%%%%%%%%%%%%%%%%%%%%%%%%%%%%%%%%%%%%%%%%
%                                                                              %
%  Probability of Scintillation                                                %
%                                                                              %
%%%%%%%%%%%%%%%%%%%%%%%%%%%%%%%%%%%%%%%%%%%%%%%%%%%%%%%%%%%%%%%%%%%%%%%%%%%%%%%

%Column 1: Cell number
%Column 2: Number of particles interacting with that cell
%Column 3: Probability of scintillation given a neutron event
%Column 4: Probability of scintillation given a charged particle event
%Column 5: Energy deposited in cell
%Column 6: Average energy deposited in cell per particle
%Column 7: Standard Deviation of energy deposited in cell
%Column 8: Tracks entering cell

%Array to store unique event numbers per cell
events_per_cell = zeros(1,2);

if run_triton==1
    charged_per_cell_triton = zeros(1,5);
    charged_per_cell_triton =
scintillation(triton_stats,charged_per_cell_triton,num_source,bnk_t_created);
    events_per_cell = total_scintillation(triton_stats,events_per_cell);
end
```

```
if run_alpha==1
    charged_per_cell_alpha = zeros(1,5);
    charged_per_cell_alpha =
scintillation(alpha_stats,charged_per_cell_alpha,num_source,bnk_a_created);
    events_per_cell = total_scintillation(alpha_stats,events_per_cell);
end

if run_heavy==1
    charged_per_cell_heavy = zeros(1,5);
    charged_per_cell_heavy =
scintillation(heavy_stats,charged_per_cell_heavy,num_source,bnk_h_created);
    events_per_cell = total_scintillation(heavy_stats,events_per_cell);
end

if run_electron==1
    charged_per_cell_electron = zeros(1,5);
    charged_per_cell_electron =
scintillation(electron_stats,charged_per_cell_electron,num_source,bnk_e_created
);
    events_per_cell = total_scintillation(electron_stats,events_per_cell);
end

if run_proton==1
    charged_per_cell_proton = zeros(1,5);
    charged_per_cell_proton =
scintillation(proton_stats,charged_per_cell_proton,num_source,bnk_h_created);
    events_per_cell = total_scintillation(proton_stats,events_per_cell);
end

% if run_he3==1
%     charged_per_cell_he3 = zeros(1,5);
%     charged_per_cell_he3 =
scintillation(he3_stats,charged_per_cell_he3,num_source,bnk_s_created);
%     events_per_cell = total_scintillation(he3_stats,events_per_cell);
% end




%Total probability of scintillation (across all particles)
%Column 1: Cell number
%Column 2: Scintillation probability
total_per_cell = zeros(size(events_per_cell,1),2);
total_per_cell(:,1) = events_per_cell(:,1);
total_per_cell(:,2) = events_per_cell(:,2)./num_source;

%%%%%%%%%%%%%%%%%%%%%%%%%%%%%%%%%%%%%%%%%%%%%%%%%%%%%%%%%%%%%%%%%%%%%%%%%%%%
% Graphing
% Change bucket size if results are inaccurate
%%%%%%%%%%%%%%%%%%%%%%%%%%%%%%%%%%%%%%%%%%%%%%%%%%%%%%%%%%%%%%%%%%%%%%%%%%%%
% Set up buckets for histogram
x=0:.02:3;

if run_triton==1
    %First graph shows total energy lost among all triton particles
    %Dump triton energy into histogram buckets
    Histogram = hist(multiplier*triton_stats(1,2:size(triton_stats,2)),x);
    figure(); %Create new bar graph
    bar(x,Histogram);
```

```
    title(['File: ',filename,', Histogram of energy lost among each triton
particle event'])
    xlabel('Energy (MeV)')
    ylabel('# of Events')
    axis([0 5 0 1]);
    axis 'auto y';
%     text(1,1,'Average: %d\nStandard Deviation:
%d',mean(triton_stats(1,2:size(triton_stats,2))),...
%         std(triton_stats(1,2:size(triton_stats,2))),'Units','normalized')
end

if run_alpha==1
    %Second graph shows total energy lost among all alpha particles
    Histogram = hist(multiplier*alpha_stats(1,2:size(alpha_stats,2)),x);
    figure();
    bar(x,Histogram);
    title(['File: ',filename,', Histogram of energy lost among each alpha
particle event'])
    xlabel('Energy (MeV)')
    ylabel('# of Events')
    axis([0 5 0 1]);
    axis 'auto y';
    text(.8,.8,['Average:
',num2str(mean(alpha_stats(1,2:size(alpha_stats,2)))),],'Units','normalized')
    text(.8,.65,['Standard Deviation:
',num2str(std(alpha_stats(1,2:size(alpha_stats,2))))],'Units','normalized')
end

if run_heavy ==1
    %Fifth graph shows total energy lost among all heavy
    Histogram = hist(multiplier*heavy_stats(1,2:size(heavy_stats,2)),x);
    figure();
    bar(x,Histogram);
    title(['File: ',filename,', Histogram of energy lost among all heavy
events'])
    xlabel('Energy (MeV)')
    ylabel('# of Events')
    axis([0 5 0 1]);
    axis 'auto y';
%     text(1,1,'Average: %d\nStandard Deviation:
%d',mean(heavy_stats(1,2:size(heavy_stats,2))),...
%         std(heavy_stats(1,2:size(heavy_stats,2))),'Units','normalized')
end

if run_electron==1
    %Third graph shows total energy lost among all electrons
    Histogram = hist(multiplier*electron_stats(1,2:size(electron_stats,2)),x);
    figure();
    bar(x,Histogram);
    title(['File: ',filename,', Histogram of energy lost among each electron
event'])
    xlabel('Energy (MeV)')
    ylabel('# of Events')
    axis([0 5 0 1]);
    axis 'auto y';
%     text(1,1,'Average: %d\nStandard Deviation:
%d',mean(electron_stats(1,2:size(electron_stats,2))),...
%         std(electron_stats(1,2:size(electron_stats,2))),'Units','normalized')
end

if run_proton ==1
```

```
    %Fourth graph shows total energy lost among all protons
    Histogram = hist(multiplier*proton_stats(1,2:size(proton_stats,2)),x);
    figure();
    bar(x,Histogram);
    title(['File: ',filename,', Histogram of energy lost among each proton
event'])
    xlabel('Energy (MeV)')
    ylabel('# of Events')
    axis([0 5 0 1]);
    axis 'auto y';
%     text(1,1,'Average: %d\nStandard Deviation:
%d',mean(proton_stats(1,2:size(proton_stats,2))),...
%         std(proton_stats(1,2:size(proton_stats,2))),'Units','normalized')
end

% if run_he3 ==1
%     %Fifth graph shows total energy lost among all helium3
%     Histogram = hist(multiplier*he3_stats(1,2:size(he3_stats,2)),x);
%     figure();
%     bar(x,Histogram);
%     title(['File: ',filename,', Histogram of energy lost among all he3
events'])
%     xlabel('Energy (MeV)')
%     ylabel('# of Events')
%     axis([0 5 0 1]);
%     axis 'auto y';
%     text(1,1,'Average: %d\nStandard Deviation:
%d',mean(he3_stats(1,2:size(he3_stats,2))),...
%         std(he3_stats(1,2:size(he3_stats,2))),'Units','normalized')
% end

%%%%%%%%%%%%%%%%%%%%%%%%%%%%%%%%%%%%%%%%%%%%%%%%%%%%%%%%%%%%%%%%%%%%%%%
%Separate charged particle energy by cell
%%%%%%%%%%%%%%%%%%%%%%%%%%%%%%%%%%%%%%%%%%%%%%%%%%%%%%%%%%%%%%%%%%%%%%%


%Create array to store each instance of energy deposition in a particular
%cell (dynamically allocated for any number of cells)
%Width is the larger of either num_tritons or num_alpha
bin_energy = zeros(1,1);

%S_alpha = solve('x/3*905^3 + y/2*905^2 + 905 = 353','x/3*774.2^3 + y/2*774.2^2
+ 774.2 = 1170');
%S_triton = solve('x/3*905^3 + y/2*905^2 + 905 = 353','x/3*774.2^3 +
y/2*774.2^2 + 774.2 = 1170');

if run_triton == 1
    bin_energy = add_energy(triton_stats,bin_energy);
end
if run_alpha == 1
    bin_energy = add_energy(alpha_stats,bin_energy);
end
if run_heavy ==1
    bin_energy = add_energy(heavy_stats,bin_energy);
end
if run_electron == 1
    bin_energy = add_energy(electron_stats,bin_energy);
end
if run_proton ==1
    bin_energy = add_energy(proton_stats,bin_energy);
end
```

```
% if run_he3 ==1
% bin_energy = add_energy(he3_stats,bin_energy);
% end


%Create one graph for each cell (of energy lost in that cell)
%Number of cell appears in title of graph
for i=2:size(bin_energy,1)
    a = hist(multiplier*bin_energy(i,2:size(bin_energy,2)),x);
    a = a(2:size(a,2));
    b = max(a);
    c = find(a == b);
    peak = x(c);

    figure();
    bar(x(2:size(x,2)),a);
    title(['File: ',filename,': Histogram of energy lost in Cell Number
',num2str(bin_energy(i,1))])
    xlabel('Energy (MeV)')
    ylabel('# of Events')
    text(.4,.8,['Peak Energy: ',num2str(peak)],'Units','normalized');
    axis([0 7 0 1]);
    axis 'auto y';

    total_particles = 0;
    total_energy = 0;
    if run_triton == 1 && i <= size(charged_per_cell_triton,1)
        total_particles = total_particles + charged_per_cell_triton(i,2);
        total_energy = total_energy + charged_per_cell_triton(i,5);
    end
    if run_alpha == 1 && i <= size(charged_per_cell_alpha,1)
        total_particles = total_particles + charged_per_cell_alpha(i,2);
        total_energy = total_energy + charged_per_cell_alpha(i,5);
    end
    if run_heavy ==1
        total_particles = total_particles + charged_per_cell_heavy(i,2);
        total_energy = total_energy + charged_per_cell_heavy(i,5);
    end
    if run_electron == 1 && i <= size(charged_per_cell_electron,1)
        total_particles = total_particles + charged_per_cell_electron(i,2);
        total_energy = total_energy + charged_per_cell_electron(i,5);
    end
    if run_proton ==1 && i <= size(charged_per_cell_proton,1)
        total_particles = total_particles + charged_per_cell_proton(i,2);
        total_energy = total_energy + charged_per_cell_proton(i,5);
    end
    % if run_he3 ==1
%       total_particles = total_particles + charged_per_cell_he3(i,2);
%         total_energy = total_energy + charged_per_cell_he3(i,5);
    % end
%     cell_average = total_energy/total_particles;
%     text(1,1,'Average: ',num2str(cell_average),'Units','normalized');
end


%%%%%%%%%%%%%%%%%%%%%%%%%%%%%%%%%%%%%%%%%%%%%%%%%%%%%%%%%%%%%%%%%%%%%%%%%%%%%%%
%                                                                              %
%  Surface Events (EVENT=3000)                                                 %
%                                                                              %
%%%%%%%%%%%%%%%%%%%%%%%%%%%%%%%%%%%%%%%%%%%%%%%%%%%%%%%%%%%%%%%%%%%%%%%%%%%%%%%
```

```
% Surface event detection included in bank events section


%%%%%%%%%%%%%%%%%%%%%%%%%%%%%%%%%%%%%%%%%%%%%%%%%%%%%%%%%%%%%%%%%%%%%%%%%%%%%%%%
%                                                                               %
%  Collision Events (EVENT=4000)                                                %
%                                                                               %
%%%%%%%%%%%%%%%%%%%%%%%%%%%%%%%%%%%%%%%%%%%%%%%%%%%%%%%%%%%%%%%%%%%%%%%%%%%%%%%%

% Initialize Tallies
col_n_inelastic_scatter = 0;
col_n_elastic_scatter = 0;
col_n_other = 0;
col_p_incoherent_scatter = 0;
col_p_coherent_scatter = 0;
col_p_fluorescence_scatter = 0;
col_p_pair_prod_scatter = 0;
col_p_other = 0;
col_other = 0;

% Filter out only collison event types (EVENT=4000)
col_eventtype = find(Data(:,1) == 4000);
for i=1:length(col_eventtype)
    % Check to see if the particle type is a neutron (IPT=1)
    if(Data(col_eventtype(i,1),5)==1)
        % Check to see if the col event was n inelastic scat (MTP=4)
        if(Data(col_eventtype(i,1),4)==4)
            col_n_inelastic_scatter = col_n_inelastic_scatter + 1;

        % Check to see if the col event was n elastic scat (MTP=2)
        elseif(Data(col_eventtype(i,1),4)==2)
            col_n_elastic_scatter = col_n_elastic_scatter + 1;

        % Check to see if there are any other neutron collision events
        else
            col_n_other = col_n_other + 1;
        end

    % Check to see if the particle type is a photon (IPT=2)
    elseif(Data(col_eventtype(i,1),5)==2)
        % Check to see if the col event was p fluorescence scat (MTP=-3)
        if(Data(col_eventtype(i,1),4)==-3)
            col_p_fluorescence_scatter = col_p_fluorescence_scatter + 1;

        % Check to see if the col event was p pair prod scat (MTP=-4)
        elseif(Data(col_eventtype(i,1),4)==-4)
          col_p_pair_prod_scatter = col_p_pair_prod_scatter + 1;


        % Check to see if there are any other photon scattering events
        else
          col_p_other = col_p_other + 1;


        end
    % Check to see if there are any other particle scattering events
    else
       col_other = col_other + 1;
    end
end
```

```
%%%%%%%%%%%%%%%%%%%%%%%%%%%%%%%%%%%%%%%%%%%%%%%%%%%%%%%%%%%%%%%%%%%%%%%%%%%%%%%%
%                                                                                 %
%  Termination Events (EVENT=5000)                                               %
%                                                                                 %
%%%%%%%%%%%%%%%%%%%%%%%%%%%%%%%%%%%%%%%%%%%%%%%%%%%%%%%%%%%%%%%%%%%%%%%%%%%%%%%%

% Initialize Tallies
ter_n_absorptions = 0;
ter_n_escape = 0;
ter_n_other = 0;
ter_p_escape = 0;
ter_p_energy_cut = 0;
ter_p_compt_scatt = 0;
ter_p_capture = 0;
ter_p_pair_prod = 0;
ter_p_photonuclear_abs = 0;
ter_p_other = 0;
ter_t_escape = 0;
ter_t_energy_cut = 0;
ter_t_other = 0;
ter_a_escape = 0;
ter_a_energy_cut = 0;
ter_a_other = 0;
ter_e_escape = 0;
ter_e_energy_cut = 0;
ter_e_other = 0;
ter_h_escape = 0;
ter_h_energy_cut = 0;
ter_h_other = 0;
ter_other = 0;

% Filter out only termination event types (EVENT=5000)
ter_eventtype = find(Data(:,1) == 5000);
for i=1:length(ter_eventtype)
    % Check to see if the particle type is a neutron (IPT=1)
    if(Data(ter_eventtype(i,1),5)==1)
        % Check to see if the ter event was a neutron abs (NTER=12)
        if(Data(ter_eventtype(i,1),3)==12)
            ter_n_absorptions = ter_n_absorptions + 1;

        % Check to see if the ter event was a neutron escape (NTER=1)
        elseif(Data(ter_eventtype(i,1),3)==1)
            ter_n_escape = ter_n_escape + 1;

        % Check to see if there are any other neutron termination events
        else
            ter_n_other = ter_n_other + 1;
        end


    % Check to see if the particle type is a photon (IPT=2)
    elseif(Data(ter_eventtype(i,1),5)==2)
        % Check to see if the ter event was a photon escape (NTER=1)
        if(Data(ter_eventtype(i,1),3)==1)
            ter_p_escape = ter_p_escape + 1;

        % Check to see if the ter event was a photon energ cutoff (NTER=2)
        elseif(Data(ter_eventtype(i,1),3)==2)
            ter_p_energy_cut = ter_p_energy_cut + 1;
```

```
        % Check to see if the ter event was a photon Compt. Scatt (NTER=11)
        elseif(Data(ter_eventtype(i,1),3)==11)
            ter_p_compt_scatt = ter_p_compt_scatt + 1;

        % Check to see if the ter event was a photon Capture (NTER=12)
        elseif(Data(ter_eventtype(i,1),3)==12)
            ter_p_capture = ter_p_capture + 1;

        % Check to see if the ter event was a photon pair prod. (NTER=13)
        elseif(Data(ter_eventtype(i,1),3)==13)
            ter_p_pair_prod = ter_p_pair_prod + 1;

        % Check to see if the ter event was a photon photonuclear absorption
(NTER=14)
        elseif(Data(ter_eventtype(i,1),3)==14)
           ter_p_photonuclear_abs = ter_p_photonuclear_abs + 1;

        else
            ter_p_other = ter_p_other + 1;
        end
    % Check to see if the particle type is a triton (IPT=32)
    elseif(Data(ter_eventtype(i,1),5)==32) && run_triton ==1
        % Check to see if the ter event was a triton escape (NTER=1)
        if(Data(ter_eventtype(i,1),3)==1)
            ter_t_escape=ter_t_escape+1;
        % Check to see if the ter event was a triton energ cutoff (NTER=2)
        elseif(Data(ter_eventtype(i,1),3)==2)
            ter_t_energy_cut=ter_t_energy_cut+1;
        % Check to see if there are any other triton termination events
        else
        ter_t_other = ter_t_other + 1;
        end
    % Check to see if the particle type is an alpha (IPT=34)
    elseif(Data(ter_eventtype(i,1),5)==34) && run_alpha ==1
        % Check to see if the ter event was an alpha escape (NTER=1)
        if(Data(ter_eventtype(i,1),3)==1)
            ter_a_escape=ter_a_escape+1;
        % Check to see if the ter event was an alpha energ cutoff (NTER=2)
        elseif(Data(ter_eventtype(i,1),3)==2)
            ter_a_energy_cut=ter_a_energy_cut+1;
        % Check to see if there are any other alpha termination events
        else
        ter_a_other = ter_a_other + 1;
        end
        %%%%%%%%%%%%%%%%%%%%%%%%% Check to see if there are any other particle
termination events
    else
      ter_other = ter_other + 1;
    end
end

if mx==1
    % Get photon event data
    bnk_g_from_n_created = g_from_n_reader(mxfilename);
    bnk_g_from_brem_created = g_from_brem_reader(mxfilename);
    col_p_fluorescence_scatter = p_fluorescence_reader(mxfilename);
    col_p_pair_prod_scatter = p_pair_prod_reader(mxfilename);
    ter_p_escape = p_escape_reader(mxfilename);
    ter_p_energy_cut = p_energy_cut_reader(mxfilename);
    ter_p_compt_scatt = p_compt_scatt_reader(mxfilename);
    ter_p_capture = p_capture_reader(mxfilename);
```

```
    ter_p_pair_prod = p_pair_prod_reader(mxfilename);
    ter_p_photonuclear_abs = p_photonuclear_abs_reader(mxfilename);

    % Get neutron event data
    ter_n_absorptions = n_abs_reader(mxfilename);
    ter_n_escape = n_escape_reader(mxfilename);
      % May want to add other events later

    % Get triton event data
    if run_triton==1
        ter_t_escape = ter_t_escape_reader(mxfilename);
        ter_t_energy_cut = ter_t_energy_cut_reader(mxfilename);
    end
    % Get alpha event data
    if run_alpha==1
        ter_a_escape = ter_a_escape_reader(mxfilename);
        ter_a_energy_cut = ter_a_energy_cut_reader(mxfilename);
    end
    % Get electron event data
    if run_electron==1
        ter_e_escape = ter_e_escape_reader(mxfilename);
        ter_e_energy_cut = ter_e_energy_cut_reader(mxfilename);
    end
    % Get proton event data
    if run_proton==1
        ter_h_escape = ter_h_escape_reader(mxfilename);
        ter_h_energy_cut = ter_h_energy_cut_reader(mxfilename);
    end

end



%%%%%%%%%%%%%%%%%%%%%%%%%%%%%%%%%%%%%%%%%%%%%%%%%%%%
% Random Calculations
%%%%%%%%%%%%%%%%%%%%%%%%%%%%%%%%%%%%%%%%%%%%%%%%%%%%

total_energy_deposited = 0;

if run_alpha==1
    prob_alpha_creation = bnk_a_created/num_source;
    alpha_energy_avg = mean(alpha_stats(1,7:size(alpha_stats,2)));
    alpha_energy_stddev = std(alpha_stats(1,7:size(alpha_stats,2)));
    alpha_distance_avg = mean(alpha_stats(4,7:size(alpha_stats,2)));
    alpha_distance_stddev = std(alpha_stats(4,7:size(alpha_stats,2)));
    total_energy_deposited = total_energy_deposited +
sum(charged_per_cell_alpha(:,5));
end

if run_triton==1
    prob_triton_creation = bnk_t_created/num_source;
    triton_energy_avg = mean(triton_stats(1,7:size(triton_stats,2)));
    triton_energy_stddev = std(triton_stats(1,7:size(triton_stats,2)));
    triton_distance_avg = mean(triton_stats(4,7:size(triton_stats,2)));
    triton_distance_stddev = std(triton_stats(4,7:size(triton_stats,2)));
    total_energy_deposited = total_energy_deposited +
sum(charged_per_cell_triton(:,5));
end

if run_heavy==1
    prob_heavy_creation = bnk_h_created/num_source;
```

```
    heavy_energy_avg = mean(heavy_stats(1,7:size(heavy_stats,2)));
    heavy_energy_stddev = std(heavy_stats(1,7:size(heavy_stats,2)));
    heavy_distance_avg = mean(heavy_stats(4,7:size(heavy_stats,2)));
    heavy_distance_stddev = std(heavy_stats(4,7:size(heavy_stats,2)));
    total_energy_deposited = total_energy_deposited +
sum(charged_per_cell_heavy(:,5));
end

if run_electron==1
    prob_electron_creation = bnk_e_created/num_source;
    electron_energy_avg = mean(electron_stats(1,7:size(electron_stats,2)));
    electron_energy_stddev = std(electron_stats(1,7:size(electron_stats,2)));
    electron_distance_avg = mean(electron_stats(4,7:size(electron_stats,2)));
    electron_distance_stddev = std(electron_stats(4,7:size(electron_stats,2)));
    total_energy_deposited = total_energy_deposited +
sum(charged_per_cell_electron(:,5));
end

if run_proton==1
    prob_proton_creation = bnk_h_created/num_source;
    proton_energy_avg = mean(proton_stats(1,7:size(proton_stats,2)));
    proton_energy_stddev = std(proton_stats(1,7:size(proton_stats,2)));
    proton_distance_avg = mean(proton_stats(4,7:size(proton_stats,2)));
    proton_distance_stddev = std(proton_stats(4,7:size(proton_stats,2)));
    total_energy_deposited = total_energy_deposited +
sum(charged_per_cell_proton(:,5));
end

% if run_he3==1
%     prob_he3_creation = bnk_s_created/num_source;
%     he3_energy_avg = mean(he3_stats(1,7:size(he3_stats,2)));
%     he3_energy_stddev = std(he3_stats(1,7:size(he3_stats,2)));
%     he3_distance_avg = mean(he3_stats(4,7:size(he3_stats,2)));
%     he3_distance_stddev = std(he3_stats(4,7:size(he3_stats,2)));
%     total_energy_deposited = total_energy_deposited +
sum(charged_per_cell_he3(:,5));
% end

prob_n_abs = ter_n_absorptions/num_source;


% Trim our stats arrays so that they don't show "zero" columns
alpha_stats = alpha_stats(:,2:size(alpha_stats,2));
triton_stats = triton_stats(:,2:size(triton_stats,2));
heavy_stats = heavy_stats(:,2:size(heavy_stats,2));
electron_stats = electron_stats(:,2:size(electron_stats,2));
proton_stats = proton_stats(:,2:size(proton_stats,2));
%he3_stats = he3_stats(:,2:size(he3_stats,2));

% Create a summary block for printing
summary = {5,2};
summary{1,1} = 'Number of source particles'; summary{1,2}=num_source;
summary{2,1} = 'Number of charged particles'; summary{2,2} =
bnk_a_created+bnk_t_created+bnk_h_created+bnk_e_created;


%Insert blank line at end of output
disp(' ');
```

SELECTION_GUI.m

```
function varargout = selection_gui(varargin)
% SELECTION_GUI M-file for selection_gui.fig
%      SELECTION_GUI, by itself, creates a new SELECTION_GUI or raises the
existing
%      singleton*.
%
%      H = SELECTION_GUI returns the handle to a new SELECTION_GUI or the
handle to
%      the existing singleton*.
%
%      SELECTION_GUI('CALLBACK',hObject,eventData,handles,...) calls the local
%      function named CALLBACK in SELECTION_GUI.M with the given input
arguments.
%
%      SELECTION_GUI('Property','Value',...) creates a new SELECTION_GUI or
raises the
%      existing singleton*.  Starting from the left, property value pairs are
%      applied to the GUI before selection_gui_OpeningFunction gets called.  An
%      unrecognized property name or invalid value makes property application
%      stop.  All inputs are passed to selection_gui_OpeningFcn via varargin.
%
%      *See GUI Options on GUIDE's Tools menu.  Choose "GUI allows only one
%      instance to run (singleton)".
%
% See also: GUIDE, GUIDATA, GUIHANDLES

% Edit the above text to modify the response to help selection_gui

% Last Modified by GUIDE v2.5 27-Sep-2010 09:20:49

% Begin initialization code - DO NOT EDIT
gui_Singleton = 1;
gui_State = struct('gui_Name',       mfilename, ...
                   'gui_Singleton',  gui_Singleton, ...
                   'gui_OpeningFcn', @selection_gui_OpeningFcn, ...
                   'gui_OutputFcn',  @selection_gui_OutputFcn, ...
                   'gui_LayoutFcn',  [] , ...
                   'gui_Callback',   []);
if nargin && ischar(varargin{1})
    gui_State.gui_Callback = str2func(varargin{1});
end

if nargout
    [varargout{1:nargout}] = gui_mainfcn(gui_State, varargin{:});
else
    gui_mainfcn(gui_State, varargin{:});
end
% End initialization code - DO NOT EDIT


% --- Executes just before selection_gui is made visible.
function selection_gui_OpeningFcn(hObject, eventdata, handles, varargin)
% This function has no output args, see OutputFcn.
% hObject    handle to figure
% eventdata  reserved - to be defined in a future version of MATLAB
% handles    structure with handles and user data (see GUIDATA)
% varargin   command line arguments to selection_gui (see VARARGIN)
handles.guifig = gcf;
```

```
movegui(handles.guifig,'center');

guidata(handles.guifig,handles);
% Choose default command line output for selection_gui
handles.output = hObject;

% Update handles structure
guidata(hObject, handles);

% UIWAIT makes selection_gui wait for user response (see UIRESUME)
% uiwait(handles.figure1);


% --- Outputs from this function are returned to the command line.
function varargout = selection_gui_OutputFcn(hObject, eventdata, handles)
% varargout  cell array for returning output args (see VARARGOUT);
% hObject    handle to figure
% eventdata  reserved - to be defined in a future version of MATLAB
% handles    structure with handles and user data (see GUIDATA)

% Get default command line output from handles structure
set(handles.guifig,'WindowStyle','Modal'); %make figure modal

uiwait; %wait till the figure is destroyed  or asked to resume
varargout={};
try %this statement is necessary if figure is destroyed , then output argument
will be empty by default
    handles = guidata(handles.guifig);
    varargout{1} = {handles.mcnpx, handles.ptrac, handles.filtered,...
        handles.electron, handles.proton, handles.triton,...
        handles.alpha, handles.multiplier, handles.pfilter, ...
        handles.heavy};
    closereq; % close the gui if done is pressed
catch
    varargout{1} = [];
end



% --- Executes on button press in done.
function done_Callback(hObject, eventdata, handles)
% hObject    handle to done (see GCBO)
% eventdata  reserved - to be defined in a future version of MATLAB
% handles    structure with handles and user data (see GUIDATA)

% if isfield(handles,'value');%if there is no selection of radio button and OK
is pressed then the selection is Radio Button1 by default
%     handles.selection = handles.value;
% else
%     handles.selection = 'Radio Button1';
% end
%
% guidata(hObject, handles);
% guidata(handles.guifig, handles);

uiresume;



% % --------------------------------------------------------------------
% function uipanel1_SelectionChangeFcn(hObject, eventdata, handles)
```

```
% % hObject    handle to uipanel1 (see GCBO)
% % eventdata  reserved - to be defined in a future version of MATLAB
% % handles    structure with handles and user data (see GUIDATA)
%
% switch get(hObject,'Tag')   % Get Tag of selected object
%     case 'radio1'
%         handles.value = 'Radio Button1'; %if Radio Button1 is selected then
update handles.value
%     case 'radio2'
%         handles.value = 'Radio Button2';%if Radio Button2 is selected then
update handles.value
% end
% guidata(hObject, handles);
%
% % --- Executes on button press in cancel.
% function cancel_Callback(hObject, eventdata, handles)
% % hObject    handle to cancel (see GCBO)
% % eventdata  reserved - to be defined in a future version of MATLAB
% % handles    structure with handles and user data (see GUIDATA)
% closereq;


% --- Executes when user attempts to close figure1.
function figure1_CloseRequestFcn(hObject, eventdata, handles)
% hObject    handle to figure1 (see GCBO)
% eventdata  reserved - to be defined in a future version of MATLAB
% handles    structure with handles and user data (see GUIDATA)

% Hint: delete(hObject) closes the figure
delete(hObject);



function mcnpx_Callback(hObject, eventdata, handles)
% hObject    handle to mcnpx (see GCBO)
% eventdata  reserved - to be defined in a future version of MATLAB
% handles    structure with handles and user data (see GUIDATA)

handles.mcnpx = get(hObject,'String');
guidata(hObject, handles);

% --- Executes during object creation, after setting all properties.
function mcnpx_CreateFcn(hObject, eventdata, handles)
% hObject    handle to mcnpx (see GCBO)
% eventdata  reserved - to be defined in a future version of MATLAB
% handles    empty - handles not created until after all CreateFcns called

% Hint: edit controls usually have a white background on Windows.
%       See ISPC and COMPUTER.
if ispc && isequal(get(hObject,'BackgroundColor'),
get(0,'defaultUicontrolBackgroundColor'))
    set(hObject,'BackgroundColor','white');
end



function ptrac_Callback(hObject, eventdata, handles)
% hObject    handle to ptrac (see GCBO)
% eventdata  reserved - to be defined in a future version of MATLAB
% handles    structure with handles and user data (see GUIDATA)
```

```
handles.ptrac = get(hObject,'String');
guidata(hObject, handles);


% --- Executes during object creation, after setting all properties.
function ptrac_CreateFcn(hObject, eventdata, handles)
% hObject    handle to ptrac (see GCBO)
% eventdata  reserved - to be defined in a future version of MATLAB
% handles    empty - handles not created until after all CreateFcns called

% Hint: edit controls usually have a white background on Windows.
%       See ISPC and COMPUTER.
if ispc && isequal(get(hObject,'BackgroundColor'),
get(0,'defaultUicontrolBackgroundColor'))
    set(hObject,'BackgroundColor','white');
end


% --- Executes on button press in filtered.
function filtered_Callback(hObject, eventdata, handles)
% hObject    handle to filtered (see GCBO)
% eventdata  reserved - to be defined in a future version of MATLAB
% handles    structure with handles and user data (see GUIDATA)

% Hint: get(hObject,'Value') returns toggle state of filtered
if (get(hObject,'Value') == get(hObject,'Max'))
    handles.filtered = 'y';
elseif (get(hObject,'Value') == get(hObject,'Min'))
    handles.filtered = 'n';
end
guidata(hObject, handles);



function multiplier_Callback(hObject, eventdata, handles)
% hObject    handle to multiplier (see GCBO)
% eventdata  reserved - to be defined in a future version of MATLAB
% handles    structure with handles and user data (see GUIDATA)

handles.multiplier = get(hObject,'String');
handles.multiplier = str2num(handles.multiplier);
guidata(hObject, handles);



% --- Executes during object creation, after setting all properties.
function multiplier_CreateFcn(hObject, eventdata, handles)
% hObject    handle to multiplier (see GCBO)
% eventdata  reserved - to be defined in a future version of MATLAB
% handles    empty - handles not created until after all CreateFcns called

% Hint: edit controls usually have a white background on Windows.
%       See ISPC and COMPUTER.
if ispc && isequal(get(hObject,'BackgroundColor'),
get(0,'defaultUicontrolBackgroundColor'))
    set(hObject,'BackgroundColor','white');
end



% --- Executes on button press in electron.
```

```
function electron_Callback(hObject, eventdata, handles)
% hObject    handle to electron (see GCBO)
% eventdata  reserved - to be defined in a future version of MATLAB
% handles    structure with handles and user data (see GUIDATA)

% Hint: get(hObject,'Value') returns toggle state of electron
if (get(hObject,'Value') == get(hObject,'Max'))
    handles.electron = 1;
elseif (get(hObject,'Value') == get(hObject,'Min'))
    handles.electron = 0;
end
guidata(hObject, handles);


% --- Executes on button press in proton.
function proton_Callback(hObject, eventdata, handles)
% hObject    handle to proton (see GCBO)
% eventdata  reserved - to be defined in a future version of MATLAB
% handles    structure with handles and user data (see GUIDATA)

% Hint: get(hObject,'Value') returns toggle state of proton
if (get(hObject,'Value') == get(hObject,'Max'))
    handles.proton = 1;
elseif (get(hObject,'Value') == get(hObject,'Min'))
    handles.proton = 0;
end
guidata(hObject, handles);


% --- Executes on button press in triton.
function triton_Callback(hObject, eventdata, handles)
% hObject    handle to triton (see GCBO)
% eventdata  reserved - to be defined in a future version of MATLAB
% handles    structure with handles and user data (see GUIDATA)

% Hint: get(hObject,'Value') returns toggle state of triton
if (get(hObject,'Value') == get(hObject,'Max'))
    handles.triton = 1;
elseif (get(hObject,'Value') == get(hObject,'Min'))
    handles.triton = 0;
end
guidata(hObject, handles);



% --- Executes on button press in alpha.
function alpha_Callback(hObject, eventdata, handles)
% hObject    handle to alpha (see GCBO)
% eventdata  reserved - to be defined in a future version of MATLAB
% handles    structure with handles and user data (see GUIDATA)

% Hint: get(hObject,'Value') returns toggle state of alpha
if (get(hObject,'Value') == get(hObject,'Max'))
    handles.alpha = 1;
elseif (get(hObject,'Value') == get(hObject,'Min'))
    handles.alpha = 0;
end
guidata(hObject, handles);
```

```
% --- Executes on button press in pfilter.
function pfilter_Callback(hObject, eventdata, handles)
% hObject    handle to pfilter (see GCBO)
% eventdata  reserved - to be defined in a future version of MATLAB
% handles    structure with handles and user data (see GUIDATA)

if (get(hObject,'Value') == get(hObject,'Max'))
    handles.pfilter = 'y';
elseif (get(hObject,'Value') == get(hObject,'Min'))
    handles.pfilter = 'n';
end
guidata(hObject, handles);


% --- Executes on button press in heavy (checkbox9).
function checkbox9_Callback(hObject, eventdata, handles)
% hObject    handle to checkbox9 (see GCBO)
% eventdata  reserved - to be defined in a future version of MATLAB
% handles    structure with handles and user data (see GUIDATA)

% Hint: get(hObject,'Value') returns toggle state of heavy
if (get(hObject,'Value') == get(hObject,'Max'))
    handles.heavy = 1;
elseif (get(hObject,'Value') == get(hObject,'Min'))
    handles.heavy = 0;
end
guidata(hObject, handles);
```

STATS.m

```
% Stats matrix row labels
% 1 = Total energy difference
% 2 = Birth cell
% 3 = Death cell
% 4 = Distance traveled
% 5 = Birth cell energy deposited
% 6 = Death cell energy deposited
% 7 = Event number
% 8 = Number of additional cells particle passed through
% 9-n = Pairs of values indicating cell number and energy deposited in cell


function particle_stats =
stats(Data,bnk_eventtype,particle_stats,i,stopping_power,kB,C,ion_num)
    %Get original 3-space coordinates, cell and energy
    birthcell = Data(bnk_eventtype(i,1),6);
    birthenergy = Data(bnk_eventtype(i,1),15);
    pos_particle_x = Data(bnk_eventtype(i,1),9);
    pos_particle_y = Data(bnk_eventtype(i,1),10);
    pos_particle_z = Data(bnk_eventtype(i,1),11);

    if ion_num == 32
        col_num = 3;
    elseif ion_num == 34
        col_num = 2;
    elseif ion_num == 35
        col_num = 2;
    end

    %Find event number by counting backward from current row
    j=bnk_eventtype(i,1)-1;
    while( sum(Data(j,2:17))~=0 ) %Stop when all columns except the first sum
to 0
        j=j-1;
    end
    event = Data(j,1);

    %Search forward to first 5000 line (to retrieve stats about death cell)
    j=bnk_eventtype(i,1)+1;
    while(Data(j,1)~=5000)
        j=j+1;
    end
    deathcell = Data(j,6);

    %Calcuate new distance and energy
    deathenergy = Data(j,15);
    dist_particle_x = pos_particle_x - Data(j,9);
    dist_particle_y = pos_particle_y - Data(j,10);
    dist_particle_z = pos_particle_z - Data(j,11);
    dist_particle_tot =
sqrt(dist_particle_x.^2+dist_particle_y.^2+dist_particle_z.^2);

    %Particle stats array will not grow beyond this number, so we can save
    %it and use the width variable for simplicity
    width = size(particle_stats,2)+1;

    %Store distance, energy, and final cell number
    particle_stats(1,width) = abs(birthenergy-deathenergy);
```

```
    particle_stats(2,width) = birthcell;
    particle_stats(3,width) = deathcell;
    particle_stats(4,width) = dist_particle_tot;

    particle_stats(7,width) = event;

    %Find other cells the particle may have passed through and record their
    %energies as well
    %Start looking at the row after this 20xx event
    previouscell=birthcell;
    surface = 0; %beginning of vector to store indices of surface events in
    k = bnk_eventtype(i,1)+1;
    while (1)
        % Stop looking when we hit the next 3000 event
        cellnum = Data(k,6);
        if Data(k,1) == 3000 && (cellnum ~= previouscell)
            %Record the row index from Data of this surface event
            surface(length(surface)+1) = k;
            previouscell=cellnum;
        %Stop looking if we find a 5000 or the next 20xx event and
        % set k to -1 to indicate error
        elseif Data(k,1) == 5000
            k=-1;
            break
        %Check whether i+1 will overflow the eventtype index
        elseif i+1 <= length(bnk_eventtype)
            %Check whether we've reached the next 20xx event(if one
            %exists)
            if  k == bnk_eventtype(i+1,1)
                k=-1;
            break
            end
        end
        %k is incrementing through single lines in Data, not
        %through event types
        k=k+1;
    end

%     u = unique(Data(surface(2:length(surface)),6));
%     if length(u) > 1
%         disp('particle passes through multiple cells');
%     end



    %Put birth cell and death cell at beginning and end of queue
    surface(1) = bnk_eventtype(i,1);
    surface(length(surface)+1)= j;
    %Calculate simple delta energy
    d_e = abs(birthenergy-deathenergy);

    %Calculate scaling factor for deposited energy
    dEdx = interp1(stopping_power(:,1),stopping_power(:,col_num),d_e);
    yield_function = ((1 + kB.*dEdx + C.*dEdx.^2).^(-1));
    d_e = d_e.*yield_function;

    %Find number of unique cells the particle passes through (excepting the
    %birth and death cells)
    u = unique(Data(surface(2:length(surface)-1),6));
```

```
    %Initialize previous cell for check later (see notes below)
    previouscell = birthcell;

    if length(u)==0
        if birthcell == deathcell
            %If particle only sees one cell, that cell gets the total
            %deposited energy (recorded in birth and death energy rows for
            %clarity)
            particle_stats(5,width)=d_e;
            particle_stats(6,width)=d_e;
%         else
%             %%%% NOTE: This block may never be needed. Uncomment if holes
%             %appear in the stats array %%%%%%%%
%             %If particle moves directly from birth cell to death cell,
%             %record birth energy - death energy in birth cell, and death
%             %energy in death cell
%             particle_stats(5,width)=d_e;
%             particle_stats(6,width)=deathenergy;
        end
    %If particle does have additional surface events, but somehow never
    %leaves the birth/death cell (all cells are identical)
    elseif length(u)==1 && Data(surface(2),6)==birthcell...
            && Data(surface(2),6)==deathcell
            particle_stats(5,width)=d_e;
            particle_stats(6,width)=d_e;
    %Otherwise there are one or more surface events and at least one of the
    %surface events involves a non-birth/death cell.
    else
        for y = 1:length(surface)
            cellnum = Data(surface(y),6);

            %Check whether particle has crossed into new cell
            if cellnum ~= previouscell

                current_energy = Data(surface(y),15);
                %Initialize birth energy to birth cell when we first find a
                %new cell to calculate a delta energy from
                if previouscell==birthcell && particle_stats(5,width)==0
                    particle_stats(5,width)=birthenergy - current_energy;
                end

                %Grab the next energy to calculate difference, or zero if
                %current cell is at the end of the queue
                if y+1 <= length(surface)
                    next_energy = Data(surface(y+1),15);
                else
                    next_energy = 0;
                end

                %Same math as for all cells, but recorded in a different
                %location for compatability with other functions
                if cellnum == birthcell
                    particle_stats(5,width) = ...
                        particle_stats(5,width) + current_energy - next_energy;
                    %Copy birthcell energy into deathcell row if they're
                    %the same cell (program works either way, but adds to
                    %readability)
                    if birthcell==deathcell
                        particle_stats(6,width)=particle_stats(5,width);
                    end
                elseif cellnum == deathcell
```

```
                    particle_stats(6,width) = ...
                        particle_stats(6,width) + current_energy - next_energy;
                else
                    %Check whether current cell already exists, create if not
                    x=find(particle_stats(:,width)==cellnum);
                    if size(x,1)==0

particle_stats(9+2*particle_stats(8,width),width)=cellnum;
                        particle_stats(8,width) = particle_stats(8,width) +1;
                        x=size(particle_stats,1);
                        particle_stats(8+2*particle_stats(8,width),width)=0;
                    end %By now, x points to the correct cell

                    d_e = current_energy - next_energy;

                    %Calculate scaling factor for deposited energy
                    dEdx =
interp1(stopping_power(:,1),stopping_power(:,col_num),d_e);
                    yield_function = ((1 + kB.*dEdx + C.*dEdx.^2).^(-1));
                    d_e = d_e.*yield_function;

                    %Simply add energy difference to cell's previous
                    %value
                    particle_stats(8+2*particle_stats(8,width),width) =...
                        particle_stats(8+2*particle_stats(8,width),width)...
                        + d_e;
                end

                previouscell = cellnum;
            end

        end
    end


end %End function
```

SCINTILLATION.m

```
%Column 1: Cell number
%Column 2: Number of particles interacting with that cell
%Column 3: Probability of scintillation given a neutron event
%Column 4: Probability of scintillation given a charged particle event
%Column 5: Energy deposited in cell
%Column 6: Average energy deposited in cell per particle
%Column 7: Standard Deviation of energy deposited in cell
%Column 8: Tracks entering cell

function charged_per_cell_particle =
scintillation(particle_stats,charged_per_cell_particle,num_source,bnk_created)

energy_events = [0,0];

for i=1:size(particle_stats,2)
        % Find locations where each cell is mentioned in particle_stats
        % If we have no cells of interest yet, take the first one and add
        % it to our list
        k=find(charged_per_cell_particle(:,1)==particle_stats(2,i));
        if size(k,1)==0

charged_per_cell_particle(size(charged_per_cell_particle,1)+1,1)=particle_stats
(2,i);
            k=size(charged_per_cell_particle,1);
            energy_events(k,1) = particle_stats(2,i);
            energy_events(k,2) = 2;
        end

        %Increment by 1 for particle's birth cell
        charged_per_cell_particle(k,2)=charged_per_cell_particle(k,2)+1;
        %Add deposited energy to particle's birth cell

charged_per_cell_particle(k,5)=charged_per_cell_particle(k,5)+particle_stats(5,
i);

        %Record this energy in vector for standard deviation calculation
        energy_events(k,energy_events(k,2)+1) = particle_stats(5,i);
        energy_events(k,2) = energy_events(k,2)+1;

        % Check whether particle was born and died in different cells
        if particle_stats(2,i) ~= particle_stats(3,i)
            j=find(charged_per_cell_particle(:,1)==particle_stats(3,i));
            if size(j,1)==0

charged_per_cell_particle(size(charged_per_cell_particle,1)+1,1)=particle_stats
(3,i);
                j=size(charged_per_cell_particle,1);
                energy_events(j,1) = particle_stats(2,i);
                energy_events(j,2) = 2;
            end

            %Increment particle count for death cell by one
            charged_per_cell_particle(j,2)=charged_per_cell_particle(j,2)+1;
            %Add deposited energy to particle's death cell

charged_per_cell_particle(j,5)=charged_per_cell_particle(j,5)+particle_stats(6,
i);
```

```
            %Record this energy in vector for standard deviation calculation
            energy_events(j,energy_events(j,2)+1) = particle_stats(6,i);
            energy_events(j,2) = energy_events(j,2)+1;
        end

        %Check whether particle passed through any additional cells
        if particle_stats(8,i)~=0
            for x=1:particle_stats(8,i)

j=find(charged_per_cell_particle(:,1)==particle_stats(7+2*x,i));
                if size(j,1)==0

charged_per_cell_particle(size(charged_per_cell_particle,1)+1,1)=particle_stats
(7+2*x,i);
                    j=size(charged_per_cell_particle,1);
                    energy_events(j,1) = particle_stats(2,i);
                    energy_events(j,2) = 2;
                end

                %Increment particle count for this cell by one

charged_per_cell_particle(j,2)=charged_per_cell_particle(j,2)+1;
                %Add deposited energy to new cell

charged_per_cell_particle(j,5)=charged_per_cell_particle(j,5)+particle_stats(8+
2*x,i);

                %Record this energy in vector for standard deviation
calculation
                energy_events(j,energy_events(j,2)+1) =
particle_stats(8+2*x,i);
                energy_events(j,2) = energy_events(j,2)+1;
            end
        end
end

%Divide num of events in cell by total events
for i=2:size(charged_per_cell_particle,1)
    charged_per_cell_particle(i,3) = charged_per_cell_particle(i,2)/num_source;
    charged_per_cell_particle(i,4) =
charged_per_cell_particle(i,2)/bnk_created;
    charged_per_cell_particle(i,6) =
charged_per_cell_particle(i,5)/charged_per_cell_particle(i,2);
    charged_per_cell_particle(i,7) =
std(energy_events(i,3:energy_events(i,2)));
end
```

ADD_ENERGY.m

```
function bin_energy = add_energy(particle_stats,bin_energy)

    %Add energy lost by particles
    for i=2:size(particle_stats,2) %look through each particle event

        %Look at the birth cell info and add up energies per event

        %Check whether this particle's cell already exists, create if not
        j=find(bin_energy(:,1)==particle_stats(2,i));
        if size(j,1)==0
            bin_energy(size(bin_energy,1)+1,1)=particle_stats(2,i);
            j=size(bin_energy,1);
        end %By now, j points to the correct cell in bin_energy no matter what


        %Check whether this particle's event already exists, create if not
        k=find(bin_energy(1,:)==particle_stats(7,i));
        if size(k,2)==0
            bin_energy(1,size(bin_energy,2)+1)=particle_stats(7,i);
            k=size(bin_energy,2);
        end %By now, k points to the correct event in bin_energy no matter what

        %Add energy from this event for this cell in the last colum
        bin_energy(j,k)=bin_energy(j,k)+particle_stats(5,i);



        %If this particle was born and died in different cells, find or create
        %the row for the death cell as well, and update its energy too
        if(particle_stats(2,i)~=particle_stats(3,i))
            %Look at the death cell info
            j=find(bin_energy(:,1)==particle_stats(3,i));
            if size(j,1)==0
                bin_energy(size(bin_energy,1)+1,1)=particle_stats(3,i);
                j=size(bin_energy,1);
            end
            k=find(bin_energy(1,:)==particle_stats(7,i));
            if size(k,2)==0
                bin_energy(1,size(bin_energy,2)+1)=particle_stats(7,i);
                k=size(bin_energy,2);
            end
            bin_energy(j,k)=bin_energy(j,k)+particle_stats(6,i);
        end



        %Check whether there are additional cells
        if particle_stats(8,i)~=0
            for x=1:particle_stats(8,i)
                %Look at energy and cell number for each additional cell
                j=find(bin_energy(:,1)==particle_stats(9+2*(x-1),i));
                if size(j,1)==0
                    bin_energy(size(bin_energy,1)+1,1)=particle_stats(9+2*(x-
1),i);
                    j=size(bin_energy,1);
```

```
                end
                k=find(bin_energy(1,:)==particle_stats(7,i));
                if size(k,2)==0
                    bin_energy(1,size(bin_energy,2)+1)=particle_stats(7,i);
                    k=size(bin_energy,2);
                end
                bin_energy(j,k)=bin_energy(j,k)+particle_stats(10+2*(x-1),i);
            end
        end

    end %end for loop

end %End function add_energy
```

NUM_SOURCE_READER.m

```
function num = num_source_reader(filename)
%filename = input('\nPlease input the MCNPX output filename:  ','s');

fid = fopen(filename);

s1 = 'start';
% This loop Search for the number of neutron histories by finding the string
%    "run terminated when"
while s1 ~= -1
    % s1 = -1 when EOF is reached - loop runs until EOF
    % Gets the first line
    s1 = fgets(fid);
    % Scans for string "run terminated when"
    while s1 ~= -1
        % Gets the next line
        s1 = fgets(fid);
        if isempty(findstr(s1,'run terminated when')) == 0
            neutron_histories = s1;
            s1 = -1;
        end
    end
    % Loop terminates when "run terminated when" is found
end
% Close the files
fclose(fid);

% Use %*s to skip a word and %d to read a number (%s to read a word)
% The number of neutron histories is the 4th "word" in this string
num = sscanf(neutron_histories,'%*s %*s %*s %d');
```

G_FROM_BREM_READER.m

```
function num = g_from_brem_reader(filename)

fid = fopen(filename);

s1 = 'start';
% This loop Search for the number of gammas from bremsstrahlung by finding the
string
%    "bremsstrahlung"
while s1 ~= -1
    % s1 = -1 when EOF is reached - loop runs until EOF
    % Gets the first line
    s1 = fgets(fid);
    % Scans for string "bremsstrahlung"
    while s1 ~= -1
        % Gets the next line
        s1 = fgets(fid);
        if isempty(findstr(s1,'bremsstrahlung')) == 0
            g_from_brem = s1;
            s1 = -1;
        end
    end
end
% Close the files
fclose(fid);

% The number of gammas from bremsstrahlung is the 2nd "word" in this string
num = sscanf(g_from_brem,'%*s %d');
```

G_FROM_N_READER.m

```
function num = g_from_n_reader(filename)

fid = fopen(filename);

s1 = 'start';
% This loop Search for the number of gammas from neutrons by finding the string
%    "from neutrons"
while s1 ~= -1
    % s1 = -1 when EOF is reached - loop runs until EOF
    % Gets the first line
    s1 = fgets(fid);
    % Scans for string "from neutrons"
    while s1 ~= -1
        % Gets the next line
        s1 = fgets(fid);
        if isempty(findstr(s1,'from neutrons')) == 0
            g_from_n = s1;
            s1 = -1;
        end
    end
end
% Close the files
fclose(fid);

% The number of gammas from neutrons is the 3rd "word" in this string
num = sscanf(g_from_n,'%*s %*s %d');
```

N_ABS_READER.m

```
function num = n_abs_reader(filename)

fid = fopen(filename);

s1 = 'start';
% This loop Search for the number of neutron absorptions by finding a line
%   in the output which has both "photonuclear" and "capture"
while s1 ~= -1
    % s1 = -1 when EOF is reached - loop runs until EOF
    % Gets the first line
    s1 = fgets(fid);
    % Scans for string for both "photonuclear" and "capture"
    while s1 ~= -1
        % Gets the next line
        s1 = fgets(fid);
        if isempty(findstr(s1,'photonuclear')) == 0
            if isempty(findstr(s1,'capture')) == 0
                n_abs = s1;
                s1 = -1;
            end
        end
    end
end
% Close the files
fclose(fid);

% The number of neutron absorptions is the 6th "word" in this string
num = sscanf(n_abs,'%*s %*s %*s %*s %*s %d');
```

N_ESCAPE_READER.m

```
function num = n_escape_reader(filename)

fid = fopen(filename);

s1 = 'start';
% This loop Search for the number of neutron escapes by finding the string
%    "escape"
while s1 ~= -1
    % s1 = -1 when EOF is reached - loop runs until EOF
    % Gets the first line
    s1 = fgets(fid);
    % Scans for string "escape"
    while s1 ~= -1
        % Gets the next line
        s1 = fgets(fid);
        if isempty(findstr(s1,'escape')) == 0
            n_escape = s1;
            s1 = -1;
        end
    end
end
% Close the files
fclose(fid);

% The number of neutron escapes is the 6th "word" in this string
num = sscanf(n_escape,'%*s %*s %*s %*s %*s %d');
```

P_CAPTURE_READER.m

```
function num = p_capture_reader(filename)

fid = fopen(filename);

s1 = 'start';
% This loop Search for the number of photon captures by finding the 1st line
%   in the output which has both "bremsstrahlung" and "capture"
while s1 ~= -1
    % s1 = -1 when EOF is reached - loop runs until EOF
    % Gets the first line
    s1 = fgets(fid);
    % Scans for string for both "bremsstrahlung" and "capture"
    while s1 ~= -1
        % Gets the next line
        s1 = fgets(fid);
        if isempty(findstr(s1,'bremsstrahlung')) == 0
            if isempty(findstr(s1,'capture')) == 0
                p_capture = s1;
                s1 = -1;
            end
        end
    end
end
% Close the files
fclose(fid);

% The number of photon captures is the 6th "word" in this string
num = sscanf(p_capture,'%*s %*s %*s %*s %*s %d');
```

P_COMPT_SCATT_READER.m

```
function num = p_compt_scatt_reader(filename)

fid = fopen(filename);

s1 = 'start';
% This loop Search for the number of photon compton scatter by finding the
string
%    "compton scatter"
while s1 ~= -1
    % s1 = -1 when EOF is reached - loop runs until EOF
    % Gets the first line
    s1 = fgets(fid);
    % Scans for string "compton scatter"
    while s1 ~= -1
        % Gets the next line
        s1 = fgets(fid);
        if isempty(findstr(s1,'compton scatter')) == 0
            p_compt_scatt = s1;
            s1 = -1;
        end
    end
end
% Close the files
fclose(fid);

% The number of compton scatters is the 8th "word" in this string
num = sscanf(p_compt_scatt,'%*s %*s %*s %*s %*s %*s %*s %d');
```

P_ENERGY_CUT_READER.m

```
function num = p_energy_cut_reader(filename)

fid = fopen(filename);

s1 = 'start';
% This loop Search for the number of photons lost by energy cutoff by
%   finding the 2nd occurance of the string which includes both
%   "nucl. interaction" and "energy cutoff"


while s1 ~= -1
    % s1 = -1 when EOF is reached - loop runs until EOF
    % Gets the first line
    s1 = fgets(fid);
    tally = 0;
    % Scans for string for both "nucl. interaction" and "energy cutoff"
    while s1 ~= -1
        % Gets the next line
        s1 = fgets(fid);
        if isempty(findstr(s1,'nucl. interaction')) == 0
            if isempty(findstr(s1,'energy cutoff')) == 0
                tally = tally + 1;
                if tally == 2;
                    p_energy_cut = s1;
                    s1 = -1;
                end
            end
        end
    end
end

% Close the files
fclose(fid);

% The number of photons lost by energy cutoff is the 8th "word" in this string
num = sscanf(p_energy_cut,'%*s %*s %*s %*s %*s %*s %*s %d');
```

P_ESCAPE_READER.m

```
function num = p_escape_reader(filename)

fid = fopen(filename);

s1 = 'start';
% This loop Search for the number of photon escapes by finding the 3rd
% occurance of the string which includes both "source" and "escape"


while s1 ~= -1
    % s1 = -1 when EOF is reached - loop runs until EOF
    % Gets the first line
    s1 = fgets(fid);
    tally = 0;
    % Scans for string for both "source" and "escape"
    while s1 ~= -1
        % Gets the next line
        s1 = fgets(fid);
        if isempty(findstr(s1,'source')) == 0
            if isempty(findstr(s1,'escape')) == 0
                tally = tally + 1;
                if tally == 3;
                    p_escape = s1;
                    s1 = -1;
                end
            end
        end
    end
end

% Close the files
fclose(fid);

% The number of photon escapes is the 6th "word" in this string
num = sscanf(p_escape,'%*s %*s %*s %*s %*s %d');
```

P_FLUORESCENCE_READER.m

```
function num = p_fluorescence_reader(filename)

fid = fopen(filename);

s1 = 'start';
% This loop Search for the number of photon 1st fluorescence by finding the
string
%    "1st fluorescence"
while s1 ~= -1
    % s1 = -1 when EOF is reached - loop runs until EOF
    % Gets the first line
    s1 = fgets(fid);
    % Scans for string "1st fluorescence"
    while s1 ~= -1
        % Gets the next line
        s1 = fgets(fid);
        if isempty(findstr(s1,'1st fluorescence')) == 0
            p_fluorescence = s1;
            s1 = -1;
        end
    end
end
% Close the files
fclose(fid);

% The number of gammas from fluorescence is the 2nd "word" in this string
num = sscanf(p_fluorescence,'%*s %d');
```

P_PAIR_PROD_READER.m

```
function num = p_pair_prod_reader(filename)

fid = fopen(filename);

s1 = 'start';
% This loop Search for the number of photon pair productions by finding the 1st
line
%   in the output which has both "p-annihilation" and "pair production"
while s1 ~= -1
    % s1 = -1 when EOF is reached - loop runs until EOF
    % Gets the first line
    s1 = fgets(fid);
    % Scans for string for both "p-annihilation" and "pair production"
    while s1 ~= -1
        % Gets the next line
        s1 = fgets(fid);
        if isempty(findstr(s1,'p-annihilation')) == 0
            if isempty(findstr(s1,'pair production')) == 0
                p_pair_prod = s1;
                s1 = -1;
            end
        end
    end
end
% Close the files
fclose(fid);

% The number of photon pair productions is the 7th "word" in this string
num = sscanf(p_pair_prod,'%*s %*s %*s %*s %*s %*s %d');
```

P_PHOTONUCLEAR_ABS_READER.m

```
function num = p_photonuclear_abs_reader(filename)

fid = fopen(filename);

s1 = 'start';
% This loop Search for the number of photon photonuclear absorption by finding
the 1st line
%   in the output which has both "photonuclear" and "photonuclear abs"
while s1 ~= -1
    % s1 = -1 when EOF is reached - loop runs until EOF
    % Gets the first line
    s1 = fgets(fid);
    % Scans for string for both "photonuclear" and "photonuclear abs"
    while s1 ~= -1
        % Gets the next line
        s1 = fgets(fid);
        if isempty(findstr(s1,'photonuclear')) == 0
            if isempty(findstr(s1,'photonuclear abs')) == 0
                p_photonuclear_abs = s1;
                s1 = -1;
            end
        end
    end
end
% Close the files
fclose(fid);

% The number of photon pair productions is the 7th "word" in this string
num = sscanf(p_photonuclear_abs,'%*s %*s %*s %*s %*s %*s %d');
```

VITA

Martin Rodney Williamson was born in Knoxville, Tennessee on April 14, 1980 to Rodney and Barbara Williamson. He has one older brother, James Andrew "Andy" Williamson. He was raised in Cosby, Tennessee, and graduated from Gatlinburg Pittman High School in May 1998. The following August he entered Walters State Community College in Morristown, Tennessee, and studied engineering for one year. While attending Walters State, he met his future wife, whom he would later marry in May of 2000. Starting in August of 1999, he entered The University of Tennessee (UTK) where he received a Bachelor of Science in Nuclear Engineering in May 2002. Immediately after graduating, he entered graduate school at UTK. He was awarded the National Academy for Nuclear Training (NANT) fellowship and received a Graduate Certificate in Nuclear Criticality Safety as well as a Master of Science degree in Nuclear Engineering with a thesis entitled "Transportable Modular Balance of Plant Study for Small Nuclear Power Plants" under the guidance of Lawrence W. Townsend, Ph.D. in May 2004. After graduation, he was hired as a Nuclear Criticality Safety Engineer at the Y-12 National Security Complex. Martin continued his education at UTK by enrolling in evening classes while working at Y-12. During this time, he also had two children, Thomas Martin and Nathaniel James. Martin became registered as a Professional Engineer in Nuclear Engineering in October 2009. He received a Graduate Certificate in Applied Statistical Strategies as well as a Doctor of Philosophy degree in Nuclear Engineering from the University of Tennessee in 2010. After completing his doctoral degree, Dr. Williamson plans to continue his current research and develop related research at the Y-12 National Security Complex.